Development and Evaluation of a Real-time Coupled Wave-Atmosphere Regional Forecast System (CWARFS)

by

Katherine Leora Howard

Bachelor of Science
Atmospheric Science
State University of New York at Albany
2006

A thesis
submitted by the Department of Marine and Environmental Systems
Florida Institute of Technology
in partial fulfillment of the requirements
for the degree of

Master of Science
in
Meteorology

Melbourne, Florida
August, 2009

© Copyright 2009 Katherine Leora Howard
All Rights Reserved

The author grants permission to make single copies _____

We the undersigned committee hereby recommend
that the attached document be accepted as fulfilling in
part the requirements for the degree of
Master of Science in Meteorology

Development and Evaluation of a Real-time Coupled Wave-Atmosphere Regional Forecast System (CWARFS)
a thesis by Katherine Leora Howard

S. M. Lazarus, Ph.D.
Assistant Professor
Marine and Environmental Systems
Major Advisor

M. E. Splitt, M.S.
Research Professor
Marine and Environmental Systems

G. Zarillo, Ph.D.
Professor
Marine and Environmental Systems

W. Shaw, Ph.D.
Dean and Kaolin Chair
Engineering, Mercer University

G. A. Maul, Ph.D.
Professor and Department Head
Marine and Environmental Systems

ABSTRACT

Development and Evaluation of a Real-time Coupled Wave-Atmosphere Regional Forecast System (CWARFS)
by
Katherine Leora Howard
Committee Chair: Dr. Steven Lazarus, Ph.D.

The configuration and evaluation of an atmosphere-wave coupled nearshore forecasting system for the National Weather Service (NWS) is discussed. The system is designed to provide the NWS with a computationally efficient, high-resolution wave forecasts (e.g., significant wave height, dominant wave period, and wave direction) for the nearshore region where a void between the coastline and WAVEWATCH III domain currently exists. The forecast system is comprised primarily of the Weather Research and Forecasting Environmental Modeling System coupled with the U.S. Army Corps of Engineers Coastal and Hydraulics Laboratory (CHL) Coastal Modeling System. The system evaluation includes key operational aspects – the variability of the forecast wave domain wind fields, the quality of both the wave model wind and wave forcings, and the performance of the wave model. Various atmosphere and wave model combinations are examined including an evaluation of the impact of model resolution and forecast wind fields from the North American Mesoscale Model, Global Forecast System, and the NWS Graphics Forecast Editor. Both wind and wave forecasts and forcing are evaluated using in situ buoy observations. Outcomes of this work form the basis of the operational configuration for transition to the NWS offices in Melbourne and Miami, FL. Results indicate that

Table of Contents

Abstract iv

List of Figures vii

List of Tables xiii

List of Abbreviations xiv

Acknowledgements xvi

Dedication xvii

1. Introduction 1

2. Methodology 9
   2.1. The Atmospheric Model 9
   2.2. The Wave Model 12
   2.3. Atmosphere/Wave Model Coupled 13
   2.4. Data 15
      2.4.1. Model Forcing and Output 15
      2.4.2. Verification Data 16
      2.4.3. Data Tiers and Wind Events 18
   2.5. Statistical Analysis 19

3. Results 22
   3.1. Atmospheric Models 23
      3.1.1. Wind Variability 24
         3.1.1.1. Theoretical Wave Height Variability 24
         3.1.1.2. Forecast Wind Subdomain Variability and Impact on Wave Forecasts 26
         3.1.1.3. Single Point Time Series vs. Domain Averaged Wind 36
      3.1.2. Wind Forecast / Forcing 45
         3.1.2.1. Tier 4 Wind Analysis 45
         3.1.2.2. Tier 2 Case Study Wind Analysis 49
         3.1.2.3. GFE Wind Forecast / Forcing 58
         3.1.2.4. Tier 1 – Tropical Storm Fay Wind Analysis 59
   3.2. Wave Model 68
      3.2.1. Wave Forcing – WAVEWATCHIII 68
      3.2.2. Wave Forecast and Impact of Varying Wind Forcing 76
         3.2.2.1. Tier 3 Wave Analysis 77

3.2.2.2. Tier 1 – Tropical Storm Fay Wave Analysis 82
3.3. Resulting Wave Model Variability 89

4. Summary 92

5. References 97

List of Figures

Figure 1: NOAA WaveWatch III (Western North Atlantic regional wave model) 12 h forecast of primary wave direction (arrows) and significant wave height (m, contours and shading) valid 18 UTC 25 June 2006. Image provided by the Melbourne FL NWS. 2

Figure 2: Locations of WRF-EMS 4.5 km, 1.5 km nest and 10 km domains. The WRF-EMS 10 km domain is in the same location as the WRF-EMS 4.5 km domain. 11

Figure 3: Locations of five CMS-Wave grids (boundaries in white and grid number in yellow) along the coastal study area of Eastern Central Florida. Approximate locations of the wind (blue circle) and wave (red circle) forcing input. The locations of the WRF 1.5 km nest and NDBC buoys also shown. Image generated using Google Earth™. 13

Figure 4: Flow chart depicting wind/wave forecast system. Paths and components shown in red are those being used and evaluated in this study. . 14

Figure 5: The NAM 218 forecast gridded tiles are shown. Outlined in black are the NAM 218 tiles used as initial and boundary conditions for WRF-EMS domains (07, 08, 16, and 17). Image provided by Environmental Modeling Center (EMC) online documentation http://www.emc.ncep.noaa.gov/mmb/research/tiles.218.html). 16

Figure 6: Approximate locations of WRF 4.5 km domain, 1.5 km nest domain and NDBC buoys used for forecast validation. The WRF 4.5 km outer and 1.5 km nested domain approximate locations are shown by semi-transparent boxes. Image generated using Google Earth™. 18

Figure 7: Theoretical equilibrium wave height (Hs - m) based on wind speed, as calculated using equation 7. 26

Figures 8a-b: Tier 3 domain averaged wind speed (ms-1) (a) and averaged wind direction (°) (b) for atmospheric models: NAM 12 km (black), and WRF-EMS (10 km – red dashed, 4.5 km – green dot dash, and 1.5 km – blue dotted) 28

Figures 9a-b: Tier 3 wind speed (ms-1) (a) and wind direction (°) (b) standard deviations as a function of wave domain for atmospheric models: NAM 12 km (black solid), and WRF-EMS (10 km – red dashed, 4.5 km – green dot dash, and 1.5 km – blue dotted) 30

Figure 10: Tier 3 percentage (%) of wind speed forecasts which fall into wind speed bins (every 2.5 ms-1). NAM 12 km (black) and WRF-NAM (10 km – red, 4.5 km – green, 1.5 km – blue). Wind speed standard deviation (seen in Figure 9a) shown by a horizontal red arrow. 31

Figures 11a-b: Theoretical equilibrium wave height (Hs - m) based on wind speed (ms-1) (as seen in Figure 7) and wave height spread (δHs - m) caused by potential wind speed spread (±0.3 ms-1). Figure 11b displays a zoomed in view around the 9 ms-1 threshold. 33

Figures 12a-b: Wave grid wind speed standard deviations (ms-1) for Tier 1 Tropical Storm Fay 19-21 August 2008 (a) and Tier 3 wind event 26 March 2009 (b). 35

Figure 13: Theoretical equilibrium wave height (Hs – m, solid black line) and wave height RMSE (Hs – m, dashed lines) based on wind speed (ms-1, x-axis) and potential wind speed RMSE (1.0 - 5.0 ms-1). 9 ms-1 threshold identified with red dashed line. 36

Figure 14: Tier 3 wind event comparisons between grid 1 average wind speed (ms-1) and average single forcing point wind speed (ms-1). All atmospheric resolutions shown: NAM 12 km (black) and WRF-EMS (10 km - red, 4.5 km - green, and 1.5 km - blue). A one-to-one line and linear best-fit trendlines for each resolution are also displayed. Red circles identify two outliers that will be examined in detail. 37

Figures 15a-b: 48h single point time series wind speed (ms-1) average (a) and standard deviation (ms-1) (b) across all Tier 3 events for atmospheric resolutions: NAM 12 km (solid black), and WRF-EMS (10 km – red dashed, 4.5 km – green dot dash, and 1.5 km – blue dotted) 42

Figures 16a-b: Tropical Storm Fay 00 UTC 20 August 2009 48 h forecast single point time series wind speed average (a, ms-1) and standard deviation (b, ms-1) for atmospheric models: NAM 12 km (solid black), and WRF-EMS (10 km – red dashed, 4.5 km – green dot dash, and 1.5 km – blue dotted) 44

Figure 17: Tier 4 wind speed (ms-1) (left) and direction (°) (right) bias (ms-1), RMSE (ms-1), and scatter index (SI - %) for two 24h forecast periods at buoy 41009: GFS (purple), NAM 12 km (black), and WRF-EMS (10 km – red, 4.5 km – green, 1.5 km – blue) 47

Figure 18: Tier 4 wind speed (ms-1) (left) and direction (°) (right) skill score versus NAM for two 24h forecast periods: GFS (purple) and WRF-EMS (10 km – red, 4.5 km – green, 1.5 km – blue) 48

Figures 19a-b: Wind speed (ms-1, a) and direction (°, b) forecasts for four 24 h periods between 00 UTC 18 January – 00 UTC 22 January 2009 from GFS (purple), NAM 12 km (orange), and WRF-NAM (10 km – red, 4.5 km – green, 1.5 km – blue) compared to buoy 41009 observations. 52

Figures 19c-d: Wind speed (ms-1, top) and direction (°, bottom) forecasts for one 24 h periods between 00 UTC 18 January – 00 UTC 19 January 2009 from GFS (purple), NAM 12 km (orange), WRF-NAM (10 km – red, 4.5 km – green, 1.5 km – blue), and WRF-GFS 10 km (pink) compared to buoy 41009 observations. 53

Figures 20a-b: Wind speed (ms-1, a) and direction (°, b) forecasts for four 24 h periods between 00 UTC 26 March – 00 UTC 30 March 2009 from GFS (purple), NAM 12 km (orange), and WRF-NAM (10 km – red, 4.5 km – green, 1.5 km – blue) compared to observations for buoy 41009. 56

Figures 20c-d: Wind speed (ms-1, c) and direction (°, d) forecasts for one 24 h period between 00 UTC 29 March – 00 UTC 30 March 2009 from GFS (purple), NAM 12 km (orange), WRF-NAM (10 km – red, 4.5 km – green, 1.5 km – blue), and WRF-GFS 10 km (pink) compared to observations for buoy 41009. 57

Figure 21: May and June 2009 bulk validation results (bias (ms-1), RMSE (ms-1), scatter index (SI - %)) for atmospheric models (GFS – purple, NAM – black, WRF-EMS (10 km – red, 4.5 km – green, 1.5 km – blue), and NWS GFE 5 km – brown) at buoy 41009. 59

Figure 22: Tier 1 event Tropical Storm Fay 00 UTC 19 August to 00 UTC 23 August 2008 observed wind speed (ms-1, solid line) and direction (°, dashed line) at buoy 41009. Onshore/offshore direction based on angle of Central Florida coastline (dotted line). 60

Figures 23a-d: NAM 10 m wind (ms-1) forecast for 00 (a), 06 (b), 12 (c), and 18 UTC (d) 20 August 2008. NAM TS Fay location (black star) and actual storm location (red star). 61

Figures 24a-b: Tier 1 event Tropical Storm Fay 00 UTC 19 August to 00 UTC 22 August 2008 observed wind speed (ms-1, a) and direction (°, b) at buoy 41009 (solid black line) compared to forecast hours 0-24 from forecasts initialized at 00 UTC 19, 20, and 21 August. Shown are the NAM (solid orange line), WRF-EMS (10 km – red, 4.5 km – green, 1.5 km – blue), and GFS (solid purple line). 63

Figures 24c-d: Tier 1 event Tropical Storm Fay 00 UTC 20 August to 00 UTC 21 August 2008 observed wind speed (ms-1, c) and direction (°, d) at buoy 41009 (solid black line) compared to forecast hours 0-24 from forecasts initialized at 00 UTC 20 August. Shown are the GFS (purple), NAM 12 km (orange), WRF-NAM (10 km – red, 4.5 km – green,1.5 km – blue), and WRF-GFS 10 km (pink). 64

Figure 25: Tier 1 (Tropical Storm Fay 19 August – 22 August 2008) wind speed (ms-1, left) and direction (°, right) bias (ms-1), RMSE (ms-1), and scatter index (SI - %) for two 48h forecast periods at buoy 41009: GFS (purple), NAM 12 km (black), WRF-NAM (10 km – red, 4.5 km – green, 1.5 km – blue), and WRF-GFS 10 km (pink). 66

Figure 26: Tier 1 (Tropical Storm Fay 19 August – 22 August 2008) skill scores for wind speed (ms-1, left) and direction (°, right) versus NAM for two 48h forecast periods: GFS (purple) , WRF-NAM (10 km - red, 4.5 km - green, and 1.5 km - blue), and WRF-GFS 10 km (pink). 67

Figure 27: Bias (ms-1), RMSE (ms-1), and Scatter Index (SI - %) for all Tier 3 (solid) & 2 (striped) WW3 Significant Wave Height (m, left) and Dominant Wave Period (s, right) forecasts at NDBC buoys 41009, 41113, and 41114 for two 24h periods: 0-24h (black) and 24-48h (turquoise). 70

Figure 28: Observed significant wave height (m, solid black line with filled circles) at buoys 41009 (top), 41113 (middle), and 41114 (bottom) versus WW3 forecasts (maroon) at the buoy locations for 00 UTC 20 August to 00 UTC 22 August 2008. 72

Figure 29: Observed dominant wave period (s, solid black line with filled circles) at buoys 41009 (top), 41113 (middle), and 41114 (bottom) compared to WW3 forecasts (maroon) at the buoy locations for 00 UTC 20 August to 00 UTC 22 August 2008. 73

Figure 30: WW3 Tropical Storm Fay wave forecast statistical results (bias (ms-1, top), RMSE (ms-1, middle), and scatter index (SI - %) (bottom)) for significant wave height (m, left) and dominant wave period (s, right) at buoys 41009, 41113, and 41114 for the first 48 h of the WW3 00 UTC 20 August 2008 forecast cycle(0-24 h – black, 24-48 h – turquoise). . . . 74

Figure 31: Tier 3 GFS wind speed RMSE (ms-1) compared to WW3 significant wave height RMSE (m). R2 correlation = 0.52. Linear trendline (black line). . 76

Figure 32: Bias (ms-1), RMSE (ms-1), and Scatter Index (SI - %) for all Tier 3 CMS-Wave Significant Wave Height (m, left) and Dominant Wave Period (s, right) forecasts at NDBC buoys 41009, 41113, and 41114. Wind forcing: NAM 12 km (black), WRF-EMS (10 km - red, 4.5 km - green, and 1.5 km - blue) 78

Figure 33: Skill score for all Tier 3 CMS-Wave Significant Wave Height (m, left) and Dominant Wave Period (s, right) forecasts at NDBC buoys 41009, 41113, and 41114. Wind forcing: NAM 12 km (black), WRF-EMS (10 km - red, 4.5 km - green, and 1.5 km - blue) 80

Figure 34: Example plot of significant wave height forecast from WW3 for 00 UTC 19 August 2008. Location of buoy 41009, 41113, and the wave input locations for wave domains 1 (C1INP), 2 (C2INP), and 3 (C3INP) are shown (triangles). The approximate location of wave domain 1 (black rectangle) is also shown. 81

Figure 35: Observed significant wave height (m, solid black line with filled circles) at buoys 41009 (top), 41113 (middle), and 41114 (bottom) compared to WW3 (dashed maroon) and differently forced CMS-Wave (GFS – purple, WRF-GFS – pink, NAM – orange, and WRF-NAM (10 km – red, 4.5 km – green, 1.5 km – blue)) forecasts at the buoy locations for 00 UTC 19 August to 00 UTC 21 August 2008. 83

Figure 36: Observed dominant wave period (s, solid black line with filled circles) at buoys 41009 (top), 41113 (middle), and 41114 (bottom) compared to WW3 (dashed maroon) and differently forced CMS-Wave (GFS – purple, WRF-GFS – pink, NAM – orange, and WRF-NAM (10 km – red, 4.5 km – green, 1.5 km – blue)) forecasts at the buoy locations for 00 UTC 19 August to 00 UTC 21 August 2008. 84

Figure 37: Bias (ms-1), RMSE (ms-1), and Scatter Index (SI - %) for Tier 1 (Tropical Storm Fay 20 August 2008) CMS-Wave Significant Wave Height (m, left) and Dominant Wave Period (s, right) forecasts at NDBC buoys 41009, 41113, and 41114. Wind forcing: GFS km (purple), NAM 12 km (black), WRF-EMS (NAM forced) (10 km - red, 4.5 km - green, and 1.5 km - blue), and WRF-EMS (GFS forced) (10 km – pink). 86

Figure 38: Skill score for Tier 1 (Tropical Storm Fay 20 August 2008) CMS-Wave Significant Wave Height (m, left) and Dominant Wave Period (s, right) forecasts at NDBC buoys 41009, 41113, and 41114. Wind forcing: GFS (purple) NAM 12 km (black), WRF-EMS (10 km - red, 4.5 km - green, and 1.5 km - blue) 87

Figures 39a-d: Figure 11a theoretical curves are plotted in Figures 39a, 39b, and 39d. Figures 39a-d all display 48 h averaged data for each Tier 3 wind event valid at buoy 41009. A – GFS forecast wind speed (ms-1, WW3 wind forcing) versus WW3 forecast Hs (m), B – WRF-NAM 10 km forecast wind speed (ms-1, CMS-Wave wind forcing) versus CMS-Wave forecast Hs (m). C - WW3 forecast Hs (m, CMS-Wave wave forcing) versus resulting CMS-Wave forecast Hs (m) (Buoy 41009 – black, 41113 – blue, 41114 – pink). D - Observed wind speed (ms-1) versus observed Hs (m). 90

List of Tables

Table 1: WRF-EMS model physics and dynamics configurations. 10

Table 2: Locations of wind and wave verification buoys used in study. 17

Table 3: Wind data and event Tiers. 19

Table 4: Various statistics used to evaluate coupled forecast system. 20

Table 5: Wind and wave model research matrix. An "X" signifies an area of research. The numbers at bottom of table denote research questions given in section 1. Introduction. 23

Table 6: Approximate number of atmospheric model grid points contained within the wave model domains. 27

Table 7: R^2 correlation values for 48 h grid average versus 48 h single point time series average wind speed. 38

Table 8: Figure 14 outlier case study results. Table presents information on the outlier 48 h forecast chosen events, the forecast model that produced the outlier, the forcing options for the event, 48 h wind forecast averages for the forcing options, and resulting CMS-Wave significant wave height 48 h RMSEs for the differing forcing time series. 39

Table 9: Spatial resolution of the various wind forcing options for the CMS-Wave model, along with the Tiers the data will be evaluated. 45

Table 10: High wind event case studies. 49

Table 11: RMSE (ms^{-1}) for 18 January 2009 24 h wind speed forecasts from GFS, NAM, WRF-NAM, and WRF-GFS. 53

Table 12: RMSE for 18 January 2009 24 h wind speed (ms^{-1}) and direction (°) forecasts from GFS, NAM, WRF-NAM, and WRF-GFS. 57

Table 13: NCEP WW3 validation statistics for 24h forecasts of significant wave height in the Western North Atlantic region between 2002 and 2004. (Results posted at: http://polar.ncep.noaa.gov/waves/valid_wna/bwaves.F024H.png) 71

Table 14: Summarized study results and recommendations for the coupled forecast system (components, models, and resolutions). 95

List of Abbreviations

ARW: Advanced Research WRF

AWIPS: Advanced Weather Interactive Processing System

CIRP: Coastal Inlets Research Program

CMS: Coastal Modeling System

GFE: Graphical Forecast Editor

IFPS: Interactive Forecast Preparation System

NAM: North American Mesoscale Model

NDBC: National Data Buoy Center

NCEP: National Centers for Environmental Prediction

NMM: Non-hydrostatic Mesoscale Model

NWP: Numerical Weather Prediction

NWS: National Weather Service

NWSFO: National Weather Service Forecast Office

SOO/STRC: NWS Science and Operations Officer Science and Training Resource Center

STWAVE: STeady State spectral WAVE

SWAN: Simulating WAves Nearshore

WABED: Wave-Action Balance Equation with Diffraction

WFO: Weather Forecast Office

WMO: World Meteorological Organization

WNA: Western North Atlantic

WRF: Weather Research and Forecasting

WRF-EMS: Weather Research and Forecasting Environmental Modeling System

WRF-GFS: GFS forced WRF

WRF-NAM: NAM forced WRF

WWIII: WAVEWATCH III

Acknowledgements

I must first thank my amazing family. You have always pushed me to be my best, while giving me unwavering love, faith, and support. Aaron…thank you for always being my anchor through all the stormy days. My friends, thank you for helping me grow and experience unforgettable new things over the last three years, I will miss you all.

Thank you to the Melbourne and Miami, FL National Weather Service Forecast Offices, as well as the NOAA CSTAR program, for giving me the opportunity to do research in the field I love.

Dr. Steven Lazarus and Mr. Michael Splitt, I couldn't have asked for better advisors. I wholeheartedly thank you for your untiring encouragement, guidance, dedication, and laughs. I will take everything you've taught me as I make like a baby…and head out.

Dedication

For Aaron.

“You are the strength that keeps me walking.
You are the hope that keeps me trusting.
You are the light to my soul.
You are my purpose...you're everything.”

1. INTRODUCTION

Coastal National Weather Service Forecast Offices (NWSFOs) are responsible for the nearshore ocean within approximately 60 nautical miles from shore, where the majority of human activity occurs. The quality of wind and wave forecasts within this coastal zone are therefore of great importance, not only to mariners and commercial users but to recreational users and local emergency management personnel who patrol and monitor these regions. Concerns within NWS county warning areas center on loss of life and property damage which, in the coastal ocean regions, can result from weather and ocean related events (e.g., erosion and flooding due to storm surge, rogue 'sneaker waves', rip currents, and storm damage to offshore platforms). These concerns constitute a high priority within coastal offices as they result in more fatalities and damage to property than other land-based weather events in these regions (Nicolini and Crawford 2005).

The National Weather Service currently obtains their nearshore wave forecasts from the National Centers for Environmental Prediction (NCEP) global wave model, WAVEWATCH III (WWIII, Tolman 2002g). An example of the full basin WWIII output (not the coastal product) as seen by a forecaster on the Advanced Weather Interactive Processing System (AWIPS) platform is shown in Figure 1. The WWIII is an integral part of operational oceanography in the coastal zone, but even at its relatively high resolution of four minutes (or approximately 7.5 km) it is not fine enough to accurately represent the nearshore wave physics. As a result, coastal

NWSFOs extrapolate (via a Graphical Forecast Editor smart tool, http://140.90.90.253/~applications/STR/generalappinfoout.php3?appnum=1080) WWIII output to the shoreline, and have identified the need for a higher resolution wave modeling system to fill-in the coastal gap (Blumberg et al. 2005). One answer to the need for a wave modeling system is a coupled atmosphere-wave forecast system implemented in the coastal zone.

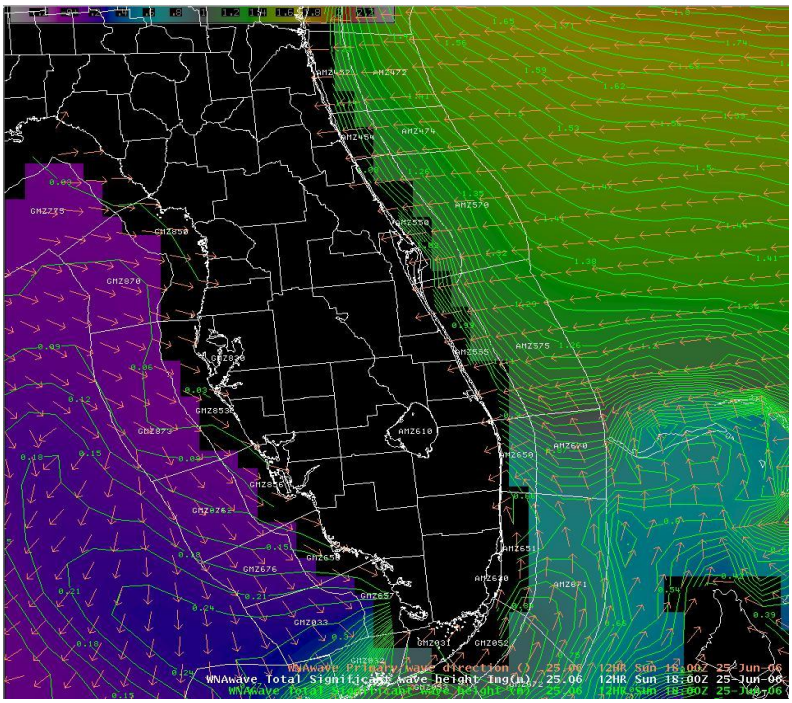

Fig. 1: NOAA WaveWatch III (Western North Atlantic regional wave model) 12 h forecast of primary wave direction (arrows) and significant wave height (m, contours and shading) valid 18 UTC 25 June 2006. Image provided by the Melbourne FL NWS.

Atmosphere-wave coupling has become an important component of wave forecasting during the last few decades as the science of air-sea interaction has demonstrated the benefits of including surface winds in calculating the generation of ocean waves in wave models. Atmosphere-wave coupled systems have been used for research purposes in Europe, Canada, and domestically in the United States (e.g., Janssen and Komen 1984; Clancy et al. 1986; Khandekar and Lalbeharry 1996; Hodur 1997; Janssen et al. 1997; Johnson et al. 1998; Makin and Kudryavtsev 1999; Blumberg et al. 2005; Nicolini and Crawford 2005; Chen et al. 2007). Wind and wave interaction forms the basis for atmosphere-wave coupling, which has been shown to improve the forecasting of both wind and waves by including feedback processes between them. Hodur (1997) demonstrated the viability of a coupled ocean-atmosphere system, as well as its future applications for forecasting, while working on COAMPS, the Naval Research Laboratory's Coupled Ocean/Atmosphere Prediction System. Other studies (e.g., Janssen 1991; Janssen et al. 1997; Makin and Kudryavtsev 1999) have also shown the strong connection between wind and waves. For example, gravity waves in the ocean were shown to extract momentum from the atmosphere (Makin and Kudryavtsev 1999).

For a coastal atmosphere-wave coupled system, the wave model should take into account the complex coastal environment including: varied topography, and irregular coastline features, inlets, etc. Ocean models such as WWIII, however, are designed to solve for deep water wave equations and do not account for

changing topography in finite-depth water where the wave physics differ from that of the deep ocean. Third-generation wave models such as WWIII are based on the energy or action balance equation (Booij et al. 1999) and can have finite-depth effects such as shoaling, refraction, and bottom friction added to them. However, they cannot be applied to coastal areas with horizontal scales (seaward boundary to shoreline) less than 30 km and water depths less than about 30 m without also including the effects of shallow-water on depth-induced wave breaking and triad wave-wave interactions (Booij et al. 1999). These shallow-water effects and nearshore topographic gradients occur on scales smaller than the resolution of many basin scale ocean wave models. The inclusion of shallow-water physics in deep water wave models would necessitate an increase in the horizontal resolution of the model. However, such a horizontal resolution increase applied over a large basin significantly adds computational time. Hence, the coastal zone is typically neglected in the basin scale wave models because of the transitional nature of the nearshore region. In nearshore zones gradients in water depth are larger, nonlinear processes dominate (Cavaleri 2005), and higher resolutions are necessary to properly capture the physical processes. A shallow water wave model is therefore needed to properly account for depth-induced wave breaking, triad wave-wave interactions, wave diffraction, and reflection (Cavaleri 2005, Lin et al. 2006).

The model used here, the CMS-Wave model (formerly known as WABED; Wave-Action Balance Equation and Diffraction), is a 2-D wave spectral

transformation (phased-averaged) model designed for shallow waters (Mase and Kitano 2000; Mase 2001; Mase et al. 2005), which contains approximations for both wave diffraction and reflection – making it suitable for conducting wave simulations at coastal inlets (Lin et al. 2006).

In addition to shallow water wave physics, an important consideration when choosing a wave model for a coastal zone coupled forecast system is the wind input, which in part, governs the evolution of the wave spectrum (Makin and Kudryavtsev 1999). Since wave models incorporate surface winds to force the generation and propagation of waves within the model domain, the accuracy of these winds is crucial. Studies have shown how errors in the wave forecast derive from inaccuracies in the wind field forcing (Janssen and Komen 1984; Clancy et al. 1986; Janssen et al. 1997; Ris et al. 1999). In an attempt to increase the accuracy of the forecast surface winds, several studies have shown the benefit of increasing horizontal resolution in an atmospheric model (Hodur 1997; Janssen et al. 1997; Dong and Oey 2005; Nicolini and Crawford 2005; Hsu et al. 2006). A recent study by Nicolini and Crawford (2005) evaluated the impact of high-resolution wave models for applications at the National Weather Service and NOAA. Just as high-resolution forecast grids in the coastal zone are better able to resolve water depth and coastline variations in the wave model, a high resolution atmospheric model can better resolve the coastal mesoscale variability, e.g., sea-breeze, coastal showers, tropical cyclones, etc.

The goals of this project are to develop and evaluate a high-resolution atmosphere-wave coupled nearshore forecasting system for the National Weather Service. The system is designed to provide nearshore wave information in the void between the coastline and WWIII domain (e.g., Fig. 1). Output from the coupled forecast system is used, in part, to populate the NWS Interactive Forecast Preparation System (IFPS) grids with high-resolution wave forecasts (e.g., significant wave height, dominant wave period and wave direction) for the nearshore region. The atmospheric component of this study includes a packaged version of the Weather Research and Forecasting (WRF) model (http://strc.comet.ucar.edu/wrf/index.htm) known as the WRF Environmental Modeling System (EMS). The WRF-EMS (herein referred to as the WRF) was developed for the NWS by the NWS Science and Operations Officer (SOO) Science and Training Resource Center (STRC) (http://strc.comet.ucar.edu/wrf/wrfems_userguide.htm) and is currently being used by several Weather Forecast Offices (WFOs). The WRF is used to provide the high-resolution (1.5, 4.5 and 10 km grid spacing) 10 m wind to drive the Florida Tech Coastal Modeling System (CMS-Wave) and flow models. The boundary conditions for the CMS-Wave model are provided by WWIII output. System evaluation includes key operational aspects -- especially the balance between resolution and computation time. As a result, various atmosphere and wave model

configurations are tested in an effort to provide a high-quality yet computationally efficient wave forecast for the coastal region.

The forecasts produced by the coupled system are evaluated by direct comparison with coastal buoy observations, described in the methods section. This analysis includes factors such as wind direction (onshore vs. offshore flow), and significant wind events (e.g., Tropical Storm Fay in August 2008). Analysis topics for this study are:

1. Atmospheric model component options
    a. Variability of wind within forecast zones
    b. Quality of the atmospheric model wind forcing options for the wave model
    c. Validation of wind forecasts
2. Wave model component
    a. Quality of wave forcing for the wave model
    b. Impact of varying atmospheric model input on wave forecasts
    c. Validation of wave forecasts

A more detailed summary of analysis areas and techniques will be shown in the results section (Table 5). A series of research questions, designed to evaluate the forecast system, are listed below.

Research questions:

1. What is the forecasted wind variability within the wave forecast domain?
2. How does atmospheric model resolution impact the wind variability?
3. How good are the wind forecasts? / What is the quality of the wave model wind forcing?
4. What is the quality of the wave model wave boundary forcing?
5. Does atmospheric model resolution matter, in terms of wind forcing?
6. Does the wave model perform differently for onshore versus offshore winds?
7. How well does the wave model perform for high wind events (10 m wind speed > 9m/s)?

The work presented herein is structured to directly address these seven questions with the results to be used to form the basis of recommendations regarding the operational configuration of the forecast system at the NWS offices in Melbourne and Miami, FL.

2. METHODOLOGY

2.1: The Atmospheric Model

As mentioned previously, wind input from a high-resolution atmospheric model is one of two forcings used to drive the wave model. The effect of model resolution on the wind forcing of wave forecasts is addressed, by examining a number of different model configurations and options, which include three WRF resolutions (10 km, 4.5 km, and 1.5 km). The WRF is the main component of this study as it is the high-resolution atmospheric model to be tested, but other options to force the wave model are also investigated (e.g., 12 km resolution North American Mesoscale Model (NAM) 218, Global Forecast System (GFS), and 5 km NWS Graphical Forecast Editor (GFE) winds).

The NWS WRF is a complete, full-physics, numerical weather prediction (NWP) software package that incorporates dynamical cores from both the National Center for Atmospheric Research (NCAR) Advanced Research WRF (ARW) and the National Center for Environmental Predictions' (NCEP) Non-hydrostatic Mesoscale Model (NMM-WRF) into a single end-to-end forecasting system (http://strc.comet.ucar.edu/wrf/wrfems_userguide.htm). The WRF version 2.1.2.2e with the ARW core is used in this study with the following configuration options shown in Table 1 below.

The configurations of the WRF that are used herein to force the wave model includes a high resolution domain that consists of a 4.5 km outer domain and a

nested 1.5 km inner domain (Figure 2). One-way coupling is setup in which the 4.5 km outer domain provides the boundary conditions for the 1.5 km nest. Hourly initial and boundary conditions for the WRF 4.5 outer domain are provided by the 12 km NAM 218 or GFS forecast grids which, as mentioned before, will also be used to force the wave model for the resolution sensitivity tests. Specifics on the NAM 218 data, as well as GFS and NWS GFE winds, used to force the WRF are described in the data section.

Table 1. WRF-EMS model physics and dynamics configurations.

WRF Model Configurations	
Model Physics	
Cumulus Parameterization	Turned off because of high resolution dx
Microphysics scheme	Lin et al. scheme, for high resolution dx
Planetary Boundary Layer	Yonsei University scheme
Land Surface	Noah Land Surface Model
Surface Layer	MM5 similarity
Long Wave Radiation	RRTM scheme
Short Wave Radiation	Dudhia scheme
Model Dynamics	
Time-integration scheme	Runge-Kutta 3rd Order
Diffusion option	Simple diffusion
Eddy coefficient option	Horizontal Smagorinsky First Order Closure
Upper-level Damping	No damping
Vertical Velocity Damping	Yes

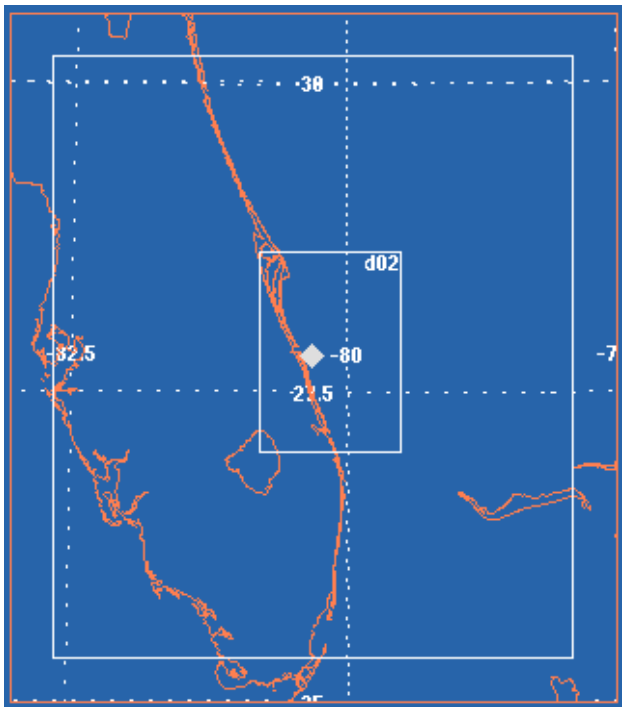

Fig. 2: Locations of WRF-EMS 4.5 km, 1.5 km nest and 10 km domains. The WRF-EMS 10 km domain is in the same location as the WRF-EMS 4.5 km domain.

A lower resolution (10 km) WRF configuration, seen in Figure 2, with the same physics as the WRF 4.5 km is also constructed. The WRF 10 km, which does not have a nest, has the same outer domain size as that of WRF 4.5 km and is also forced by the NAM 218 or GFS. Running on the 00 UTC cycle NAM or GFS forecast, all three of the WRF domains (10 km, 4.5 km, 1.5 km) execute daily on an 8 node cluster. 10 m winds from both simulations are used to force CMS-Wave. Wave model performance is then evaluated via comparison to buoy and satellite observations. All input and output data are processed automatically using scripts which are discussed later in the data discussion section. The impact of forcing the

wave model with the different WRF configurations, as well as the NAM 218, GFS, and NWS GFE, is presented in the results section.

2.2: The Wave Model

CMS-Wave (formerly known as WABED) is one of the components of the Coastal Inlets Research Program's (CIRP's) Coastal Modeling System (CMS) (CMS, Buttolph et al. 2006). The **W**ave-**A**ction **B**alance **E**quation with **D**iffraction (WABED) model is a wave model developed for the U.S. Army Engineering Research and Development Center (ERDC) for convenient coupling with 2 and 3-dimension hydrodynamic models designed for high resolution predictions in coastal waters (Mase and Kitano 2000; Mase et al., 2005). CMS-Wave/WABED is a 2-D wave spectral transformation (phase-averaged) model, which means it neglects changes in the wave phase while calculating wave and other nearshore processes (Lin et al. 2006). Designed for nearshore regions, CMS-Wave is ideal for this study as the wave diffraction scheme in WABED is more robust compared to schemes included in other nearshore wave models like SWAN or STWAVE (Mase and Kitano 2000; Mase et al., 2005). For this study, CMS-Wave is setup with five high resolution (100 m) grids approximately 50 x 50 km, oriented parallel to the coastline from Playlinda Beach, FL just north of Cape Canaveral south to Jupiter, FL (e.g., Fig. 3). The wave grids cover an area that lies, for the most part, within the WRF 1.5 km nest. CMS-Wave is forced by two time series inputs: boundary wave conditions from WAVEWATCH III (WW3) and wind forcing. The wind forcing can be obtained from

WRF or from the NAM, GFS, GFE, etc. Each of the five wave grids are driven by an independent time series at three hourly resolutions and are run out 48 hours.

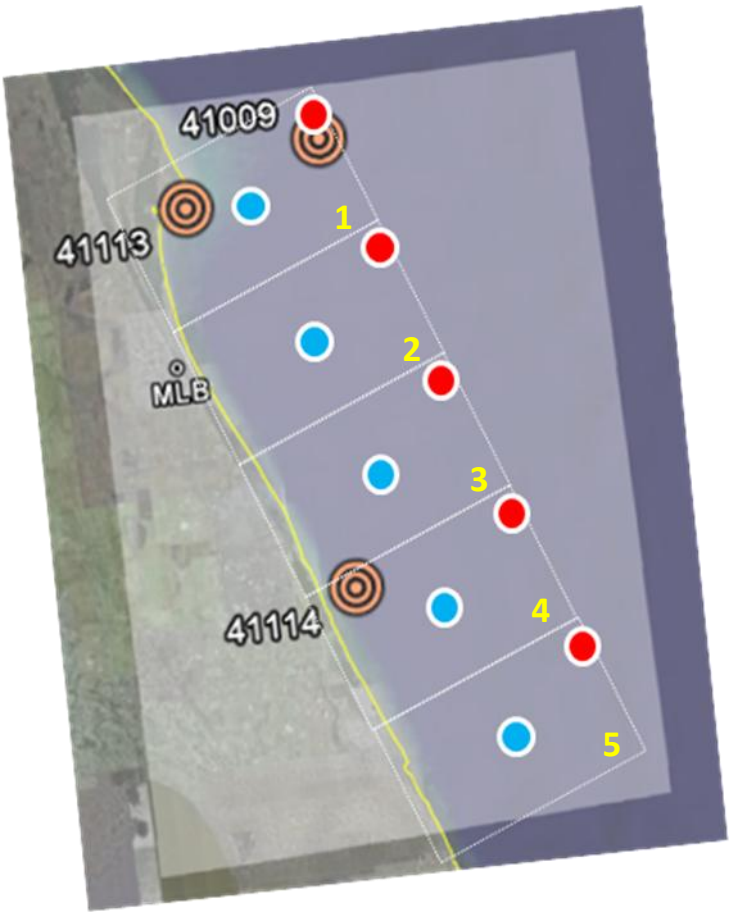

Fig. 3: Locations of five CMS-Wave grids (boundaries in white and grid number in yellow) along the coastal study area of Eastern Central Florida. Approximate locations of the wind (blue circle) and wave (red circle) forcing input. The locations of the WRF 1.5 km nest and NDBC buoys also shown. Image generated using Google Earth™.

2.3: Atmosphere/Wave Model Coupling

This study focuses on the components highlighted in red as shown in Figure 4 but will also include other atmospheric model options for testing (i.e., GFS and NWS generated GFE). The NAM 218 or GFS provide the initial and lateral boundary

conditions for the WRF simulations. The WRF (or other wind forcing option) 10 m winds and WWIII wave fields are then used to force CMS-Wave. With the exception of the WRF (which comes with its own scripts) the one-way coupled system is driven by scripts and code developed explicitly for this study. Figure 4 also shows a flow model (M2D) which is not tested in this study but will be a future addition to the forecast system.

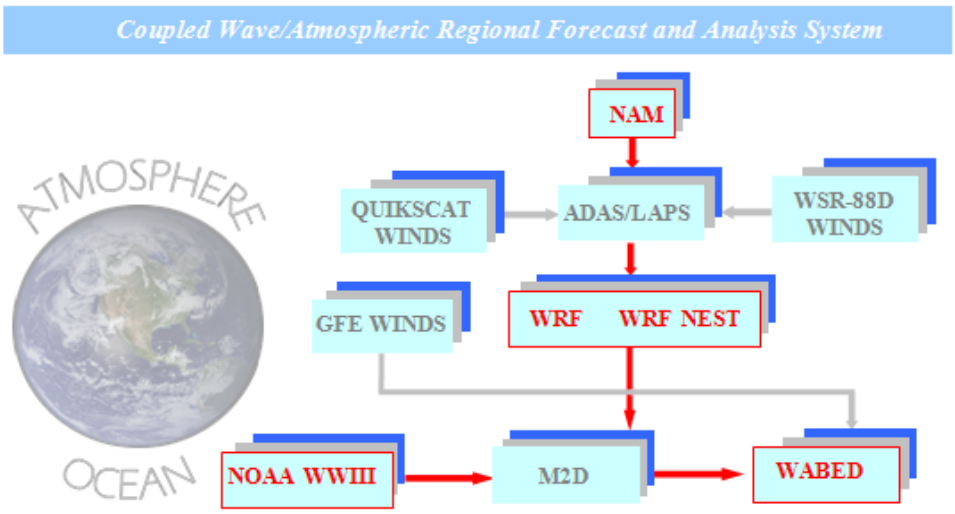

Fig. 4: Flow chart depicting wind/wave forecast system. Paths and components shown in red are those being used and evaluated in this study.

2.4: Data

The model output and observation data used to compare, validate, and test the forecast system is described in the following subsections.

2.4.1: Model Forcing and Output

The forecast grids used to force the WRF is comprised of four NAM 218 tiles (shown in Figure 5) or the 0.5° GFS grid which provide the initial conditions and three-hourly boundary conditions. Prior to initiation of a WRF run the NAM 218 forecast tiles are automatically downloaded from the National Centers for Environmental Prediction/Environmental Modeling Center (NCEP/EMC) server (ftp://ftpprd.ncep.noaa.gov/pub/data/nccf/com/nam/prod/nam.YYYYMMDD). The NAM model data are archived and used as an alternative wind forcing for the CMS-Wave. The GFS 0.5° is also obtained from the NCEP server (ftp://ftpprd.ncep.noaa.gov/pub/data/nccf/com/gfs/prod/gfs.YYYYMMDDFH) for WRF forcing, as well as another option for wind forcing for the wave model. The WW3 uses the GFS as its wind forcing; therefore the GFS was also obtained by extraction from the WW3 forecast output. NWS generated GFE (Graphical Forecast Editor) data is obtained from the local NWSFO in Melbourne, FL. The data is posted nightly by the office for download, archival, and use as wave model wind forcing. Data processing scripts extract the forecast data from each dataset obtained at user

specified locations (e.g., buoys) within the model domains (Fig. 6) and compared to observations.

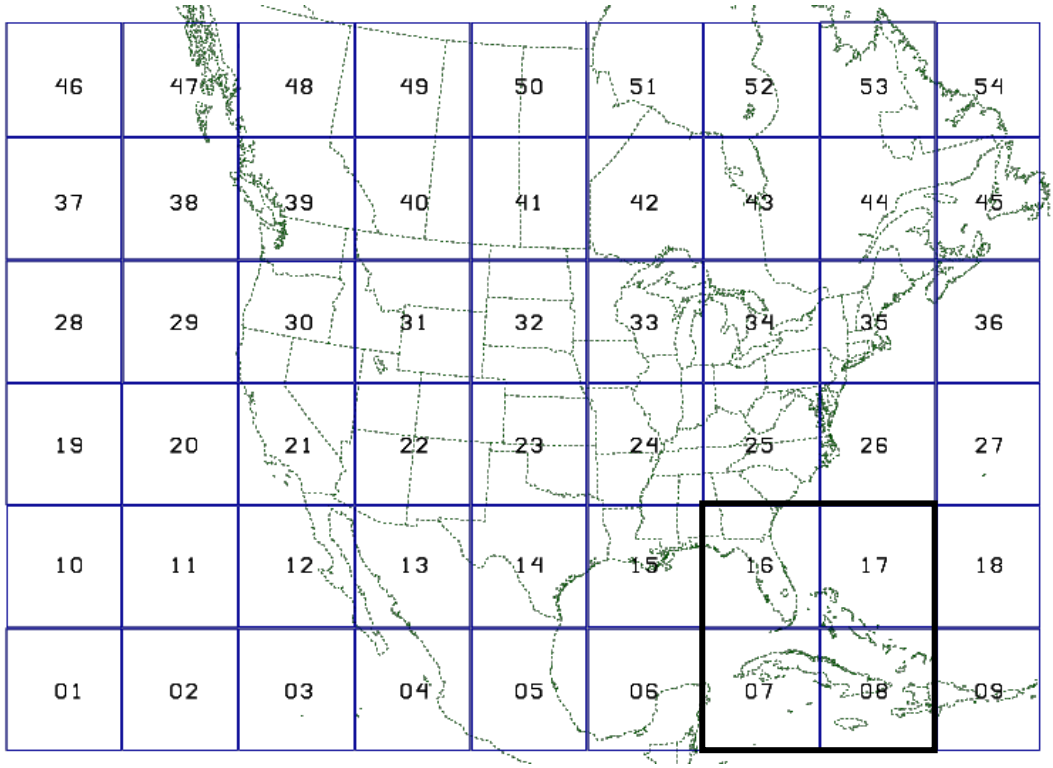

Fig. 5: The NAM 218 forecast gridded tiles are shown. Outlined in black are the NAM 218 tiles used as initial and boundary conditions for WRF-EMS domains (07, 08, 16, and 17). Image provided by Environmental Modeling Center (EMC) online documentation (http://www.emc.ncep.noaa.gov/mmb/research/tiles.218.html).

2.4.2: Verification Data

Quality controlled buoy data is retrieved from the National Data Buoy Center (NDBC) server for the buoys shown in Figure 6. If the anemometer on the buoy is not at the World Meteorological Organization (WMO) standard 10 m, the data is adjusted using the Power Law Method (Hsu et al. 1994),

$$u_2 = u_1 \left(z_2/z_1\right)^p, \qquad (1)$$

where u_1 is the observed value, u_2 is the adjusted value to the 10 m height, z_1 is the anemometer height, z_2 is the standard height of 10 m, and the exponent P is taken to be 0.11. The value for P, the power-law wind-profile exponent for near-neutral stability conditions, has been empirically determined to be applicable over the ocean (Hsu et al. 1994). Missing NDBC buoy observation data is delineated by a "-99.00" in the data files after being collected and before being used for analysis. Data from four buoys (Table 2) are available over the WRF domains (Fig. 2). Table 2 also provides information regarding what data are available at each of the buoys.

Table 2. Locations of wind and wave verification buoys used in study.

Verification Data Buoys	
10 m Wind Speed and	**Significant Wave Height, Dominant Wave Period, and**
41009	41009
41010	41113
	41114

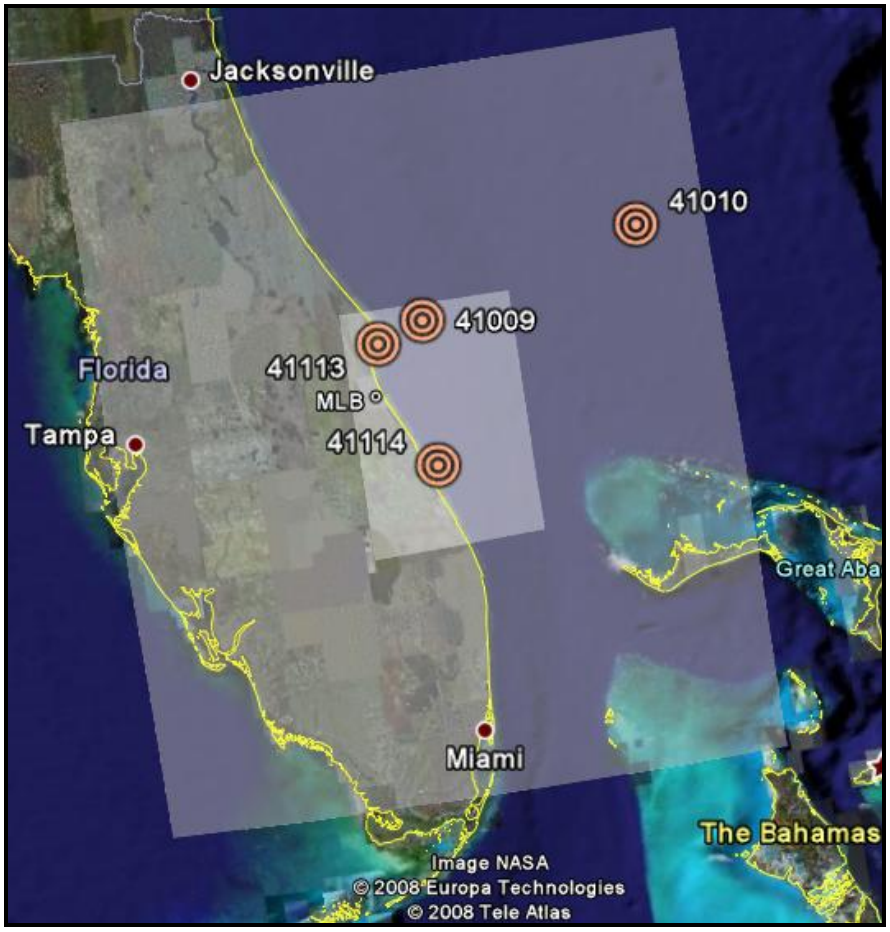

Fig. 6: Approximate locations of WRF 4.5 km domain, 1.5 km nest domain and NDBC buoys used for forecast validation. The WRF 4.5 km outer and 1.5 km nested domain approximate locations are shown by semi-transparent boxes. Image generated using Google Earth™.

2.4.3: Data Tiers and Wind Events

The data are subdivided into Tiers and as described in Table 3, based on wind events that span August 2008 to March 2009. A nine m/s (approximately 20 mph) 10 m wind speed threshold is chosen based on the NWS definition of "windy" (http://www.weather.gov/glossary/index.php?word=windy), which are wind speeds 20 to 30 mph. In an effort to gauge the performance of the wind/wave

system, error statistics are calculated and stratified by the wind Tiers with results presented in section 3. Results.

Table 3. Wind data and event Tiers.

Tier	Wind Speed Thresholds
4	All
3	Wind events (12 consecutive hours > 9 m/s)
2	Same as Tier 3 + total 48 hour forecast period wind speed average > 9 m/s
1	Tropical Cyclone events *

*Only one event, therefore will not be statistically robust

2.5: Statistical Analysis

Previous studies, involving either coupled atmosphere-wave models or wave models only, have utilized NDBC buoy observations for validation of both atmospheric and wave model output (Clancy et al. 1986; WAMDI Group 1988; Khandekar and Lalbeharry 1996; Janssen et al. 1997; Hsu et al. 2006). This section describes the statistics used to compare wind and wave model output with coastal NDBC buoy observations.

Common statistical quantities used in previous studies to validate model forecasts include root-mean-square-error (RMSE) (Clancy et al. 1986; Khandekar and Lalbeharry 1996; Tracy and Cialone 2004), mean error (bias) (Janssen et al. 1984; Khandekar and Lalbeharry 1996; Janssen et al. 1997; Tracy and Cialone 2004), standard deviation (Janssen et al. 1984; Janssen et al. 1997), skill score and correlation (Hsu et al. 2006; Tracy and Cialone 2004), and the scatter index (Janssen

et al. 1984; Clancy et al. 1986; Zambreski 1989, 1991; Romeiser 1993; Komen et al. 1994; Janssen et al. 1997; Ris et al. 1999; Tracy and Cialone 2004). Statistics used in evaluating the coupled forecast system and a description of each metric are included in Table 4.

The statistical quantities employed in this study include the following: RMSE, bias, standard deviation, skill score, and the scatter index (SI). The scatter index (SI) is a standard parameter for intercomparing wave model output (Clancy et al. 1986) but can also be used with atmospheric model output. Lower values of the SI reflect either a reduction in the scatter of the forecast error and/or an increase in the average observed variable (i.e., wind speed or wave height). The scatter index is a way of normalizing model error to account for larger forecast errors that are typically associated with higher wind speeds or significant wave heights. In the context of significant wave height, reports of the scatter index (SI) in the literature range between 20% for hindcasts with sophisticated models and high quality wind forcing fields to 60% for some operational forecasts with less accurate wind forcing (Janssen and Komen 1984; Clancy et al. 1986). The scatter index, along with bias, RMSE, standard deviation, correlation, and skill score will be used to gauge both the quality of the wave model and the 10 m wind forecasts. The following results sections will employ the statistical techniques as part of the system evaluation.

Table 4. Various statistics used to evaluate coupled forecast system.

Statistic		Description of Equation
Bias: $\frac{\sum E}{N}$	(2)	The average error where E is error (predicted X – observed Y) and N is the total number of E values. The bias will indicate if the model is over- or under-forecasting a particular variable.
Root-mean square error (RMS_{error}): $\sqrt{\frac{1}{N}\sum_{N}(X_n - Y_n)^2}$ also $RMS_{error} = (MSE_s + MSE_u)^{1/2}$	(3)	The RMS_{error} is a measure of the absolute difference between values predicted by a model and those observed. It is a good measure of accuracy. X_n is the predicted value and Y_n is the observed value.
Standard deviation $\sigma = \sqrt{\frac{1}{N}\sum_{i=1}^{n}(X_i - \bar{X})^2}$	(4)	The measure of the dispersion or spread within a data set.
Skill Score: $SKILL = \frac{\sum_i \lvert FC_i - O_i \rvert - \sum_i \lvert F_i - O_i \rvert}{\sum_i \lvert FC_i - O_i \rvert}$	(5)	The skill of a model compared to a control (i.e., another model). FC_i is the forecast using a control, F_i is the forecast value, and O_i is the observed value. Values will range from -∞ to 1; a positive value indicating the model is more accurate than the control and an errorless forecast would be a skill score
Scatter Index (SI): $SI = \frac{average\ obs}{standard\ deviation\ of\ errors} \times 100\%$	(6)	The ratio between the average observations for a forecast period and the standard deviation of the forecast errors for that same period.

3. RESULTS

The following sections are a detailed evaluation of the coupled atmosphere-wave forecast system, which addresses the key questions raised in the introduction. Table 5 outlines the evaluation of the forecast system in terms of system component, validation technique, and research question. The results section is broken into five main subsections (seen in the evaluation row in Table 5) which will be evaluated in the following ways:

1. Atmospheric model resolution – the impact of increased horizontal model resolution on the quality of the wind forecast and resulting wave forecasts from differing resolution wind forcing.

2. Wave model domains – Wind variability and the proper number of separate wave domains.

3. NDBC buoys – Validation of both wind and wave forecasts within the study area.

Table 5. Wind and wave model research matrix. An "X" signifies an area of research. The numbers at bottom of table denote research questions given in section 1. Introduction.

Forecast System Component (Options) >		**Atmospheric Model (Weather Research and Forecasting (WRF), North American Mesoscale Model (NAM), GFS, & NWS GFE)**		**Wave Model (WWIII & CMS-Wave)**	
Evaluation >		**Wind Variability**	**Wind Forecast / Forcing**	**Wave Forcing**	**Wave Forecast & Impact of Varying Wind Forcing**
Validation and Analysis	**Atmospheric Model Resolution**	X	X		X
	Wave Model Domains	X			
	NDBC Buoys		X	X	X
Research Question #'s		1,2	3	4	5,6,7

3.1: Atmospheric Models

Output from three atmospheric models (NAM 218, WRF, and GFS) and the NWS generated GFE, were each used as the wind forcing for the CMS-Wave model. The next two subsections (a - Wind Variability and b - Wind Forecast/Forcing) will discuss the wind component options in terms of their variability in forecast winds over the wave model domains and the quality of their forecasts. The NAM forced

WRF will herein be referred to as the WRF-NAM and the GFS forced WRF will be the WRF-GFS.

3.1.1: Wind Variability

The impact of the single point wind forcing approach is addressed here by evaluating the variability of the spatially varying forecast wind field across the five wave grids. The key issues are whether or not the wave subdomains are small enough such that wind variability within them is minimal and therefore, whether a single point time series is representative of the forecast area covering the specific wave domains. In an attempt to determine whether or not the single point time series is representative of winds over the entire subdomain it is compared to the domain average. Given the computational expense of running a high resolution atmospheric model, an effort is also made to discern how the wind variability changes with increasing atmospheric model resolution.

3.1.1.1: Theoretical Wave Height Variability

In order to better quantify the variability in the forecast winds, it is instructive to consider the equilibrium significant wave height and its sensitivity with respect to the wind field. The functional dependence of significant wave height (H_s) on the wind speed (U_{10}), for equilibrium conditions, is given by Janssen et al. (1997).

$$H_s = \beta U_{10}^2/g \qquad (7)$$

Where β is a constant (β = 0.22) and g is acceleration of gravity ($g = 9.81 ms^{-1}$). Eq. 7 is used to generate a graph of the equilibrium significant wave height for a range of wind speeds ranging from 0 to 15 ms^{-1} (Fig. 7). Equation 7 can be used to derive an equation (Eq. 8) representing the change in the wave height (δH_s) caused by wind speed variability, bias, or error (δU_{10}) by taking the derivative of equation 7 in terms of U_{10}.

$$\delta H_s = 2\beta U_{10} \delta U_{10}/g \qquad (8)$$

For example, by knowing the standard deviation of the wind speed, an equilibrium wave height standard deviation can be determined using Equation 8. The utility of Equation 8 is that it provides an approximation regarding what might be expected in terms of wave height forecasts with respect to wind speed variability or error. The equilibrium wave height and wave height standard deviation is used in this study to gauge whether the domain-to-domain variability is significant and if so, how it impacts the wave forecasts. Figure 7 displays the resulting curve using equation 7; showing increased wave heights with increasing wind speed.

With a value for the forecast wind speed standard deviation it is then possible to use equation 8 to add lines to Figure 7 which represent the expected standard deviation in significant wave height according to input wind speed standard deviation. In the next section (Forecast wind variability) the atmospheric

model forecast variability is examined and the observed wind speed spread is used to determine the theoretical equilibrium wave height variability.

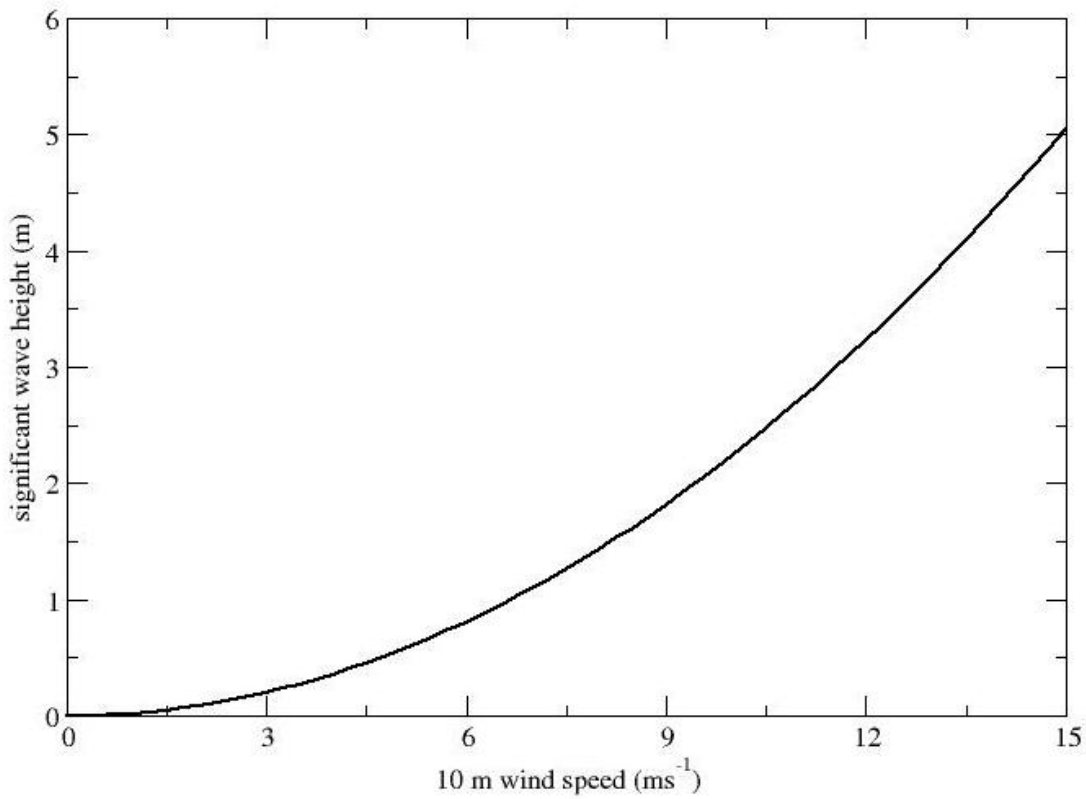

Fig. 7: Theoretical equilibrium wave height (H_s - m) based on wind speed, as calculated using equation 7.

3.1.1.2: Forecast Wind Subdomain Variability and Impact on Wave Forecasts

Table 6 lists the number of atmospheric model grid points contained within each of the five wave domains. Only grid points over water (LANDMASK = 0) were considered here since the study focuses on winds over the coastal region. For each Tier 3 event, model (NAM, WRF-NAM) grid points (Table 6) are used to produce a

single 48 h mean wind and standard deviation for each wave domain. Temporal variations in wind are not considered. The mean and standard deviation are then averaged across all Tier 3 forecasts for each wave domain and for both wind speed and direction. The mean wind speed and wind direction for all 67 wind events (Tier 3), in terms of wave domain and atmospheric model resolution, are shown in Figures 8a and 8b. The largest spread in wind speed across the five wave domains occurs in the NAM model which has a 0.8 ms^{-1} difference between domains 1 and 2. Within any of the wave domains there is a 0.2 ms^{-1} spread in the mean wind and at most a 1° spread in average wind direction between the various WRF resolutions for the Tier 3 events. For a given WRF resolution, the difference in the mean winds across the domains is even smaller (less than 0.1 ms^{-1}).

Table 6. Approximate number of atmospheric model grid points contained within the wave model domains.

Wave Grid	NAM 12	WRF 10	WRF 4.5	WRF 1.5
1	49	64	306	1485
2	49	56	208	1716
3	49	56	224	1886
4	49	42	195	1640
5	49	49	182	840

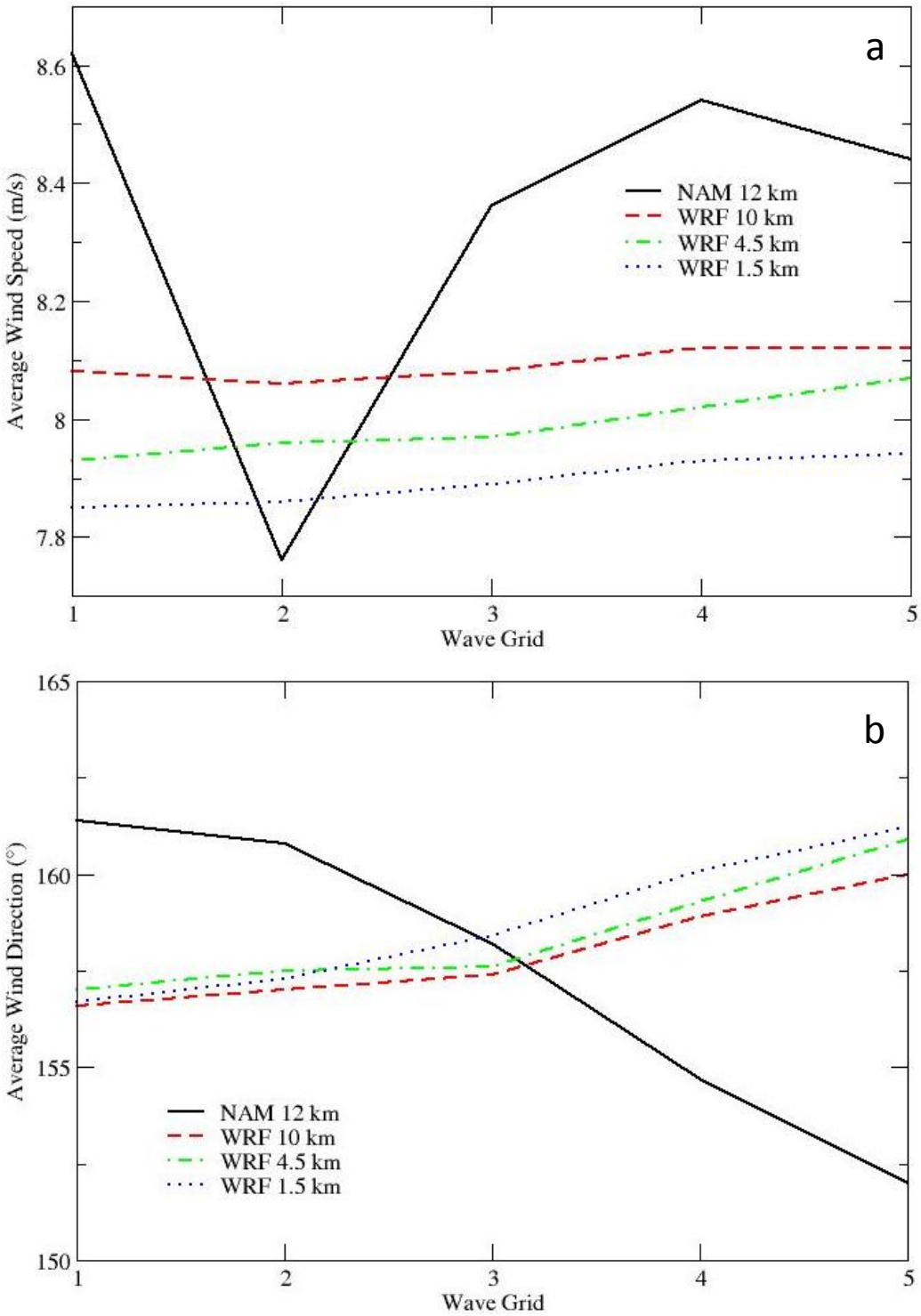

Figs. 8a-b: Tier 3 domain averaged wind speed (ms^{-1}) (a) and averaged wind direction (°) (b) for atmospheric models: NAM 12 km (black), and WRF-EMS (10 km – red dashed, 4.5 km – green dot dash, and 1.5 km – blue dotted)

Similar to Figures 8a and 8b, Figures 9a and 9b shows the standard deviation of wind speed and direction within each wave domain for all Tier 3 wind events. The standard deviations are too large to be plotted as error bars in Figures 8a and 8b without obscuring the details of the average wind speeds and directions. The 12 km NAM exhibits less wind speed variability (Fig. 9a) but greater wind direction variability (Fig. 9b) than all WRF-NAM resolutions, which have domain average wind speed standard deviations between 2.6 and 2.7 ms^{-1} and wind direction standard deviations between 68° and 71°. The variation between the three WRF resolutions is small both within and across the wave domains, which suggests that a change in the WRF horizontal resolution does not significantly impact the intradomain wind variability.

Another way at displaying the variation in forecast wind speed is in terms of wind speed bins. Figure 10 displays the percentage of Tier 3 NAM and WRF-NAM wind speed forecasts that are within a particular wind speed bin (every 2.5 ms^{-1}). The majority of Tier 3 forecast winds fall in three wind speed bins between 5.0 and 12.5 ms^{-1}, which is approximately the ±2.6 ms^{-1} standard deviation shown in Figure 9a (indicated in Figure 10 with a horizontal red arrow).

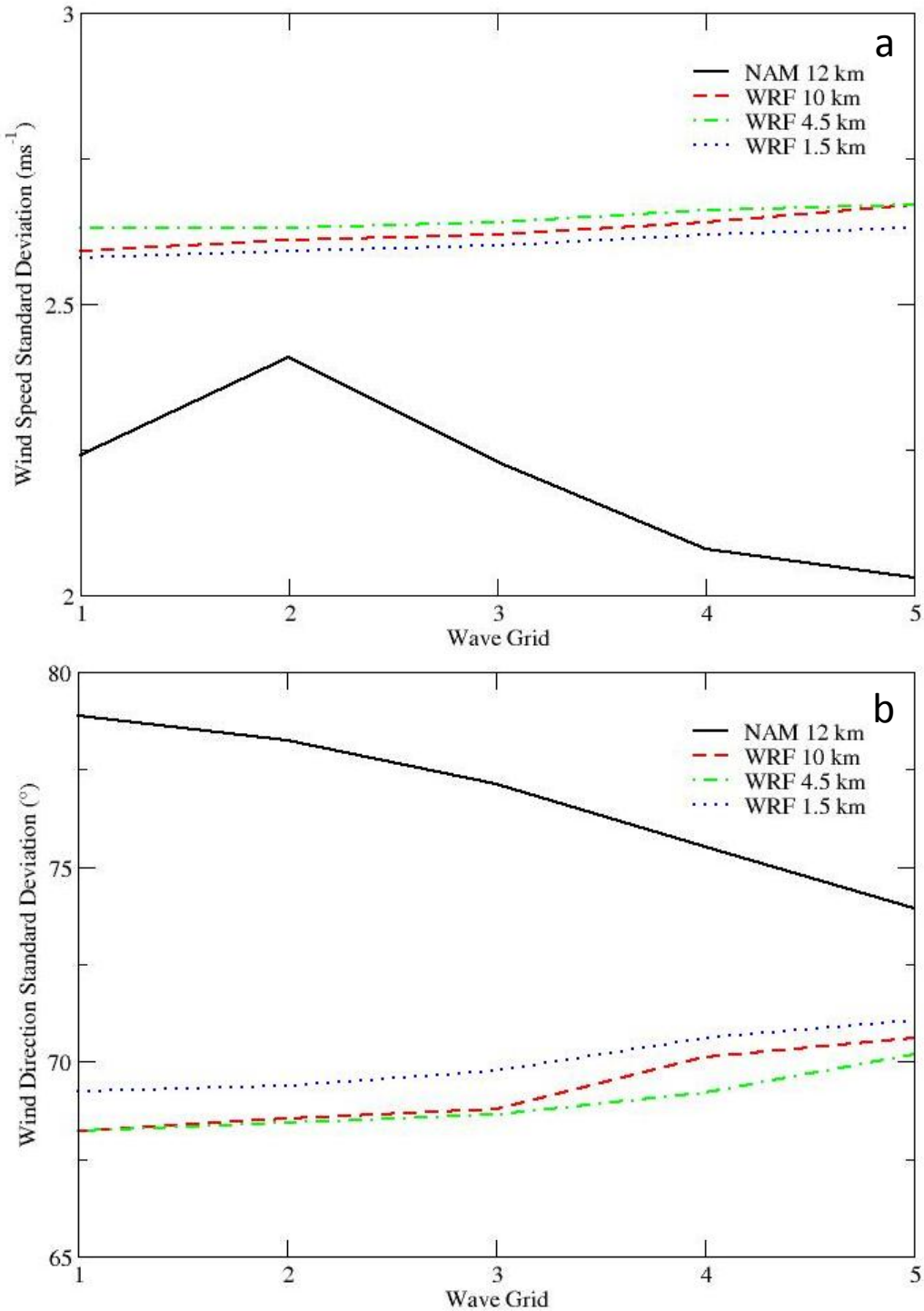

Figs. 9a-b: Tier 3 wind speed (ms^{-1}) (a) and wind direction (°) (b) standard deviations as a function of wave domain for atmospheric models: NAM 12 km (black solid), and WRF-EMS (10 km – red dashed, 4.5 km – green dot dash, and 1.5 km – blue dotted)

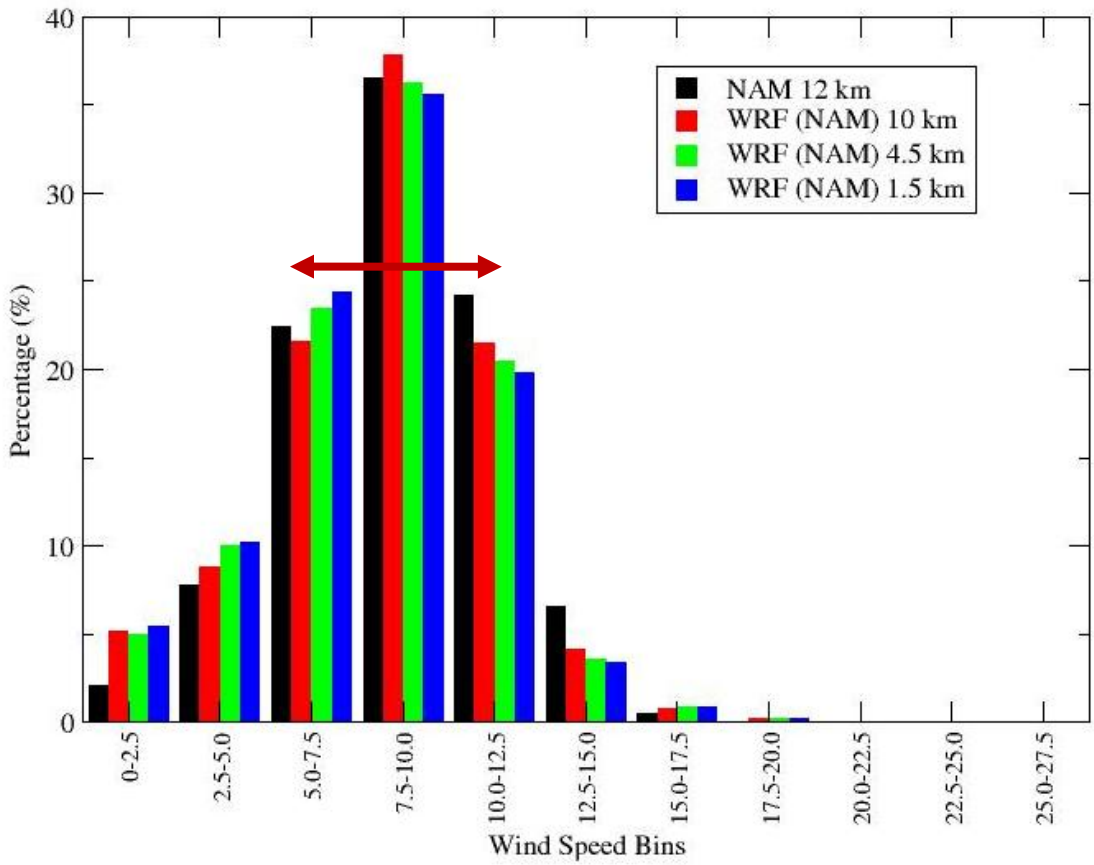

Fig. 10: Tier 3 percentage (%) of wind speed forecasts which fall into wind speed bins (every 2.5 ms^{-1}). NAM 12 km (black) and WRF-NAM (10 km – red, 4.5 km – green, 1.5 km – blue). Wind speed standard deviation (seen in Figure 9a) shown by a horizontal red arrow.

A wind speed standard deviation on the order of ±2.6 ms^{-1} for each of the wave domains may be significant over the coastal zone and may have an important influence on both the spread of wave heights that could be forecast and potential error in those predictions. The relationship between wind speed spread and wave height spread is now examined.

The intradomain standard deviation in wind speed observed in the WRF (approximately ±2.6 ms^{-1} in Figure 9a) is now used in Equation 8 to arrive at an

estimate for the significant wave height standard deviation and added to Figure 7. Similar to Figure 7, Figure 11a now includes the variability in wave height (positive and negative) that would be expected because of both the positive and negative standard deviation in the wind speed forecast within the domains. Figure 11b displays the same graph zoomed in to see the wave height variability that would be expected around an average wind speed value of 9 ms^{-1}, which is the value that was used to define the Tier 3 wind events. The theoretical spread in forecast wave height with a value of 9.0 ms^{-1} and a wind speed standard deviation of ±2.6 ms^{-1} would be approximately 2.0 m. A standard deviation of 2.0 m (or 6.5 ft) in the wave model is a significant value, especially considering the standard deviation will grow with increasing wind speed to approximately 4.0 m (or 13 ft) with winds speeds of 15 ms^{-1} (Fig. 11a). Figures 12a and 12b display the wave grid wind speed standard deviations for two events: Tier 1 Tropical Storm Fay (a) and Tier 3 26 March 2009 (b). Wind speed standard deviations during Tropical Storm Fay are as high as 4.0 ms^{-1} (see Figure 12a), which would produce a wave height standard deviation of approximately 3.5 m (using equation 8), nearly twice the Tier 3 wind event average wave height standard deviation. Similar to Tier 3 data seen in Figure 9a, compared to the WRF-NAM the NAM has lower wind speed standard deviations in all five wave domains during Tropical Storm Fay (Fig. 12a). Also, the WRF-NAM exhibits low variations in wind speed standard deviation across both resolution and wave domains.

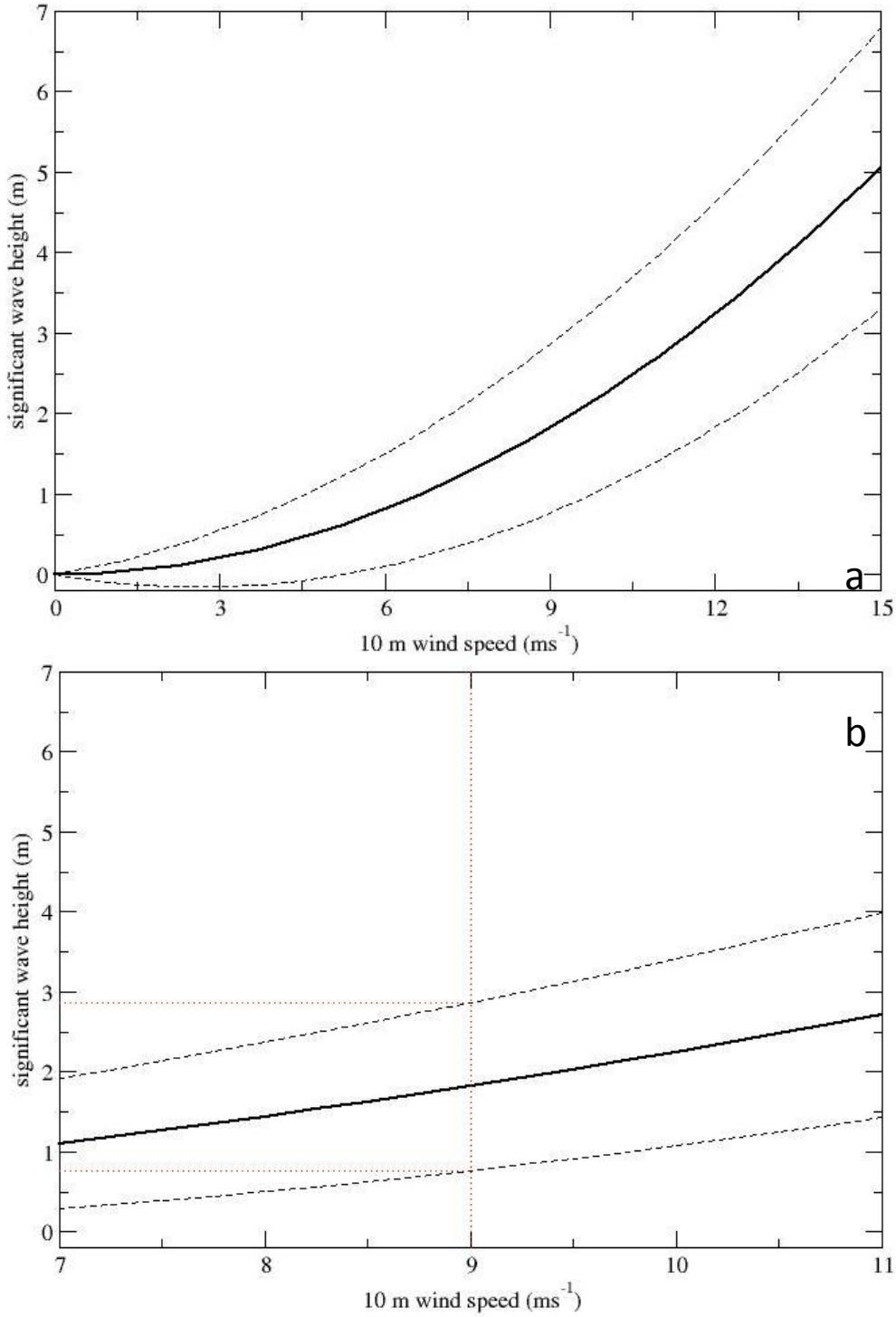

Figs. 11a-b: Theoretical equilibrium wave height (H_s - m) based on wind speed (ms^{-1}) (as seen in Figure 7) and wave height spread (δH_s - m) caused by potential wind speed spread (±0.3 ms^{-1}). Figure 11b displays a zoomed in view around the 9 ms^{-1} threshold.

The 26 March 2009 (the first day of a four day event discussed further in section 3.1.2.2 Tier 2 - Case Study Wind Analysis) wave grid wind speed standard deviations (Fig. 12b) are much lower than the Tier 3 wind event average (Fig. 9a), with only the NAM exhibiting standard deviations of approximately 2.0 ms^{-1} in the two northern wave domains. Interestingly for the 26 March case, the NAM has higher standard deviations in wind speed when compared to the three WRF-NAM resolutions, which may be because the NAM forecasts higher wind speeds for that 24 h period (see Figure 20a). Again, the WRF-NAM shows insignificant differences across both resolution and wave domains. The NAM is the only model shown in Figures 12a and 12b that shows significant variations across wave domains.

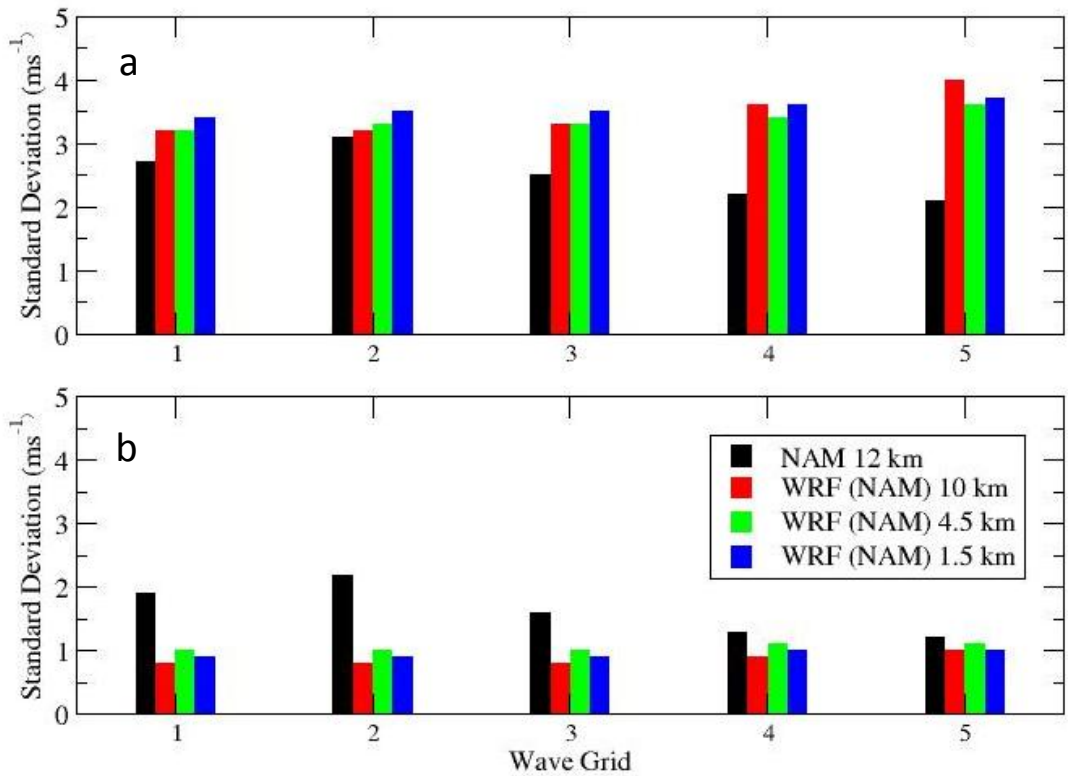

Fig. 12a-b: Wave grid wind speed standard deviations (ms^{-1}) for Tier 1 Tropical Storm Fay 19-21 August 2008 (a) and Tier 3 wind event 26 March 2009 (b).

The increasing variability with increasing wind speed (Fig. 11a) indicates that potential errors in providing representative wind forcing to the wave model will also grow. Figure 13 displays the same theoretical equilibrium wave height curve (solid black line) from Figure 11a but instead of showing wave height standard deviation, equation 8 uses wind speed RMSE as the U_{10} input to plot the potential wave height errors (colored dashed lines). A red dashed line is also plotted in Figure 13 to help illustrate the potential wave height errors that could result from potential errors in forecasting a wind speed of 9 ms^{-1} (Tier 3 wind event threshold).

A theoretical wave height error, resulting from a RMSE of 5.0 ms^{-1}, can be as high as ±3.0 m when forecasting a wind speed of 15 ms^{-1}.

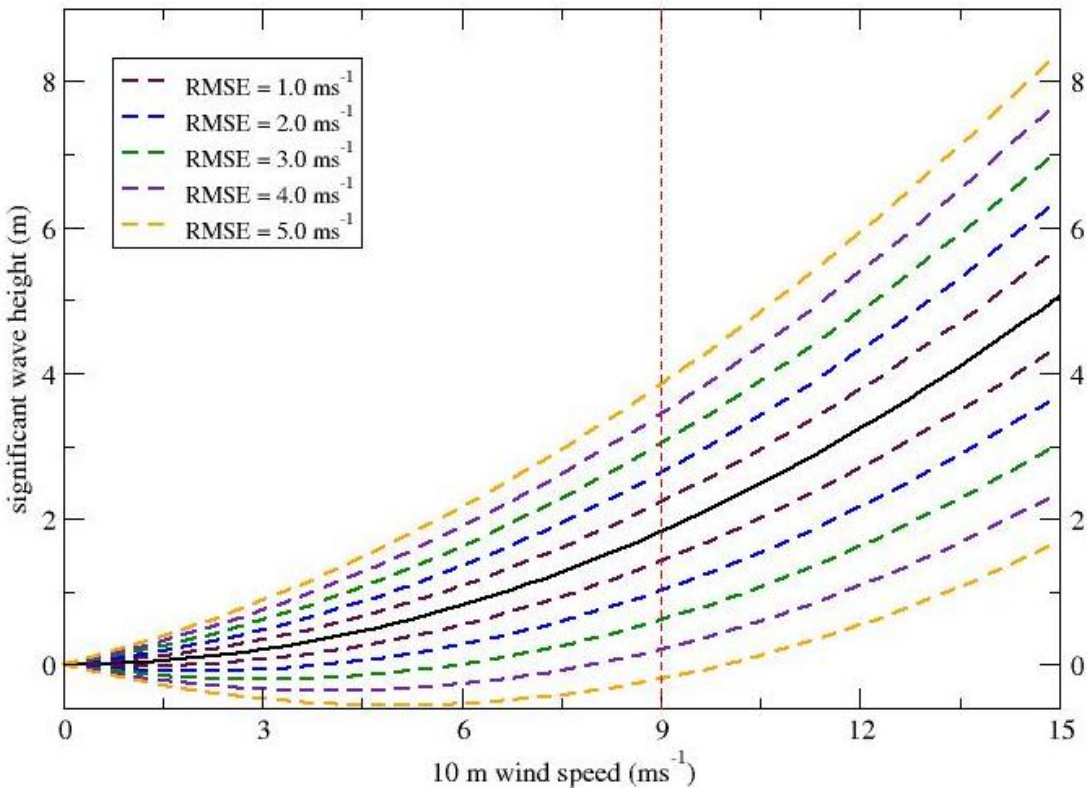

Fig. 13: Theoretical equilibrium wave height (H_s – m, solid black line) and wave height RMSE (H_s – m, dashed lines) based on wind speed (ms^{-1}, x-axis) and potential wind speed RMSE (1.0 - 5.0 ms^{-1}). 9 ms^{-1} threshold identified with red dashed line.

3.1.1.3: Single Point Time Series vs. Domain Averaged Wind

With the limitation of only being able to use a single time series of data to force an entire wave domain it is necessary to compare the average wind across a wave domain to a single point taken from the wind forecast, located in the center of the wave domain. Figure 14 compares the 48 h domain average wind speed

(wave grid 1) and the 48 h average wind speed from the single point time series grid 1 forcing for each Tier 3 wind event. Comparisons are shown for four atmospheric model resolutions: NAM 12 km and WRF (10 km, 4.5 km, and 1.5 km). A one-to-one line has been included to indicate whether the single point time series is representative of domain average. Also included in the figure are linear best-fit trendlines for each model resolution. Two outliers are also identified in Figure 14 (red circles) and will be examined in this section.

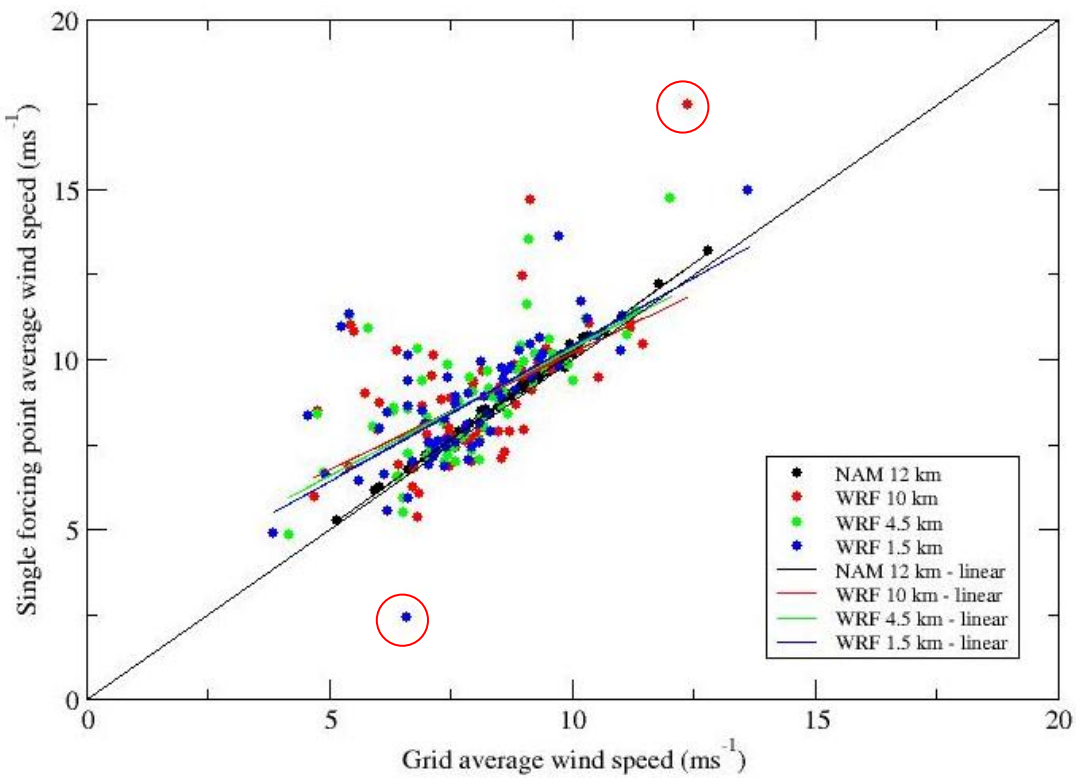

Fig. 14: Tier 3 wind event comparisons between grid 1 average wind speed (ms^{-1}) and average single forcing point wind speed (ms^{-1}). All atmospheric resolutions shown: NAM 12 km (black) and WRF-EMS (10 km - red, 4.5 km - green, and 1.5 km - blue). A one-to-one line and linear best-fit trendlines for each resolution are also displayed. Red circles identify two outliers that will be examined in detail.

Table 7 shows the square of the correlation coefficient (R^2) for each of the WRF-NAM resolutions and the NAM in Figure 14. The NAM single point is highly correlated with the domain average and thus suggests that a single point forcing time series extracted from NAM is indeed representative of the wave domain wind field. There is a decrease in correlation from the NAM to the WRF-NAM 10 km, indicating more variability exists in the WRF. Interestingly, the correlation increases in the WRF with increasing resolution, suggesting that increasing resolution adds redundant information to the wind field instead of resolving addition features.

Table 7. R^2 correlation values for 48 h grid average versus 48 h single point time series average wind speed.

Model and resolution		R^2 value
NAM 218	**12 km**	**0.9953**
WRF-NAM	**10 km**	**0.3113**
	4.5 km	**0.4293**
	1.5 km	**0.4592**

The impact of the spatial averaging of the wind forcing on the wave forecast is now briefly examined by selecting two outliers from Figure 14 (red circles) . For these two cases, CMS-Wave is executed with both a single point and domain averaged wind forcing time series. A 25 pt average about the forcing point location was also used to force CMS-Wave for the first of the two cases. Table 8 displays the information and results for the two outliers circled in Figure 14. In the first case, WRF-NAM 10 km wind forecasts during the passage of Tropical Storm Fay on 20

August 2008 had a higher average wind forecast for the single point time series than for either of the forcing time series produced using a domain or 25 pt average of winds. Note in Table 8 that the single point time series for the TS Fay case matches more closely the average wind speed observed at buoy 41009 for the forecast time period. When using a 25 point average (centered on the location of the single point time series) or a domain average to force the wave model the resulting H_s RMSE values are higher for the 48 h forecast period compared to the results when using the single point time series. Hence for the TS Fay case, the single point time series is a better representation of the observed wind field at buoy 41009 and thereby produces the best wave forecast.

Table 8. Figure 14 outlier case study results. Table presents information on the outlier 48 h forecast chosen events, the forecast model that produced the outlier, the forcing options for the event, 48 h wind forecast averages for the forcing options, and resulting CMS-Wave significant wave height 48 h RMSEs for the differing forcing time series.

48 h Forecast Event	Model and Resolution	Grid 1 Wind input or Buoy obs	48 hr Avg. WSPD (ms^{-1})	48 h H_s RMSE (m)
TS Fay 20-21 Aug 2008	WRF-NAM 10 km	Grid average	12.40	1.89
		25 pt avg	14.88	1.83
		Single point	17.48	1.54
		Buoy 41009	17.36	-
18-19 Jan 2009	WRF-NAM 1.5 km	Grid average	6.60	0.34
		Single point	2.41	0.94
		Buoy 41009	6.82	-

The second outlier case in Table 8, a frontal passage on 18 January 2008, gives an example of when the the grid average more closely matched the average wind speed observed at buoy 41009. The 18 January 2009 Tier 3 wind event single point time series taken from the WRF-NAM 1.5 km provided lower wind speeds to the wave model than if one were to use the hourly domain averaged value. For this case, the use of the domain averaged forecast winds resulted in lower H_s RMSE values than when the single point time series was used to force the wave model. Overall, a single point time series closely matches a domain average on a daily basis (Fig. 14) but the outlier cases illustrate that there will be days when a single point time series is not the best wind to use as wind forcing for the wave model.

Since Figure 14 illustrated that the single point time series wind forcing data are similar to the domain averaged wind, the wind speed and direction averages and standard deviations for each wave domain forcing point are now examined for further comparison. Figures 15a and 15b show the average and standard deviations for the Tier 3 wind event single point time series of wind speed and direction for each of the five wave domains and the four atmospheric model resolutions. The averages and standard deviations computed here are similar to those produced for the wave domains earlier (Figs. 8a, 8b, 9a, and 9b), except only the single point time series wave forcing data was used, instead of the spatially varying data contained within the wave domains. These results are similar to Figures 8a, 8b, 9a, and 9b, in terms of higher standard deviations in the WRF-NAM compared to the NAM and

the differences between the WRF-NAM resolutions. However, compared to the domain averaged values, the single point forcing time series average wind speeds are higher overall for each wave domain and the standard deviations are smaller. Compared to wave model variability produced by the domain averaged standard deviations the lower standard deviations in the single point forcing time series should produce a smaller standard deviation in the wave model forecasts. With the standard deviation of 1.9 ms^{-1} in the WRF-NAM (Fig. 15a) and a forecast wind speed of 9 ms^{-1} the standard deviation in the wave model (using Eq. 8) will be approximately 1.5 m (compare to the domain averaged forcing wave model standard deviation value of 2.0 m).

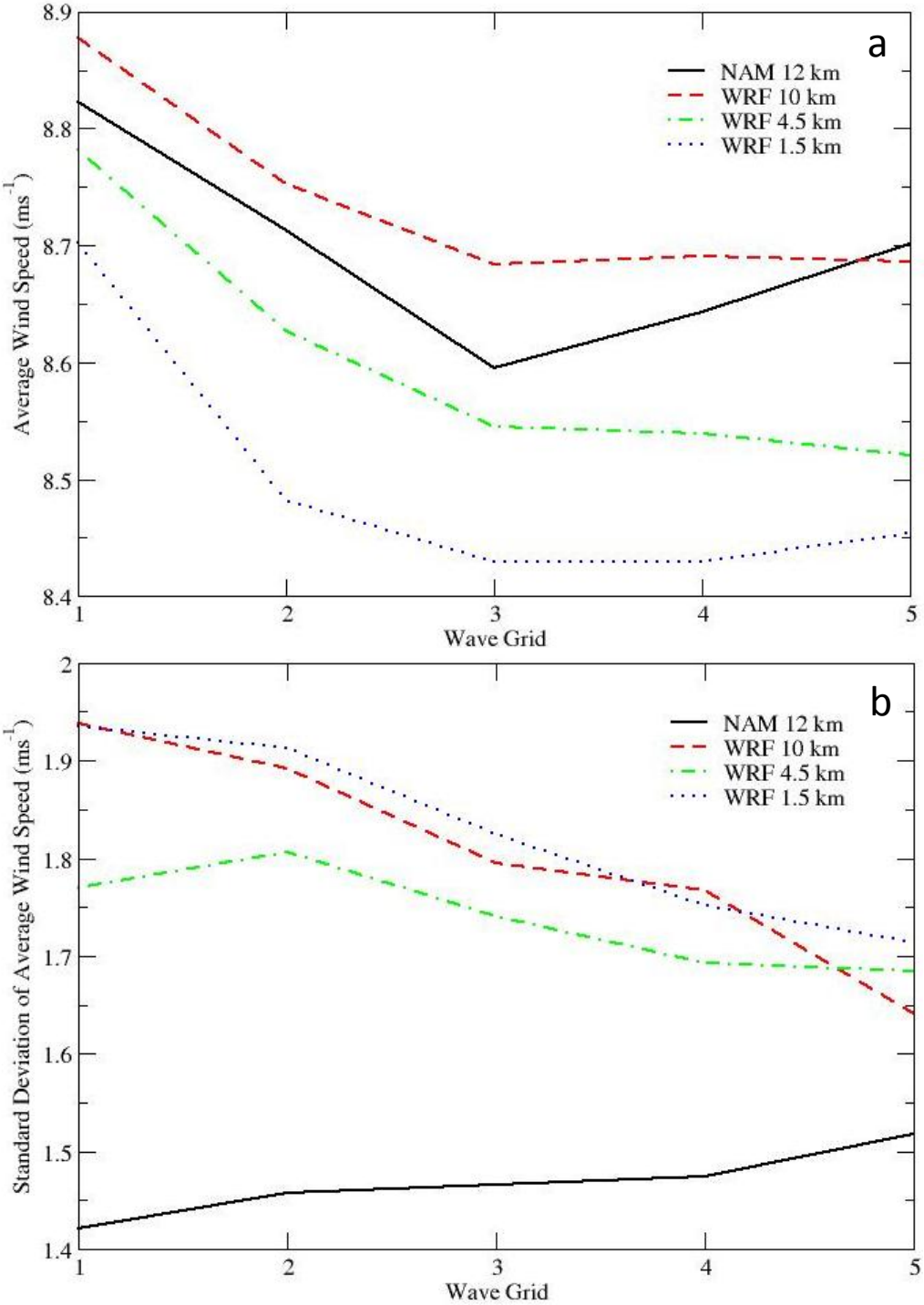

Figs. 15a-b: 48h single point time series wind speed (ms^{-1}) average (a) and standard deviation (ms^{-1}) (b) across all Tier 3 events for atmospheric resolutions: NAM 12 km (solid black), and WRF-EMS (10 km – red dashed, 4.5 km – green dot dash, and 1.5 km – blue dotted)

For a more detailed look at wind speed variability within the wave forecast domains, the Tier 1 Tropical Storm Fay event is now examined. Similar to Figures 15a and 15b, Figures 16a and 16b displays the average forecast wind speed and standard deviation for each wave domain 48 h single point time series produced for the Tropical Storm Fay Tier 1 wind event on 20 August 2008. Figure 16a clearly indicates greater variability than the Tier 3 events with respect to both model resolutions and between domains, which is not surprising since a tropical cyclone would likely produce the upper limit on wind variability within the forecast areas of this project. A difference between the NAM and WRF-NAM 10 km in the average forecast wind speed of approximately 5.0 ms^{-1} in wave domain 1 is a significant variation —indicating that there may be large differences in the resulting wave forecasts among some of the wave model runs. Using equation 8 again, the standard deviation of approximately 3.25 ms^{-1} in wind speed observed in the WRF-NAM (Fig. 14b) and a wind speed of 9 ms^{-1} would produce a standard deviation in the wave model of 2.6 m (8.5 ft). The impact on the wave model simulations will be discussed in more detail in section 3.2.2.

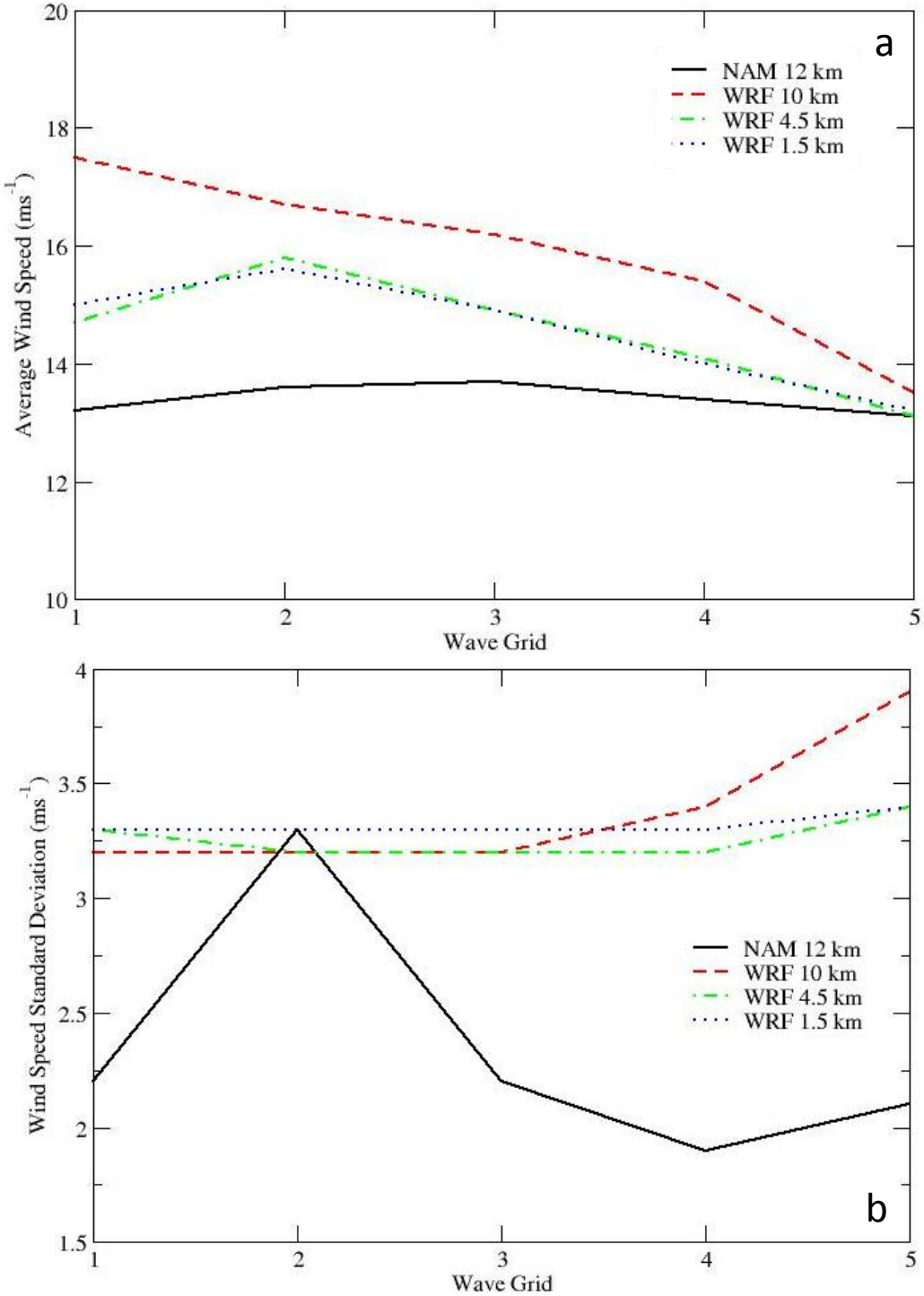

Fig. 16a-b: Tropical Storm Fay 00 UTC 20 August 2009 48 h forecast single point time series wind speed average (a, ms^{-1}) and standard deviation (b, ms^{-1}) for atmospheric models: NAM 12 km (solid black), and WRF-EMS (10 km – red dashed, 4.5 km – green dot dash, and 1.5 km – blue dotted)

3.1.2: Wind Forecast / Forcing

The quality of both the wind forecasts and forcing for the CMS-Wave model are examined in this section. The evaluation consists of statistical analysis of the 10 m wind forecasts validated against buoy observations. Results are stratified by wind event Tiers, which contain a total of 213 48 h forecasts between August 2008 and March 2009. The CMS-Wave model wind forcing options are listed in Table 9.

Table 9. Spatial resolution of the various wind forcing options for the CMS-Wave model, along with the Tiers the data will be evaluated.

Model	Forcing*	Resolution	Tiers
GFS		0.5°	All
NAM 218		12 km	All
WRF	NAM 218	10 km	All
WRF	GFS	10 km	1
NWS GFE		5 km	Select days
WRF	GFS	4.5 km	1
WRF	NAM 218	4.5 km	All
WRF	NAM 218	1.5 km	All

*Only listed for WRF

3.1.2.1: Tier 4 Wind Analysis

Figure 17 displays statistical results for 213 00 UTC 48h atmospheric model runs between August 2008 and March 2009. Bias, RMSE, and scatter index values were calculated for each 24h forecast period (0-24h and 24-48h) and were averaged across the eight month period. All five atmospheric model options underforecast wind speed, with the NAM underforecasting the 24-48h wind speed

the least. RMSE values for each of the five atmospheric options are similar for wind speed, ranging only between 1.7 ms^{-1} and 2 ms^{-1}, but vary between 50° and 70° for wind direction, with the GFS standing out with the lowest overall directional bias and error. The RMSE is slightly larger during the 24-48 forecast period for all atmospheric model options and variables. Scatter index values indicate all models performed well in terms of wind speed, with values between 20% and 30%, however, wind direction scatter index values are higher. Figure 18 displays the skill score values for wind forecasts produced by the GFS and the three resolutions of WRF-NAM against NAM. With respect to this metric, the NAM outperforms the WRF-NAM for both wind speed and direction (Fig. 18), suggesting that, on average, the WRF-NAM does not provide an improvement over the NAM. Compared to GFS, NAM has a larger directional bias but a lower wind speed bias. Based on the skill score it appears that NAM outperforms GFS and WRF-NAM for wind speed but the GFS outperforms the NAM in terms of wind direction. Therefore, it is of interest to force the WRF with GFS instead of NAM and compare the results again. The GFS was used to force the WRF for the Tier 1 event, results of which will be shown in the Tier 1 section.

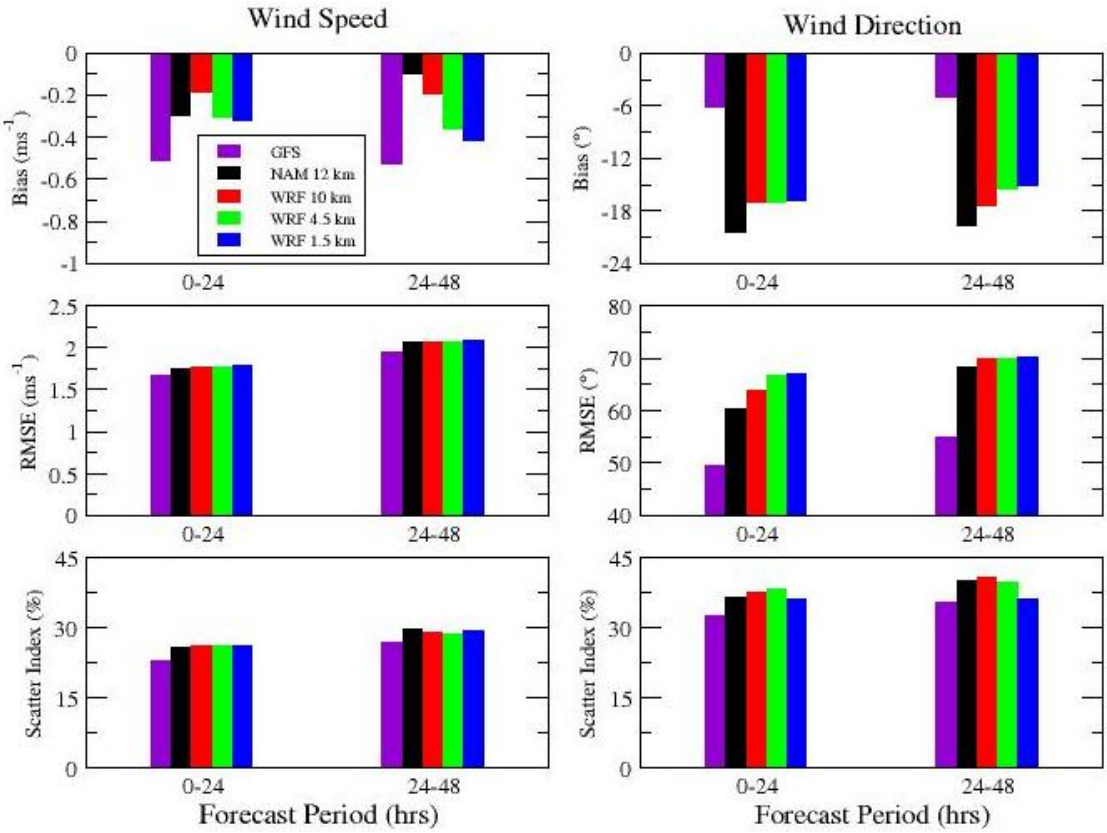

Fig. 17: Tier 4 wind speed (ms^{-1}) (left) and direction (°) (right) bias (ms^{-1}), RMSE (ms^{-1}), and scatter index (SI - %) for two 24h forecast periods at buoy 41009: GFS (purple), NAM 12 km (black), and WRF-EMS (10 km – red, 4.5 km – green, 1.5 km – blue)

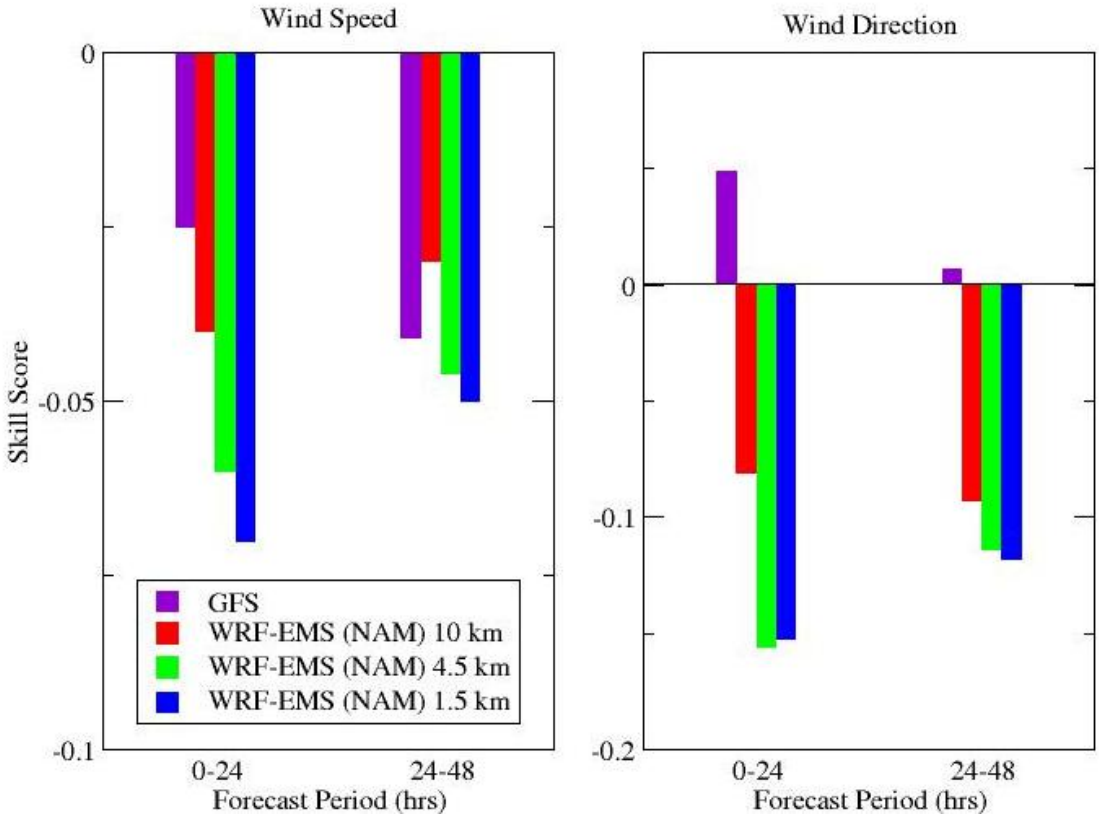

Fig. 18: Tier 4 wind speed (ms^{-1}) (left) and direction (°) (right) skill score versus NAM for two 24h forecast periods: GFS (purple) and WRF-EMS (10 km – red, 4.5 km – green, 1.5 km – blue)

To better quantify the Tier 4 results presented here, they are compared directly to previous results involving atmospheric-ocean coupling. Janssen et al. (1997), validated the ECMWF wave forecast system by calculating ECMWF wind forcing scatter index values for wind speed along the U.S. east coast. Their SI values ranged between approximately 16% and 27%, averaging approximately 23% for the 16 month study period. The same study also found, that on average, the ECMWF atmospheric model tended to overforecast wind speeds over the ocean. In addition, wind speed RMSE values were between approximately 1.4 ms^{-1} and 1.8 ms^{-1} for the

U.S. east coast. Janssen et al. (1997) claimed that wind speed scatter index values as high as 25% were indicative of a "poor performance" but it is important to recognize that these values are for open ocean forecasts. Earlier work in shallow water (Janssen et al. 1984) produced wind speed scatter index values greater than 30%, suggesting that results seen in their later (1997) study were actually an improvement. The lower SI may be due to increases in model resolution, however this assumption can be disputed in this study due to the fact that the wind forecasts from the GFS had lower overall errors when compared to the higher resolution forecasts produced by both NAM and WRF-NAM. The impact of model resolution on the wind forecasts is examined further in section 3.2.2.

3.1.2.2: Tier 2 – Case Study Wind Analysis

Tier 2 and 3, when compared to Tier 4 (i.e., Figs. 17 and 18), show only slight differences and are thus not presented here. Instead, the wind forecast evaluation presented here will now focus on specific case studies selected from the Tier 2 events (Table 10) and the Tropical Storm Fay Tier 1 event (section 3.1.2.4). The NWS generated GFE wind option will also be examined in section 3.1.2.3.

Table 10. High wind event case studies.

Dates	Event information
1/18/09 – 1/22/09	**Frontal passage**
3/26/09 – 3/30/09	**Four day event with frontal passage at end**

Figures 19a and 19b displays the wind forecasts from GFS, NAM 12 km, and WRF-NAM (10 km, 4.5km, and 1.5 km) valid at buoy 41009 for the first Tier 2 case study (00 UTC 18 January – 00 UTC 22 January 2009) compared to observations. Four 24 h forecasts make up the time series in Figures 19a and 19b, which display wind speed (a) and wind direction (b). The first day of this case study happens to be the same day used for one of the outlier cases discussed in the wind variability section. In terms of the wind speed, all atmospheric models perform relatively well, capturing the trends as the front passes through the forecast region. As the winds shift from northerly to southerly and increase in magnitude on 18 January, neither the NAM or the WRF-NAM resolutions capture the correct evolution of the directional shift as the actual winds rotate to the south in a counterclockwise fashion while the NAM and WRF-NAM winds rotate clockwise on the 18th. In this case, the GFS is superior to both the NAM and WRF-NAM simulations. More importantly, these results are consistent with all Tier 4 events for which the GFS shows skill over that of the NAM wind direction for both the 0 to 24 h and 24 to 48 h forecast windows (Fig. 18). This is also a great example of how strongly NAM boundary conditions influence the resulting WRF forecasts and is an argument to test using GFS as the WRF forcing.

Figures 19c and 19d display the first set of 18 January 24 h forecasts from Figures 19a and 19b, with the addition of the WRF-GFS 10 km forecast wind speed and direction. Table 11 displays the RMSEs for wind speed forecasts shown in

Figures 19c and 19d. Although the GFS wind speed forcing is inferior to the NAM for this case (see Table 11), the WRF-GFS 10 km outperforms the other model configurations with respect to wind speeds for the 0 to 24 h forecast period. In terms of the wind direction, the WRF-GFS 10 km is similar to the GFS forcing during the first few forecast hours each of which have northerly flow. Both the observed and GFS winds back, however the directional change in the GFS lags the observations by several hours. Interestingly the WRF-GFS winds do not follow the GFS – and instead veer along with the NAM and WRF-NAM simulations. However, the WRF-GFS 10 km does a better job capturing the wind direction during the last six hours, compared to the other models.

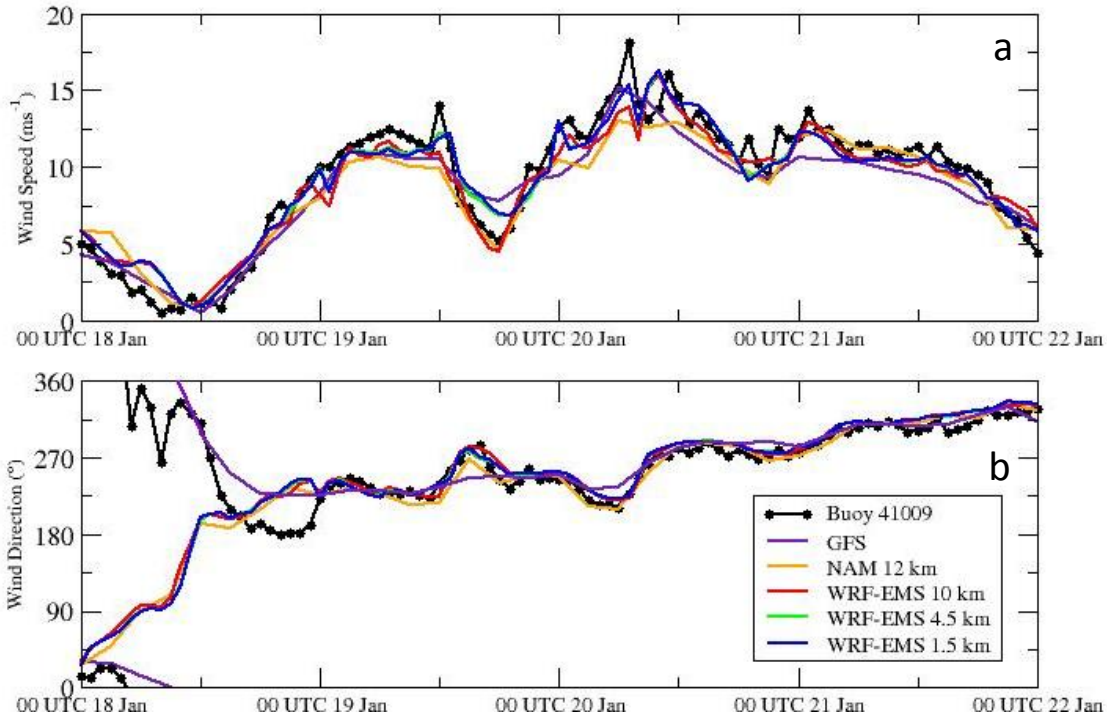

Fig. 19a-b: Wind speed (ms^{-1}, a) and direction (°, b) forecasts for four 24 h periods between 00 UTC 18 January – 00 UTC 22 January 2009 from GFS (purple), NAM 12 km (orange), and WRF-NAM (10 km – red, 4.5 km – green, 1.5 km – blue) compared to buoy 41009 observations.

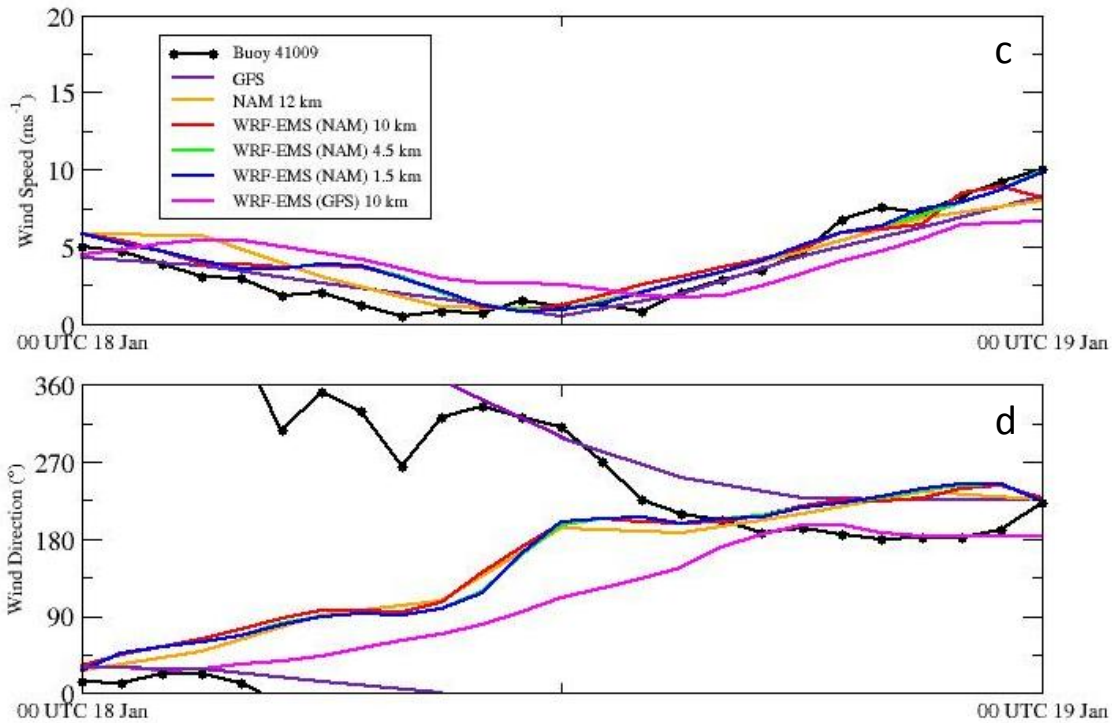

Fig. 19c-d: Wind speed (ms^{-1}, top) and direction (°, bottom) forecasts for one 24 h periods between 00 UTC 18 January – 00 UTC 19 January 2009 from GFS (purple), NAM 12 km (orange), WRF-NAM (10 km – red, 4.5 km – green, 1.5 km – blue), and WRF-GFS 10 km (pink) compared to buoy 41009 observations.

Table 11. RMSE (ms^{-1}) for 18 January 2009 24 h wind speed forecasts from GFS, NAM, WRF-NAM, and WRF-GFS.

Model and Resolution	Wind Speed RMSE (ms^{-1})
GFS	**2.06**
NAM 12 km	**1.04**
WRF-GFS 10 km	**0.92**
WRF-NAM 10 km	**1.18**
WRF-NAM 4.5 km	**1.12**
WRF-NAM 1.5 km	**1.12**

Similar to Figures 19a and 19b, Figures 20a and 20b displays the wind speed and direction forecasts for four 24 h periods between 00 UTC 26 March and 00 UTC 30 March 2009. In terms of wind speed all models experience problems capturing the correct evolution of the 10 m wind, exhibiting, at times, maxima and minima that are out of synch with the observed winds. The spike in the 00 UTC 28 March WRF-NAM 1.5 km initial conditions suggests that some sort of averaging (either grid, 25 point, or other) would help in reducing spurious or unrepresentative model winds spikes. With the wind event already in progess at the start of the 26 March forecast period all models perform well in capturing the southeasterly wind direction that continues into the 27 March. All of the models forecast and the buoy observes a diurnal backing of the winds during the day on the 27th, which is most likely due to land surface heating. While the models capture the wind direction on the 27th, they all underforecast the wind speeds during the day. As the front approaches 29 March, both the NAM and the WRF-NAM prematurely shift the winds southwesterly before shifting back to southerly (compare to buoy, solid black line). The GFS tends to handle the gradual wind shift much better than either the NAM or the WRF-NAM. During the latter half of 29 March, all models capture the clockwise rotation of the winds to a westerly direction as the front passes. The error in the NAM (which is passed along to the WRF via the boundary conditions) is clear at the beginning of the 24 h forecast period on 29 March as the initial conditions from the NAM are off by about 60 degrees. Again the WRF follows the NAM

boundary conditions and, in terms of wind direction, would suggest the use of GFS would be a better choice for WRF forcing.

Figures 20c and 20d display the wind speed (c) and direction (d) forecasts for the 00 UTC 29 March to 00 UTC 30 March 24 h period with the addition of the WRF-GFS 10 km. In this case and in terms of wind direction, the WRF-GFS is more strongly influenced by the GFS boundary conditions than it was during the first Tier 2 case study as it is nearly identical to the GFS during the first 12 hours of the 24 h period. The WRF-GFS deviates from the GFS during the second half of the forecast period, with a clockwise rotation of the winds to the west. This westerly rotation is also seen in the other WRF-NAM forecasts, indicating that the WRF may be responsible for the error in the wind direction forecast, and not either of the model forcings (NAM or GFS). Table 12 displays the RMSE values for the wind speed and direction forecasts shown in Figures 20c and 20d. The GFS has both the lowest wind speed and direction errors for the 29 March 24 h forecast. The WRF-NAM was an improvement over its NAM forcing, however, the WRF-GFS did not improve upon the GFS for this case.

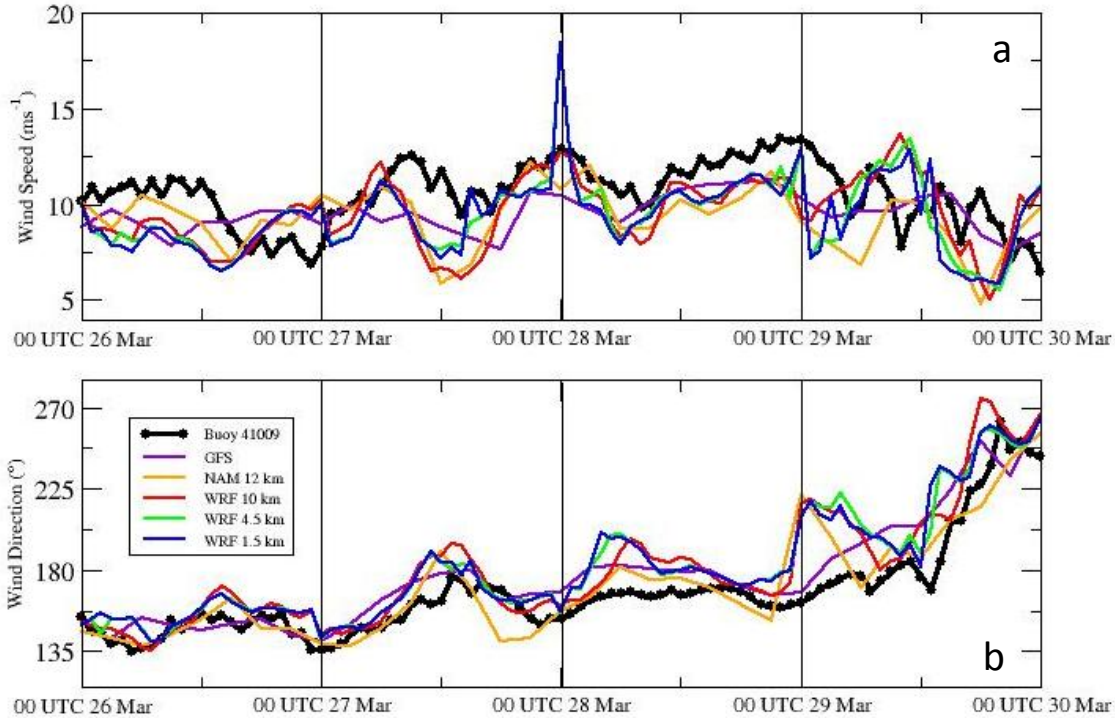

Fig. 20a-b: Wind speed (ms^{-1}, a) and direction (°, b) forecasts for four 24 h periods between 00 UTC 26 March – 00 UTC 30 March 2009 from GFS (purple), NAM 12 km (orange), and WRF-NAM (10 km – red, 4.5 km – green, 1.5 km – blue) compared to observations for buoy 41009.

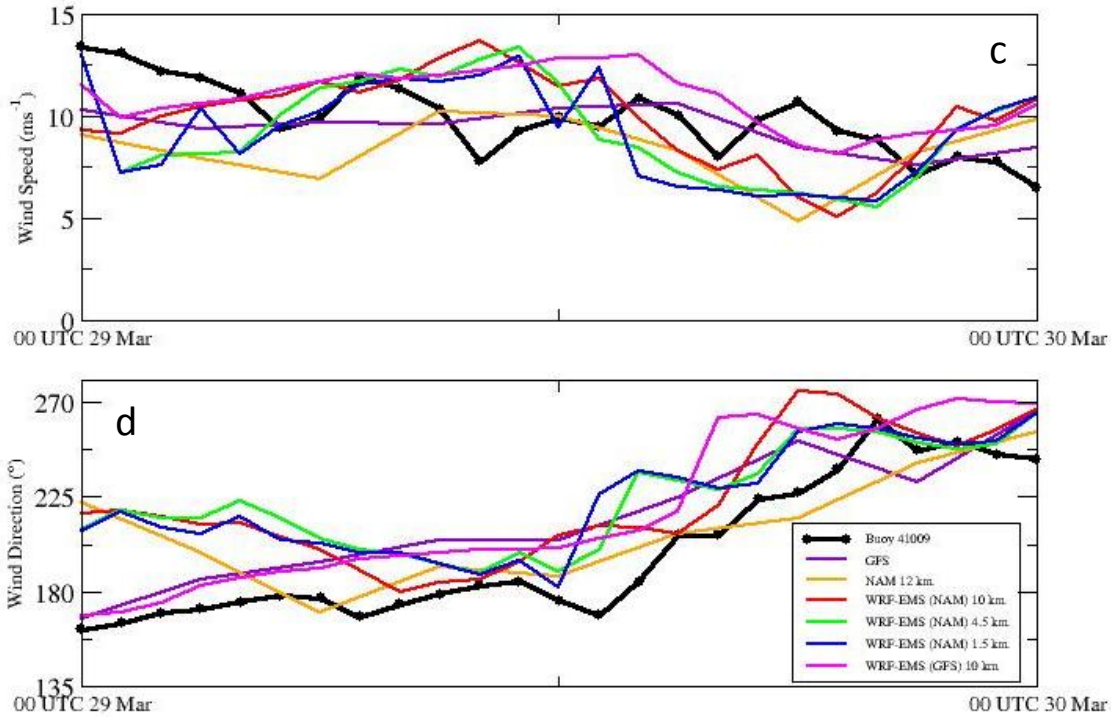

Fig. 20c-d: Wind speed (ms^{-1}, c) and direction (°, d) forecasts for one 24 h period between 00 UTC 29 March – 00 UTC 30 March 2009 from GFS (purple), NAM 12 km (orange), WRF-NAM (10 km – red, 4.5 km – green, 1.5 km – blue), and WRF-GFS 10 km (pink) compared to observations for buoy 41009.

Table 12. RMSE for 18 January 2009 24 h wind speed (ms^{-1}) and direction (°) forecasts from GFS, NAM, WRF-NAM, and WRF-GFS.

Model and Resolution	Wind Speed RMSE (ms^{-1})	Wind Direction RMSE (°)
GFS	**1.67**	**19.6**
NAM 12 km	**3.21**	**24.6**
WRF-GFS 10 km	**2.23**	**23.1**
WRF-NAM 10 km	**2.72**	**29.5**
WRF-NAM 4.5 km	**2.91**	**30.0**
WRF-NAM 1.5 km	**2.90**	**29.9**

3.1.2.3: GFE Wind Forecast / Forcing

Figure 21 displays the validation stats for five atmospheric model wind forcing options (GFS, NAM 12 km, GFE 5 km, and WRF-NAM 10 km, 4.5 km, and 1.5 km) for May and June 2009. The statistics (RMSE and scatter index) for both wind speed and direction indicate that GFE does not perform as well as the models at buoy 41009 for the months of May and June. Early summer conditions are typically quiesent in the region, thus a longer time period is needed to fully evaluate the GFE as a possible option for forcing the wave model. It would be more beneficial to evaluate how the GFE performs in the fall and winter months when the wind speeds are normally higher and there is more mesoscale variability.

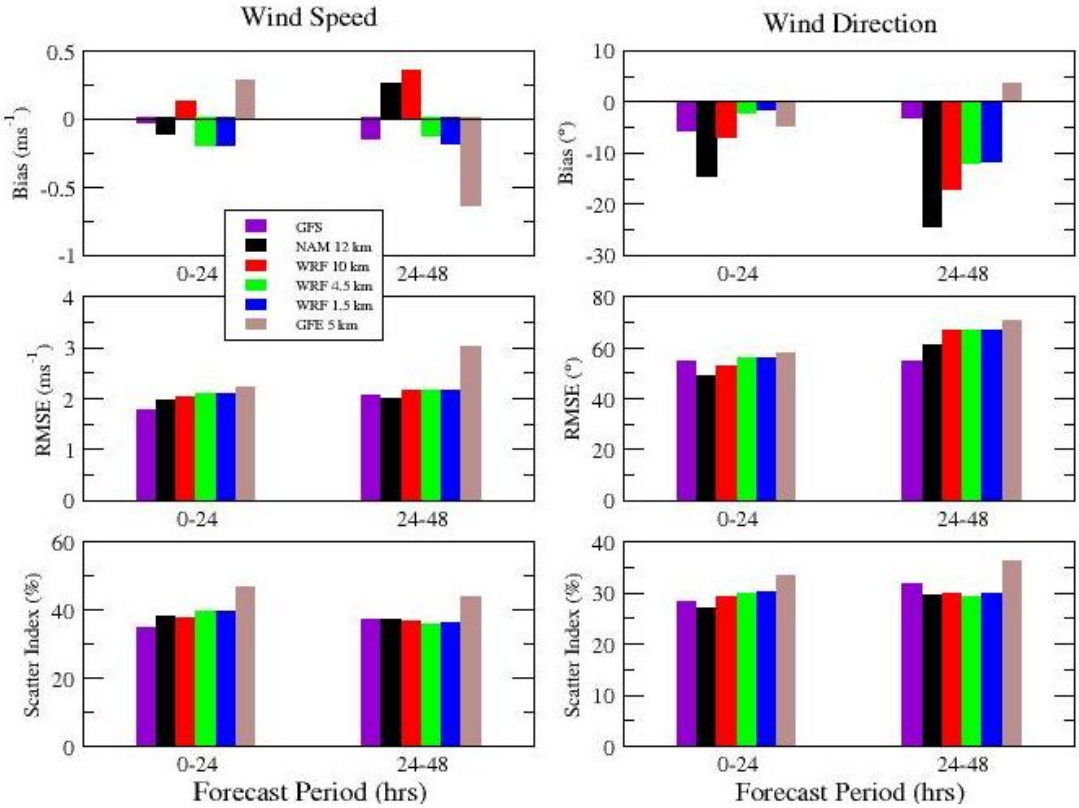

Fig. 21: May and June 2009 bulk validation results (bias (ms^{-1}), RMSE (ms^{-1}), scatter index (SI - %)) for atmospheric models (GFS – purple, NAM – black, WRF-EMS (10 km – red, 4.5 km – green, 1.5 km – blue), and NWS GFE 5 km – brown) at buoy 41009.

3.1.2.4: Tier 1 – Tropical Storm Fay Wind Analysis

Figure 22 depicts the observed wind speed and direction at buoy 41009 from 00 UTC 19 August to 00 UTC 23 August 2008. A dashed line indicates where the wind direction shifts from onshore to offshore (offshore being winds between 162° and 342° due to the orientation of the coastline). Tropical Storm Fay approached the forecast area on 19 August from the southwest, passing through on 20 August and stalling offshore on 21 August before moving onshore and northwest

on 22 August. For this event, the wind speed excedes nine m/s for more than 48 hours and the wind direction shifts from onshore to offshore during the forecast period – making Tropical Storm Fay an excellent case study to test both the wind and wave components of the forecast system.

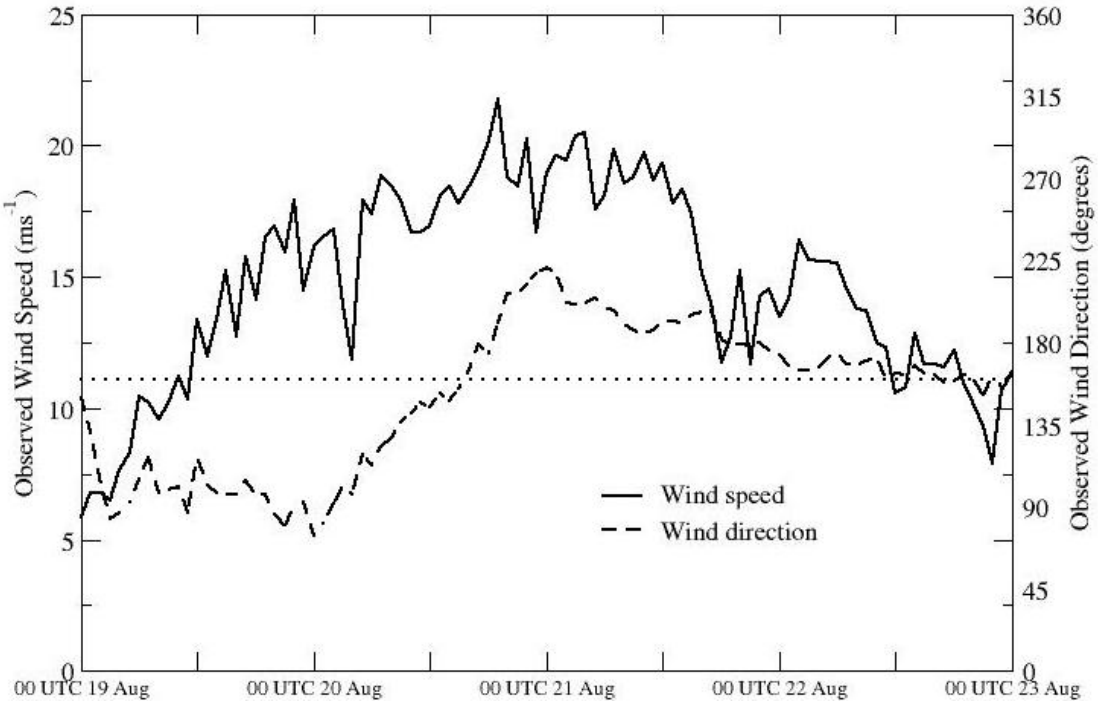

Fig. 22: Tier 1 event Tropical Storm Fay 00 UTC 19 August to 00 UTC 23 August 2008 observed wind speed (ms^{-1}, solid line) and direction (°, dashed line) at buoy 41009. Onshore/offshore direction based on angle of Central Florida coastline (dotted line).

Figures 23a-d display the NAM forecast 10 m winds at six hour intervals (00, 06, 12, and 18 UTC) on 20 August 2008. The NAM forecast locations of Tropical Storm Fay are displayed (black star), as well as the actual location of the storm (red star).

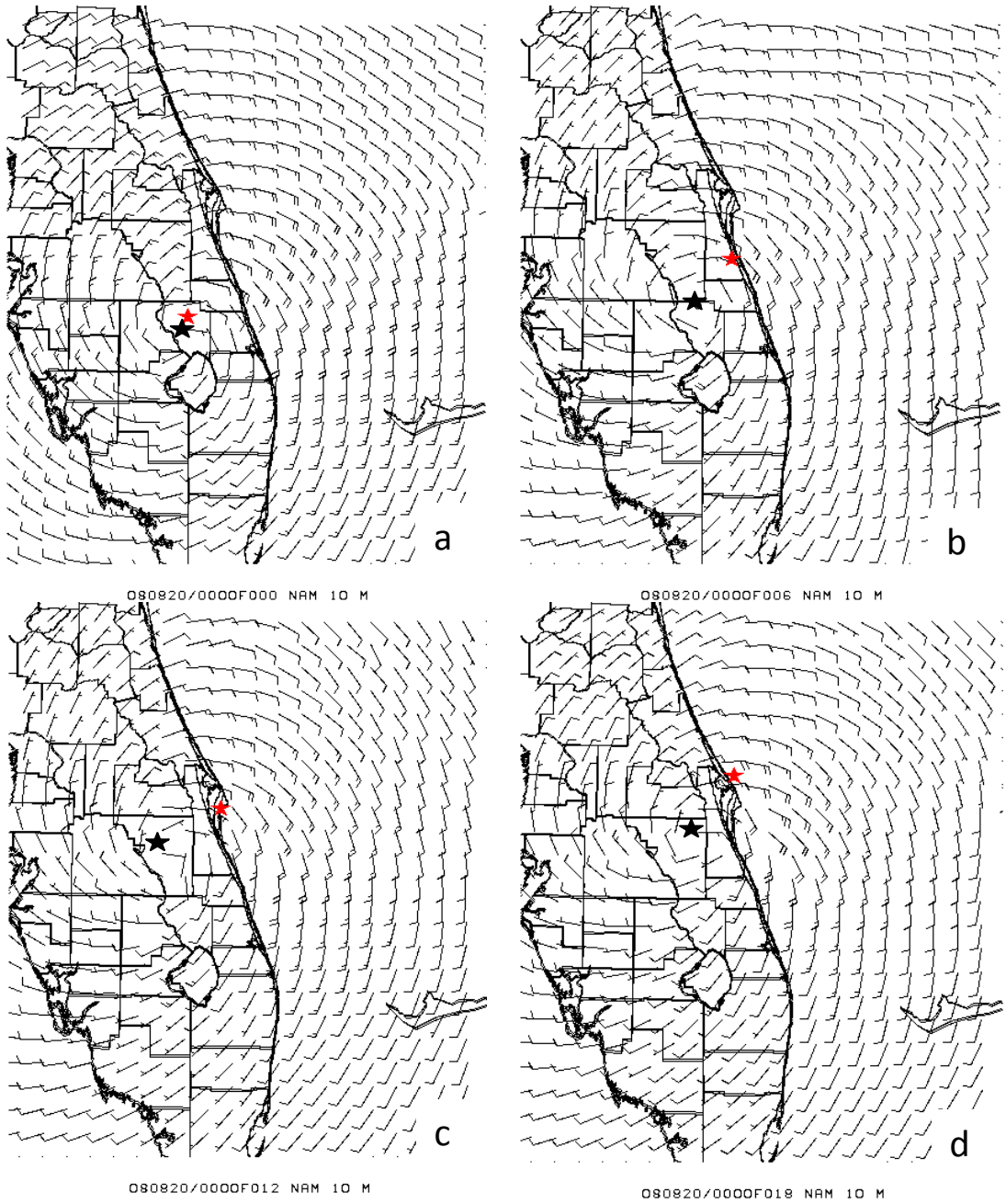

Fig. 23a-d: NAM 10 m wind (ms^{-1}) forecast for 00 (a), 06 (b), 12 (c), and 18 UTC (d) 20 August 2008. NAM TS Fay location (black star) and actual storm location (red star).

Wind speeds and directions obtained from the front end (i.e., forecast hours 0-24) of three consecutive 48 h forecasts for the 19th to 22nd of August from the GFS, NAM, and WRF-NAM are shown in Figures 24a and 24b. The forecast wind speeds are valid at buoy 41009 -- the latter of which is also shown for comparison (solid black line). During the early portion of the forecast period on 19 August, Tropical Storm Fay begins to impact the northern most wave domains and the wind speeds increase at buoy 41009. In the absence of data assimilation, the WRF initialization will reflect whatever biases are inherent in the NAM. Hence, the low bias in the NAM wind speed is mapped to the WRF grid for all configurations. All models capture the increasing wind speeds as the storm moves into the study area and approaches buoy 41009. However, as the wind speeds continue to increase during the 20 August forecast period – some relatively significant differences appear. Only the GFS captures the steady increase in wind speeds at buoy 41009, while the NAM and the WRF-NAM winds remain steady for the remainder of the 20 August 24 h period. At the beginning of the next 24 h forecast period (21 August) the NAM has corrected itself and thus so have each of the WRF-NAM configurations as wind speed and direction is in better agreement with the observations. The NAM and WRF-NAM each capture the decline in wind speed as the storm stalls over the study area on 21 August. The error in wind speed forecasts on 20 August in the NAM are due to differences in the forecast track of the storm (see Figures 23a-d). The error in the NAM forecast carries over into the WRF and suggets trying to use

the GFS for force the WRF for this case as the GFS is one of the models in the suite of ensembles used for tropical storm track forecasting.

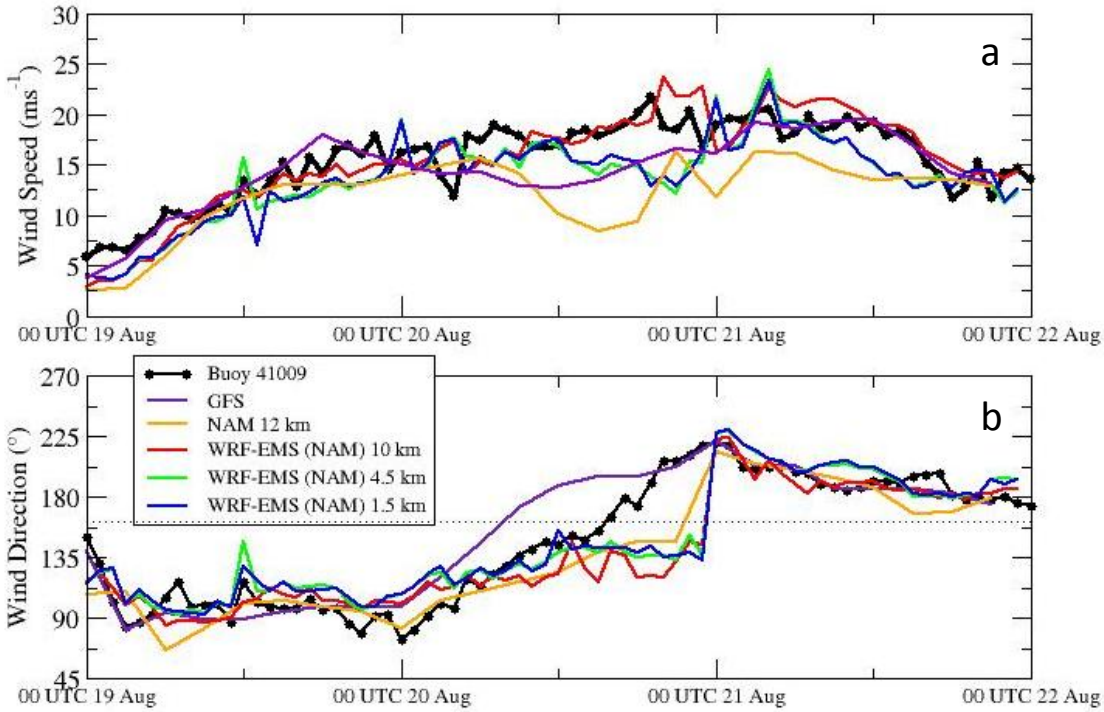

Fig. 24a-b: Tier 1 event Tropical Storm Fay 00 UTC 19 August to 00 UTC 22 August 2008 observed wind speed (ms^{-1}, a) and direction (°, b) at buoy 41009 (solid black line) compared to forecast hours 0-24 from forecasts initialized at 00 UTC 19, 20, and 21 August. Shown are the NAM (solid orange line), WRF-EMS (10 km – red, 4.5 km – green, 1.5 km – blue), and GFS (solid purple line).

Figures 24c & 24d display the wind speed and direction forecasts for the 24 h period from 00 UTC 20 August to 00 UTC 21 August, with the addition of the WRF-GFS 10 km. The WRF-GFS 10 km performs similarly to the WRF-NAM 10 km in terms of wind speed forecasts, capturing the peak in wind speeds on 20 August, however it also performs similarly to the GFS forcing in terms of wind direction and shifts the

winds offshore too early. Figure 25 presents the statistical summary of all atmospheric forecasts during TS Fay – including the GFS and WRF-GFS 10 km.

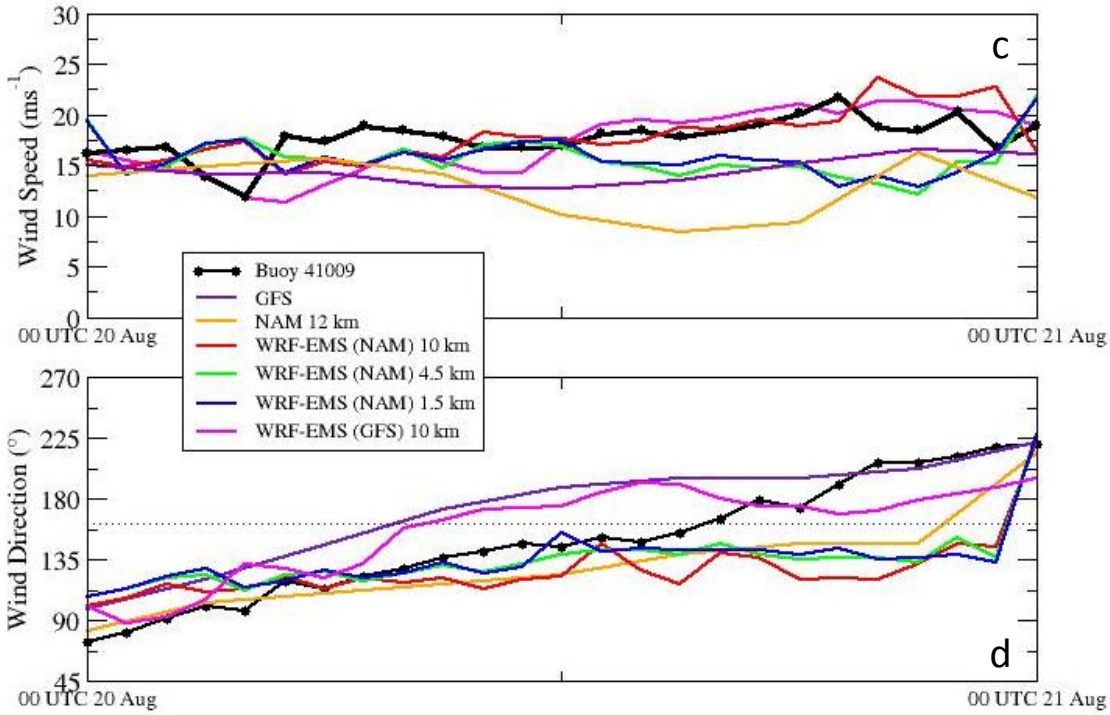

Fig. 24c-d: Tier 1 event Tropical Storm Fay 00 UTC 20 August to 00 UTC 21 August 2008 observed wind speed (ms^{-1}, c) and direction (°, d) at buoy 41009 (solid black line) compared to forecast hours 0-24 from forecasts initialized at 00 UTC 20 August. Shown are the GFS (purple), NAM 12 km (orange), WRF-NAM (10 km – red, 4.5 km – green, 1.5 km – blue), and WRF-GFS 10 km (pink).

Figures 25 and 26 present the bias, RMSE, scatter index, and skill score values for Tropical Storm Fay forecasts from GFS, NAM, WRF-NAM, and WRF-GFS. All statistics are made by comparing forecasts (Figs. 24a and 24b) and observations valid at buoy 41009. The skill score (Fig. 26) compares the GFS, WRF-NAM, and WRF-GFS to the NAM. Both the bias and RMSE represent the average over three 48 h forecasts (19, 20, and 21 August 2008). As indicated by Figure 25, all models tend

to underforecast wind speed throughout the 3-day period with biases ranging from -0.75 ms^{-1} (WRF-GFS 10 km) to -4.25 ms^{-1} (GFS and NAM). The wind direction bias for Tropical Storm Fay indicates that the WRF (NAM and GFS forced) has smaller values than either the GFS or NAM. In terms of the skill score and with the exception of the GFS 24-48 h wind speed forecast each of the configurations are an improvement over the NAM – with the largest skill observed in the WRF-GFS 10 km. Results for wind direction are more mixed, with the GFS and WRF-NAM 10 km outperforming NAM in the 0-24 h period and only the WRF-GFS 10 km outperforming in the 24-48 h period. Overall, for this Tier 1 high wind speed event, the WRF 10 km (NAM and GFS forced) provided an improvement in forecasting over NAM.

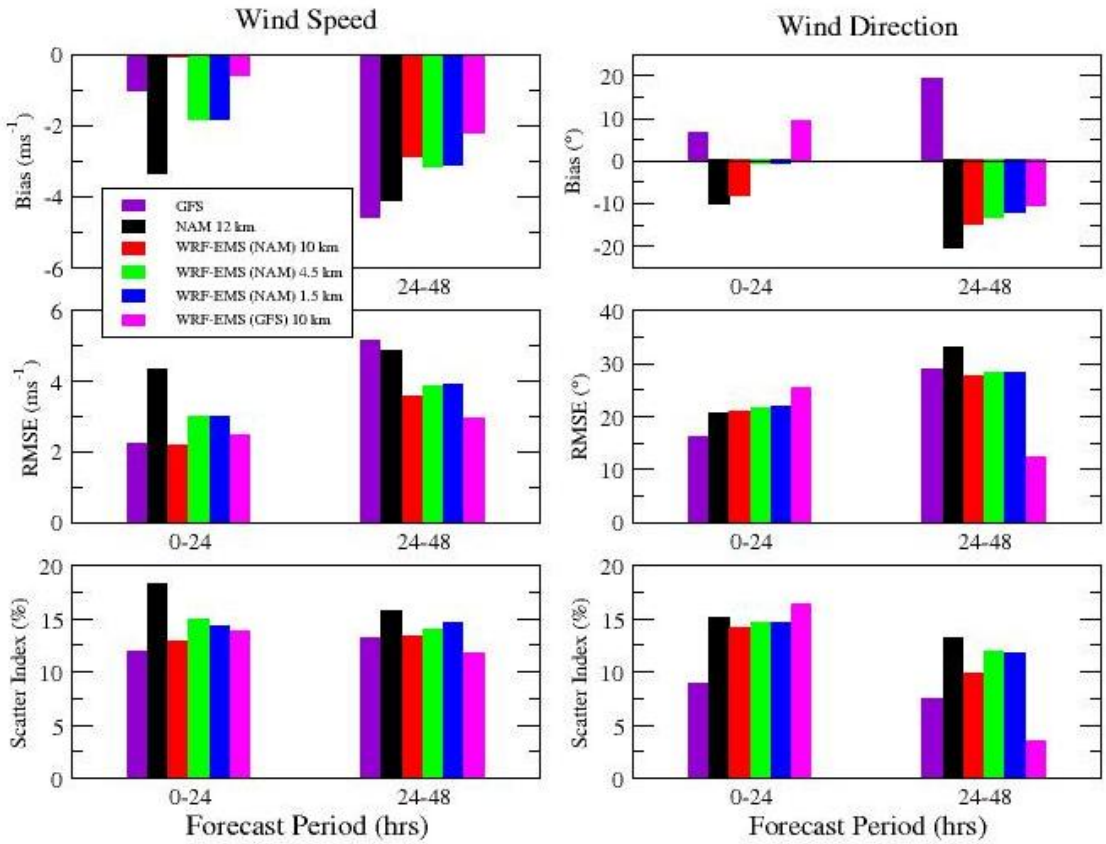

Fig. 25: Tier 1 (Tropical Storm Fay 19 August – 22 August 2008) wind speed (ms^{-1}, left) and direction (°, right) bias (ms^{-1}), RMSE (ms^{-1}), and scatter index (SI - %) for two 48h forecast periods at buoy 41009: GFS (purple), NAM 12 km (black), WRF-NAM (10 km – red, 4.5 km – green, 1.5 km – blue), and WRF-GFS 10 km (pink).

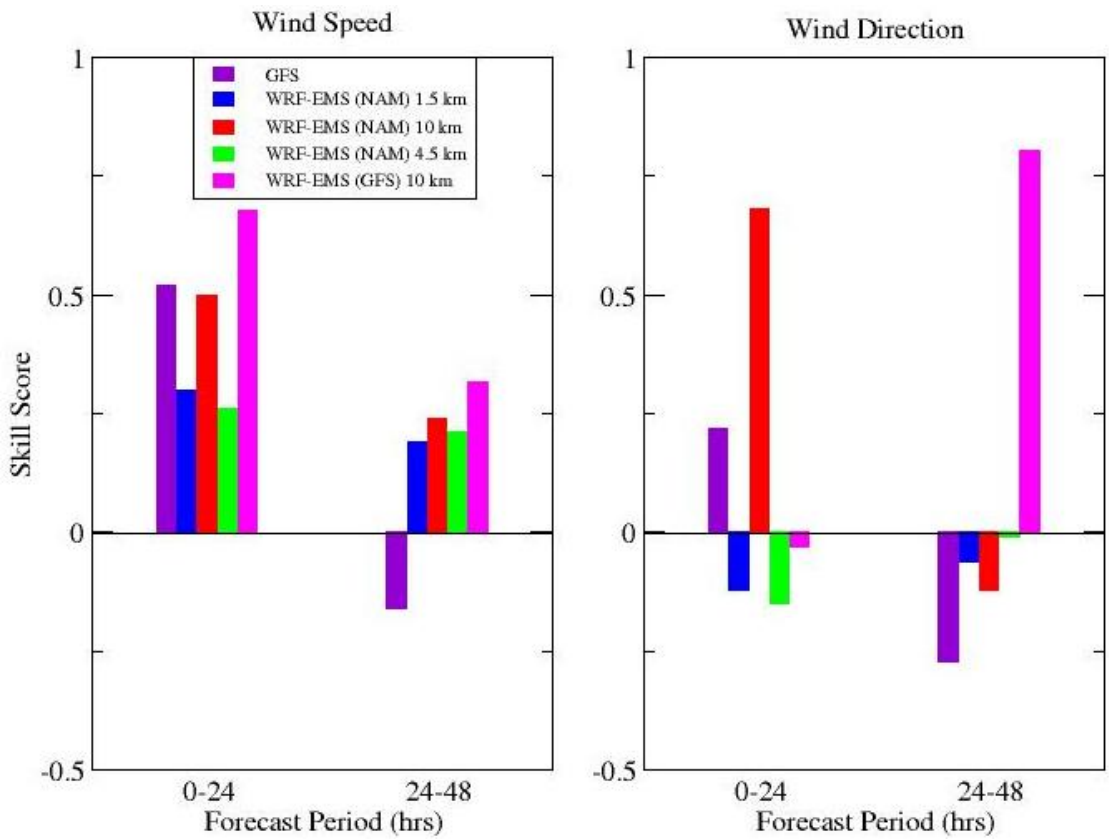

Fig. 26: Tier 1 (Tropical Storm Fay 19 August – 22 August 2008) skill scores for wind speed (ms^{-1}, left) and direction (°, right) versus NAM for two 48h forecast periods: GFS (purple) , WRF-NAM (10 km - red, 4.5 km - green, and 1.5 km - blue), and WRF-GFS 10 km (pink).

The following sections will now examine the wave model component of the coupled forecast system, which includes the quality of the wave forcing, impact of varying atmospheric model wind forcing resolution, and performance of the wave model during the Tier 3 wind events.

3.2: Wave Model

The quality of the wave forcing obtained from WW3 is evaluated in this section. The performance of CMS-Wave is also examined. Each of the wind forcing options (Table 8) evaluated in sections 3.1.2.1 through 3.1.2.4 was used to force CMS-Wave and the resulting wave forecasts are examined here. The following results are intended to assist in developing recommendations for both the wind and wave components of the coupled forecast system.

3.2.1: Wave Forcing – WAVEWATCHIII

The quality of the WW3 four minute (approximately 6.5 km) coastal product, which provides the wave forcing (significant wave height, wave period, and wave direction) for the CMS-Wave model, is assessed here. The WW3 forcing time series are obtained from the 00 UTC WW3 cycle, from which the first 48 h (out of 180 h available) are compared to corresponding wave observations from coastal NDBC buoys 41009, 41113, and 41114. Although the 00 UTC WW3 cycle was used in this study, it would not be practical in terms of forecast timeliness, as the data is not available until approximately 04 UTC (18 UTC WW3 will most likely be used in an operational setting).

Figure 27 displays the bias, RMSE, and scatter index values for all Tier 2 and 3 event WW3 significant wave height (H_s) and dominant wave period (D_p) forecasts at buoys 41009, 41113, and 41114, broken into two 24 h periods (0-24 h and 24-48

h). For these events, WW3 tends to underforecast H_s at all three buoys (see bias in Figure 27) – especially at the two nearshore buoys (41113 and 41114). The wave period is mixed, WW3 underforecasts D_p at the two coastal buoys (41113 & 41114) but forecasts longer periods than observed at 41009. The underforecasting of H_s at buoy 41009 is not surprising as the GFS underforecasts wind speeds (Fig. 17), however, because there are no wind observations at buoys 41113 and 41114, it is not possible to draw similar conclusions at the nearshore locations. Smaller RMSEs are observed at buoy 41009 for both H_s and D_p, indicating that the WW3 coastal product is somewhat degraded in the nearshore region. In terms of the SI, the WW3 performs well at all three buoys with overall SI values (Fig. 27) between 11% and 15% for significant wave height and between 15% and 30% for dominant wave period. There appears to be only a small difference in the quality of the WW3 forcing between the first and second 24h forecast periods – with both siginificant wave height and dominant wave period forecasts actually improving in time at the nearshore buoys. This fact may be due to the selection of wind events, for which the highest winds occur during the first 24h forecast period.

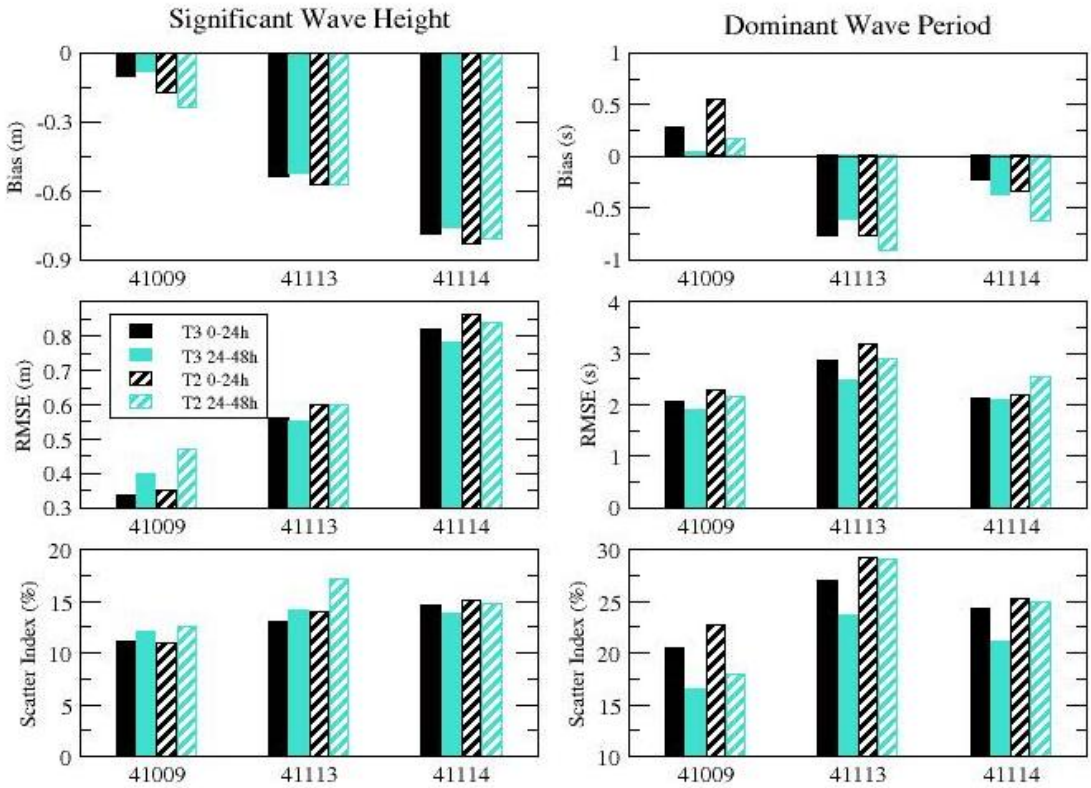

Fig. 27: Bias (ms^{-1}), RMSE (ms^{-1}), and Scatter Index (SI - %) for all Tier 3 (solid) & 2 (striped) WW3 Significant Wave Height (m, left) and Dominant Wave Period (s, right) forecasts at NDBC buoys 41009, 41113, and 41114 for two 24h periods: 0-24h (black) and 24-48h (turquoise).

The results discussed above are in agreement with a 2002 to 2004 WW3 study at NCEP for which they validated 24 h forecasts over the Western North Atlantic (WNA) WW3 domain (http://polar.ncep.noaa.gov/waves/valid_wna/bwaves.F024H.png). Statistics for significant wave height from the NCEP study are provided in Table 13. Although larger errors might be expected within coastal regions, due to changing bottom topography and wave interactions with the shore, SI values for the WW3 coastal product are actually lower than those reported for the WNA region. H_s bias and

RMSE values for buoy 41009 are also comparable to WNA results (compare Fig. 27 and Table 13), whereas values are higher at buoys 41113 (bias -0.6 ms^{-1}, rmse 0.6 ms^{-1}) and 41114 (bias -0.9 ms^{-1}, rmse 0.8 ms^{-1}). These higher errors seen in the coastal region indicate an area where CMS-Wave can play an important role in improving forecasts.

Table 13. NCEP WW3 validation statistics for 24h forecasts of significant wave height in the Western North Atlantic region between 2002 and 2004. (Results posted at **http://polar.ncep.noaa.gov/waves/valid_wna/bwaves.F024H.png)**

Statistic	Monthly Value Range
Bias (m)	-0.25 – 0.25
RMSE (m)	0.2 – 0.4
Scatter Index (%)	20 - 30

WW3 wave forecasts are evaluated for the Tropical Storm Fay Tier 1 event. Figures 28 and 29 depict both the observations and WW3 forecasts of H_s and D_p at buoys 41009, 41113, and 41114 for the 48 h period starting 00 UTC 20 August 2008. Figure 30 is the Tier 1 analog to Figure 27 (i.e., the bias, RMSE, and scatter index for TS Fay). WW3 underforecasts D_p (except for at buoy 41114 in the second 24 h forecast period) and, similar to the the Tier 2 and 3 results (Fig. 27), WW3 significantly underforecasts H_s at all three buoy locations (Fig. 29). Again the underforecasting of H_s at buoy 41009 may be an artifact of underforecasting the wind speed by the GFS (WW3 wind forcing) which is on the order of 5 ms^{-1} lower than observed on 20 August 2008 (e.g., Fig. 24c).

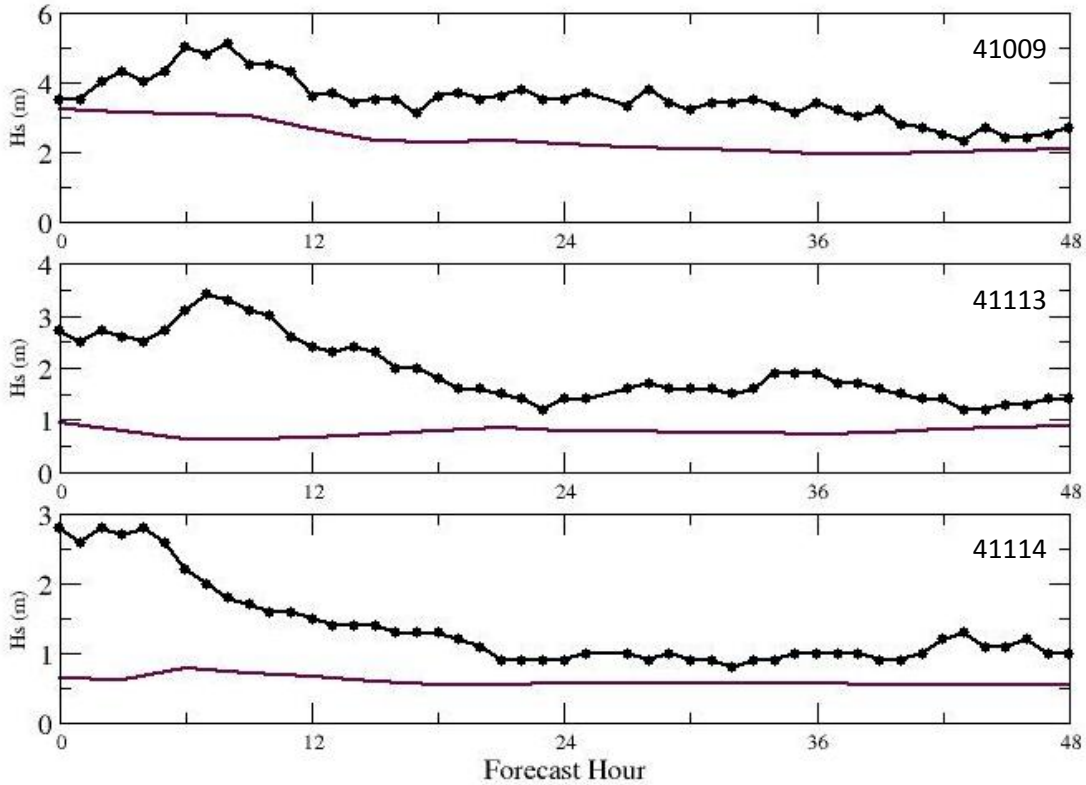

Fig. 28: Observed significant wave height (m, solid black line with filled circles) at buoys 41009 (top), 41113 (middle), and 41114 (bottom) versus WW3 forecasts (maroon) at the buoy locations for 00 UTC 20 August to 00 UTC 22 August 2008.

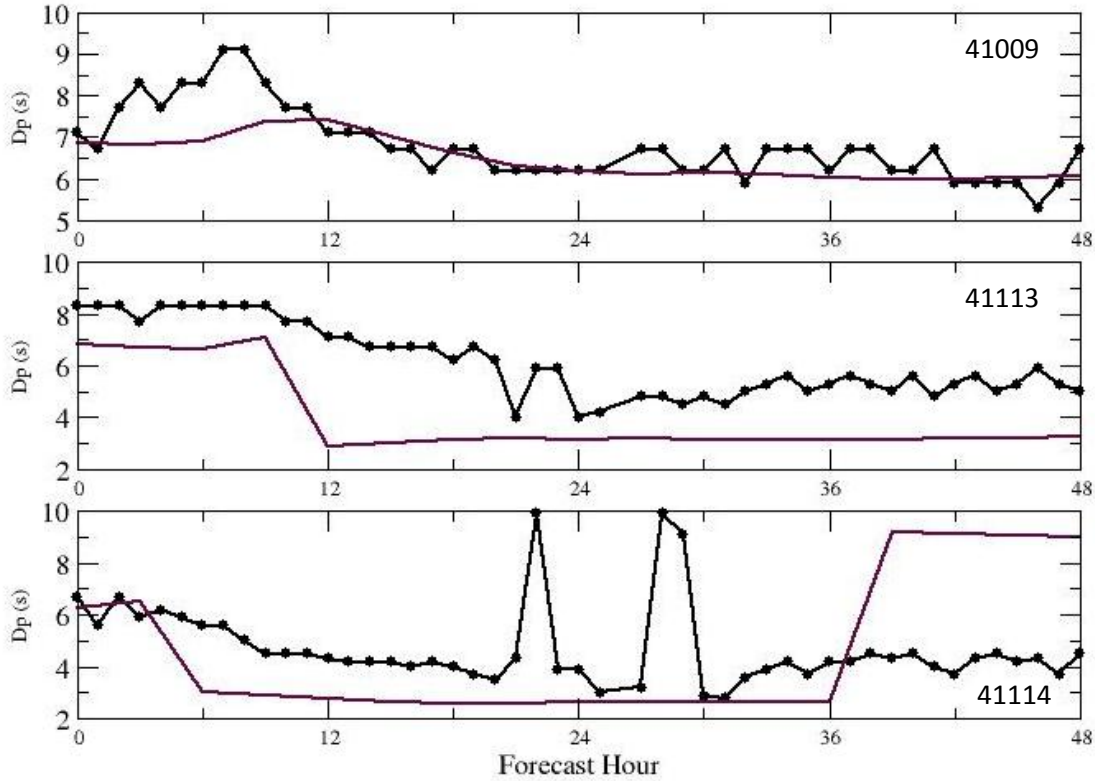

Fig. 29: Observed dominant wave period (s, solid black line with filled circles) at buoys 41009 (top), 41113 (middle), and 41114 (bottom) compared to WW3 forecasts (maroon) at the buoy locations for 00 UTC 20 August to 00 UTC 22 August 2008.

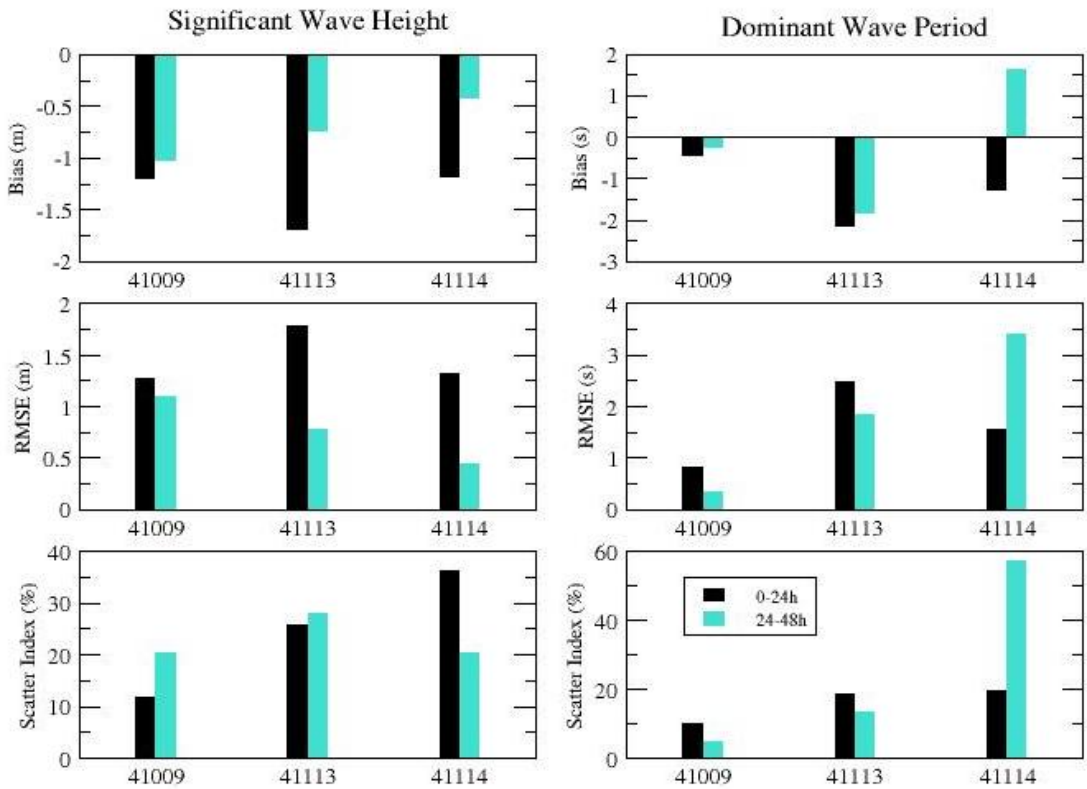

Fig. 30: WW3 Tropical Storm Fay wave forecast statistical results (bias (ms^{-1}, top), RMSE (ms^{-1}, middle), and scatter index (SI - %) (bottom)) for significant wave height (m, left) and dominant wave period (s, right) at buoys 41009, 41113, and 41114 for the first 48 h of the WW3 00 UTC 20 August 2008 forecast cycle(0-24 h – black, 24-48 h – turquoise).

RMSE values are higher for both variables and at each buoy for the Tropical Storm Fay wave forecasts when compared to Tier 2 and 3 results (Fig. 27) and are the highest for the first 24 h forecast period. The RMSEs at buoy 41113 and 41114 are due to WW3 erroneously forecasting the initial wave heights, which could once more be attributed to the GFS underforecasting the initial wind speed (Fig. 24). As observed in the Tier 2 and 3 results (Fig. 27), RMSE values for D_p are smaller at buoy 41009 and larger at both of the nearshore buoys (41113 and 41114). H_s scatter

indices during TS Fay are quite low (between 10% and 20%) at buoy 41009 but higher at the nearshore buoys (between 20% and 40%). Compared to Tier 3 results, D_p scatter index values are very low for the first 24 h period at all three buoys and for the second 24 h period at buoys 41009 and 41113. The large D_p scatter index value (57%, Fig. 30) for the 24-48 h forecast window at buoy 41114 is consistent with the time series shown in Figure 29 in which the difference between the observed and WW3 forecast periods is, at times, nearly six seconds, again most likely due in part to the GFS underforecasting of the wind speed during the event . As mentioned earlier in this section and discussed in this study, errors in the wind field can produce errors in the wave forecasts, therefore, it is not surprising that errors in the WW3 forecasts can be attributed, in part, to errors in the GFS wind forcing. The RMSE for the WW3 H_s is plotted against the GFS wind speed error at buoy 41009 for all Tier 3 events (Fig. 31). The linear trendline indicates that errors in the GFS wind field are correlated, in part, with errors in forecast significant wave height in WW3.

Overall the coastal WW3 product performs reasonably well, with errors similar to or smaller than those reported by NCEP in their open ocean WNA products. Nonetheless, the coastal WW3 still is somewhat degraded in the nearshore region – suggesting that an increase in forecast resolution for both atmosphere and wave models and the incorporation of bottom physics would potentially provide improved wave forecasts for the National Weather Service.

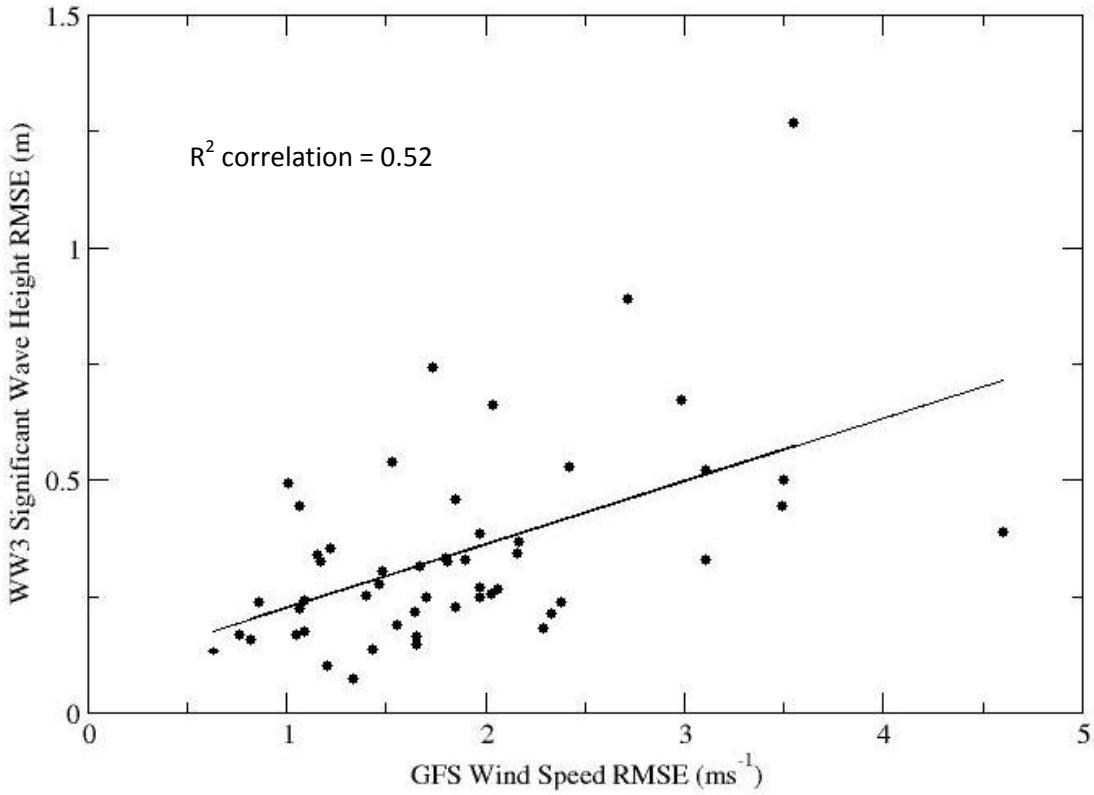

Fig. 31: Tier 3 GFS wind speed RMSE (ms^{-1}) compared to WW3 significant wave height RMSE (m). R^2 correlation = 0.52. Linear trendline (black line).

3.2.2: Wave Forecast and Impact of Varying Wind Forcing

Wind speed variations across the wave domains are relatively small for the Tier 3 events (e.g., Fig. 9b). However, it is important to discern whether or not these small differences are important in the context of the wave forecasts. This section attempts to determine whether or not the small variations in forecast wind speed have an impact on the CMS-Wave forecasts. In order to examine whether this is the case or not, the CMS-Wave is run for each Tier 3 event, *varying only the wind forcing*. Here, the NAM 12 km, WRF-NAM 10 km, WRF-NAM 4.5 km, and WRF-NAM

1.5 km winds are used to force CMS-Wave. The GFS and WRF-GFS 10 km are used as wind forcing for the Tier 1 Tropical Storm Fay case only (see section 3.2.2.2). Due to the quiescent conditions and the lack of performance during the two month analysis of the NWS generated GFE it was not used to force the wave model and will not be discussed in this section. As in previous sections, the results are organized by Tier with the focus on significant wave height and dominant wave period forecasts at buoys 41009, 41113, and 41114.

3.2.2.1: Tier 3 Wave Analysis

The bias, RMSE, and scatter index (SI) for Tier 3 CMS-Wave forecasts of H_s and D_p are shown, for the various forcings, at buoys 41009, 41113, and 41114 (Fig. 32). CMS-Wave underforecasts at all three NDBC buoys in terms of significant wave height, as well as for dominant wave period at both of the coastal buoys, which is not surprising as all atmospheric models also underforecasted the wind speeds at all three buoys. Root-mean square errors for significant wave height and dominant wave period forecasts are similar at all three buoys with the exception of NAM, which has the lowest RMSE values in the nearshore region. Scatter index values for both variables, all four wind forcing options, and at each of the three buoys are between 10% and 30%. These SI values are consistent with previous wave model study by Janssen et al. (1997) who observed SI values around 20%. The SI values are actually lower than those reported by Janssen et al. (1997) who noted increased SI

values along the east coast of the United States reaching as high as 30% in the summer months.

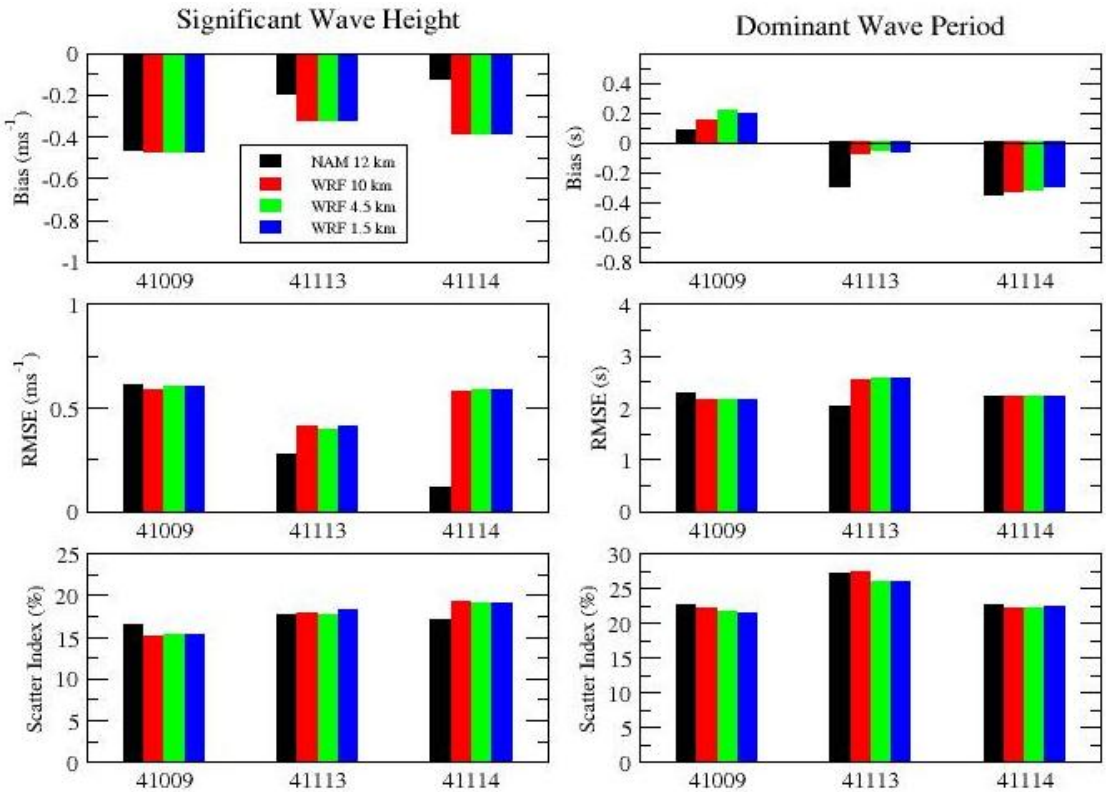

Fig. 32: Bias (ms^{-1}), RMSE (ms^{-1}), and Scatter Index (SI - %) for all Tier 3 CMS-Wave Significant Wave Height (m, left) and Dominant Wave Period (s, right) forecasts at NDBC buoys 41009, 41113, and 41114. Wind forcing: NAM 12 km (black), WRF-EMS (10 km - red, 4.5 km - green, and 1.5 km - blue)

Figure 33 depicts the skill scores for CMS-Wave forecasts for the different wind forcing, with the skill score metric being the WW3 forecasts at the buoy locations. For the Tier 3 events, CMS-Wave exhibits an improvement over WW3 forecasts for significant wave height at the nearshore buoys (41113 and 41114) and dominant wave period at buoy 41113. *In particular the NAM wind forcing yields the*

greatest improvement in significant wave height forecasts over that of WW3 at the nearshore buoys. The negative skill scores at 41009 indicate that the CMS-Wave forecasts of both H_s and D_p are inferior to those of WW3, which is not surprising as buoy 41009 is located at the eastern edge of wave domain 1 and is thus in deeper water (44 m) compared to 41113 (10 m) and 41114 (16 m). CMS-Wave is designed for the nearshore regions where the waves feel the affect of ocean bottom. In addition, the CMS-Wave boundary conditions are strongly tied to WW3 given the buoy location with respect to the model boundary (e.g., see Fig. 34). As a side note, Figure 34 is as a reminder of the gaps in wave forecsts left at the coast by the coastal WW3 product.

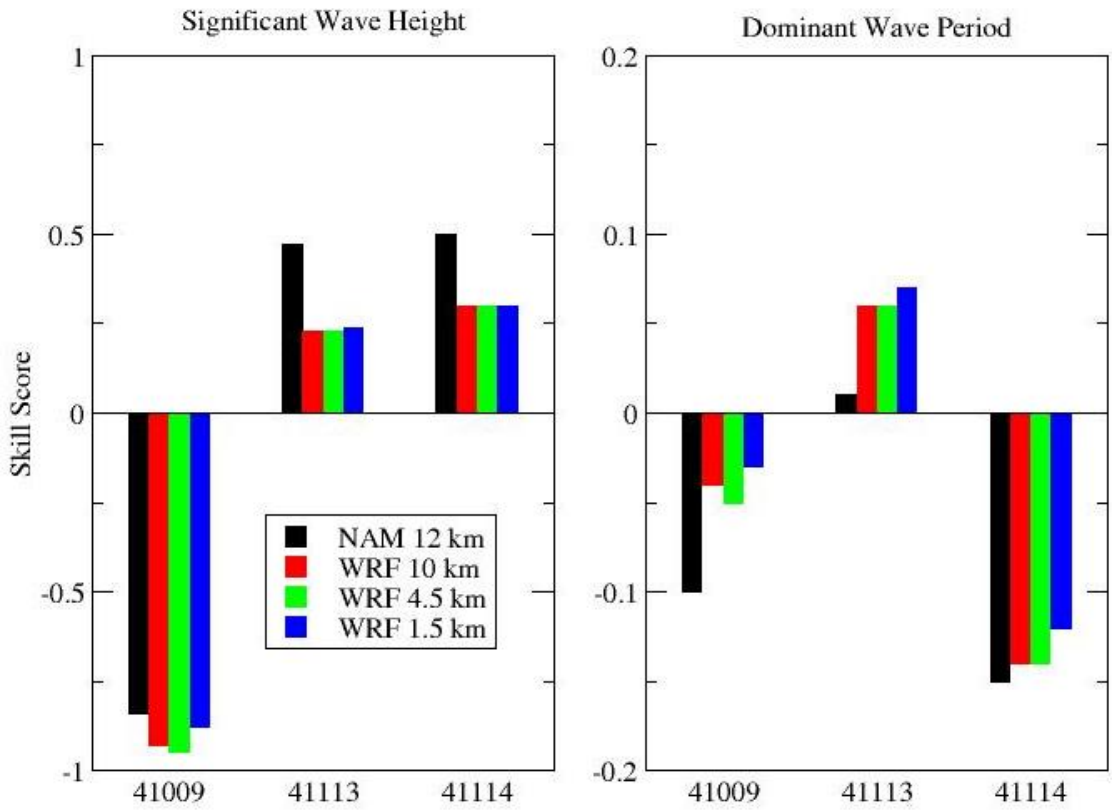

Fig. 33: Skill score for all Tier 3 CMS-Wave Significant Wave Height (m, left) and Dominant Wave Period (s, right) forecasts at NDBC buoys 41009, 41113, and 41114. Wind forcing: NAM 12 km (black), WRF-EMS (10 km - red, 4.5 km - green, and 1.5 km - blue)

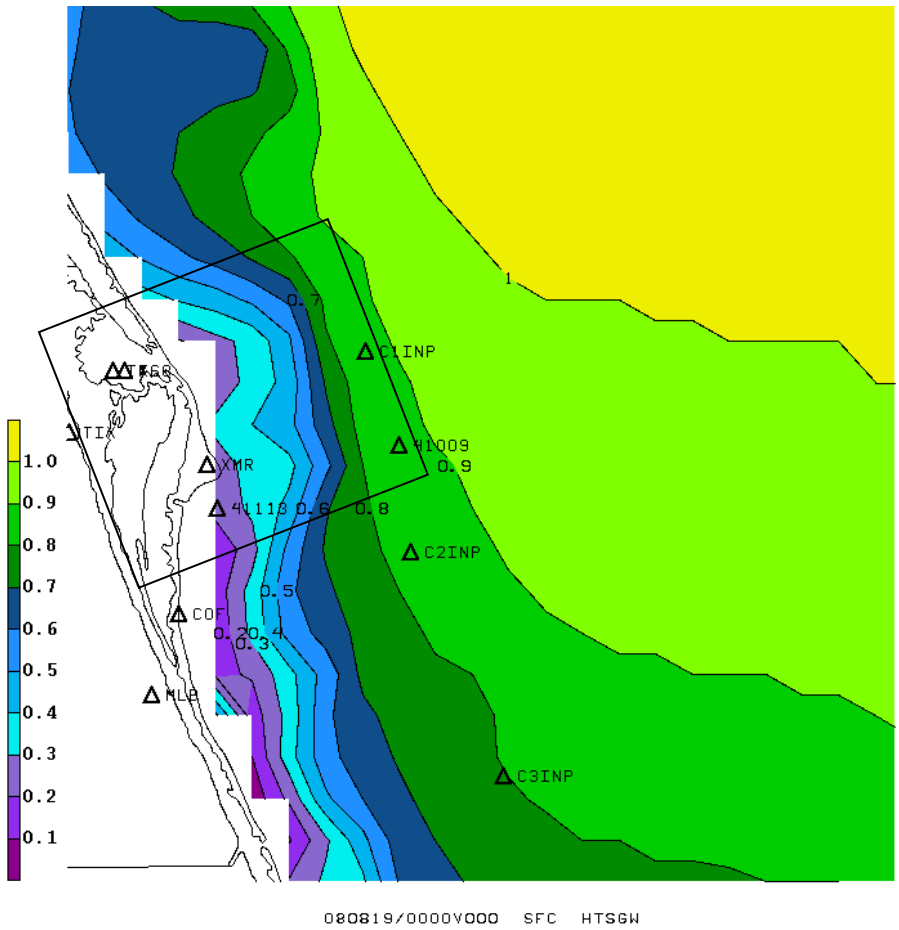

Fig. 34: Example plot of significant wave height forecast from WW3 for 00 UTC 19 August 2008. Location of buoy 41009, 41113, and the wave input locations for wave domains 1 (C1INP), 2 (C2INP), and 3 (C3INP) are shown (triangles). The approximate location of wave domain 1 (black rectangle) is also shown.

RMSE results in Figure 32 show that using NAM as wind forcing produces improvements in significant wave height at both neashore buoy locations and in dominant wave period at buoy 41113. Figure 33 presents similar results, in terms of CMS-Wave forecast skill scores, as the NAM driven wave model forecasts are clearly superior to those generated via WRF-NAM forcing, especially for significant wave height forecasts at the nearshore buoys. For the Tier 3 results shown in Figures 32

and 34, significant differences are only observed between NAM and WRF-NAM. No difference is observed amid any of the WRF-NAM results, implying that the small variations seen in the WRF-NAM wind forcing do not have an impact on the wave forecasts.

3.2.2.2: Tier 1 – Tropical Storm Fay Wave Analysis

Similar to results shown for the Tier 3 analysis (Figs. 32 and 33), the Tier 1 TS Fay case results are now presented in Figures 37 and 38. Tier 2 evaluations are quite similar to the Tier 3 results and thus, the results are not shown here. As discussed in the wind forecast results section, Tropical Storm Fay passed through the study area in August 2008. Figures 35 and 36 display the observed significant wave height and dominant wave period (solid black dotted lines) at buoy 41009 (top time series in figures) from 00 UTC 20 August to 00 UTC 22 August 2008, along with the forecasted values from CMS-Wave. Wind results from Tropical Storm Fay at buoy 41009 (Figs. 24 and 25) indicated that the GFS has more skill than NAM at forecasting for this tropical cyclone, therefore the following CMS-Wave results include model runs using GFS and WRF-GFS 10 km.

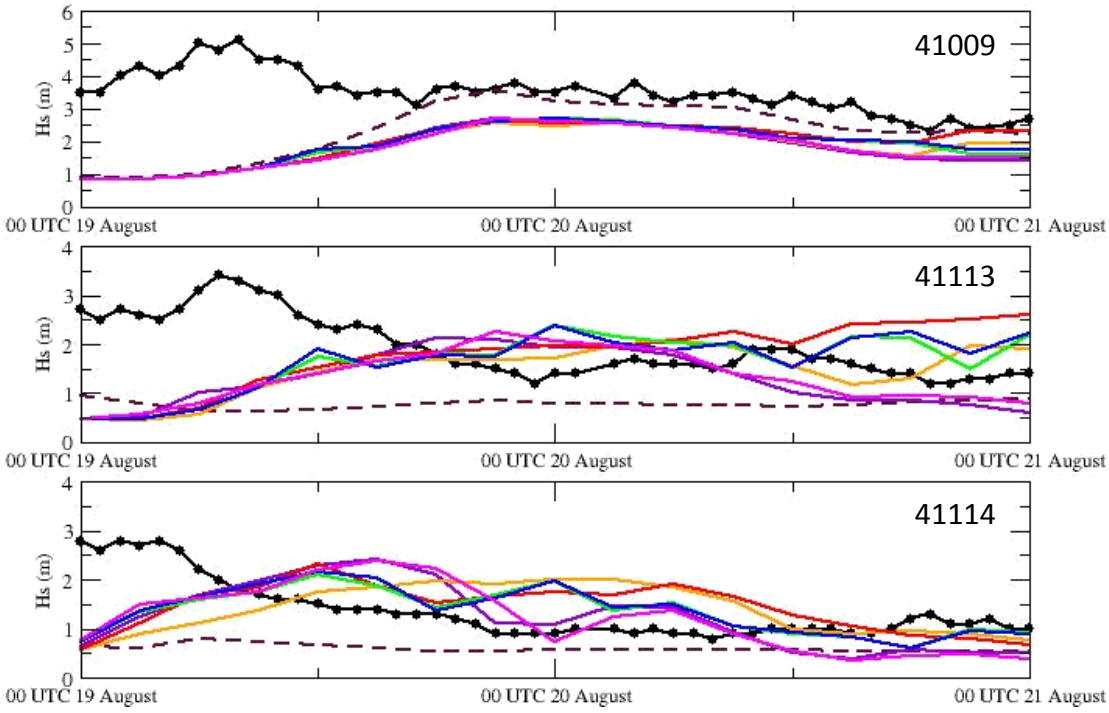

Fig. 35: Observed significant wave height (m, solid black line with filled circles) at buoys 41009 (top), 41113 (middle), and 41114 (bottom) compared to WW3 (dashed maroon) and differently forced CMS-Wave (GFS – purple, WRF-GFS – pink, NAM – orange, and WRF-NAM (10 km – red, 4.5 km – green, 1.5 km – blue)) forecasts at the buoy locations for 00 UTC 19 August to 00 UTC 21 August 2008.

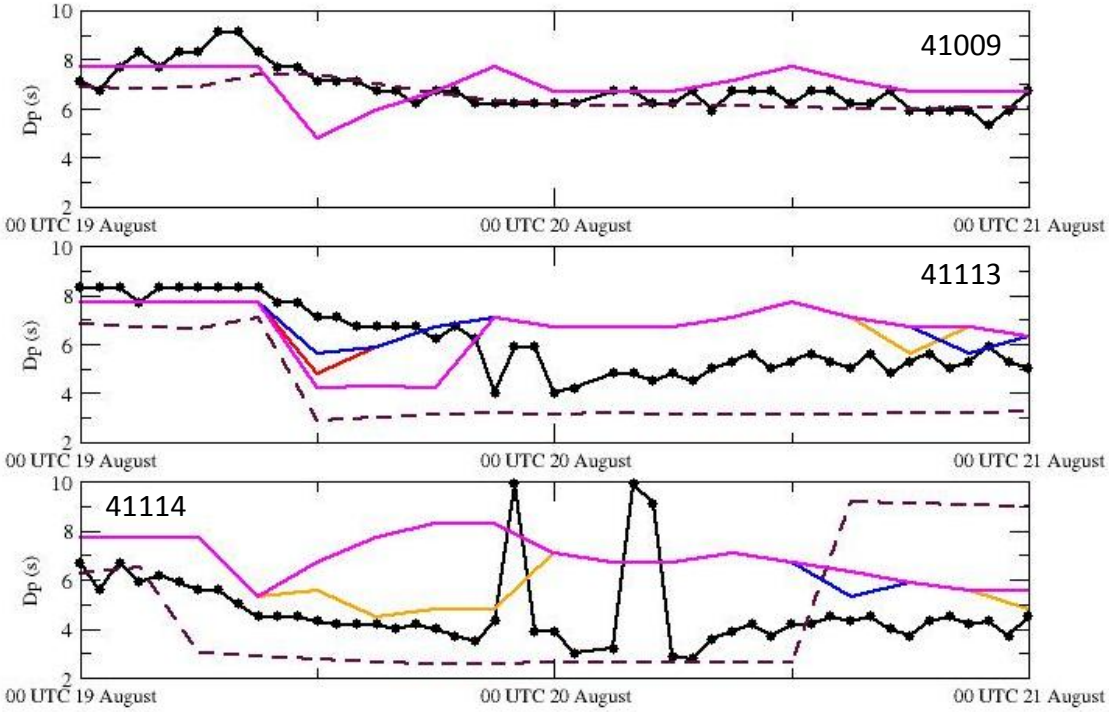

Fig. 36: Observed dominant wave period (s, solid black line with filled circles) at buoys 41009 (top), 41113 (middle), and 41114 (bottom) compared to WW3 (dashed maroon) and differently forced CMS-Wave (GFS – purple, WRF-GFS – pink, NAM – orange, and WRF-NAM (10 km – red, 4.5 km – green, 1.5 km – blue)) forecasts at the buoy locations for 00 UTC 19 August to 00 UTC 21 August 2008.

GFS, NAM 12 km, WRF-NAM (10 km, 4.5 km, 1.5 km), and WRF-GFS 10 km were used to force CMS-Wave during the passage of Tropical Storm Fay on 20 August 2008. Figures 37 and 38 display the validation statistics for all differently forced 48 h forecast runs of CMS-Wave for this Tier 1 event. Figure 38 displays the skill score values for the CMS-Wave forecasts compared to those of WW3 at buoys 41009, 41113, and 41114. Consistent with the Tier 3 results, CMS-Wave performs better than WW3 in the nearshore region in terms of significant wave height RMSE; however, the scatter index values at buoys 41113 and 41114 for all differently

forced CMS-Wave runs for Tropical Storm Fay are higher than at buoy 41009. The higher scatter index values at the nearshore buoys are due to the SI equation incorporation of lower observed wave heights, typical of nearshore regions, causing larger SI values even though the error is similar at all three buoys. Getting back to the RMSEs, larger values observed at buoy 41009 are again not surprising as CMS-Wave is not designed to forecast at open ocean locations where WW3 will still be the more accurate model. Also, model predictions are generally known to be bad near the boundary of model grids, where buoy 41009 is located.

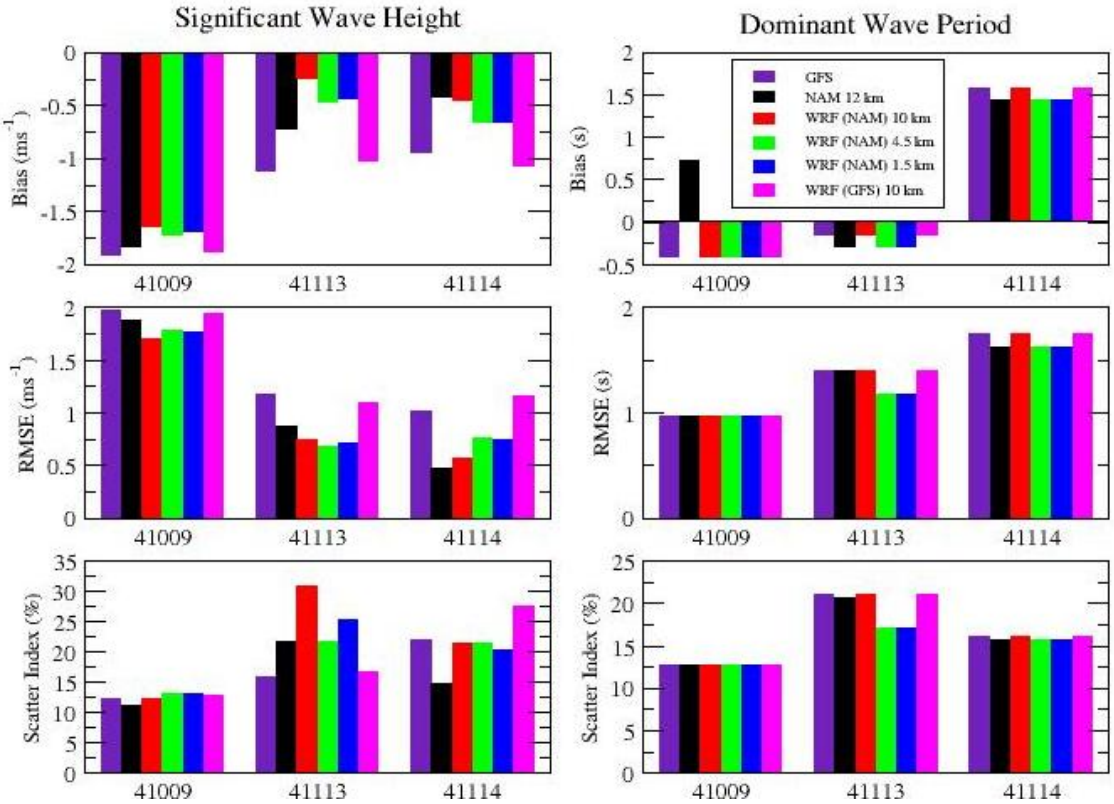

Fig. 37: Bias (ms^{-1}), RMSE (ms^{-1}), and Scatter Index (SI - %) for Tier 1 (Tropical Storm Fay 20 August 2008) CMS-Wave Significant Wave Height (m, left) and Dominant Wave Period (s, right) forecasts at NDBC buoys 41009, 41113, and 41114. Wind forcing: GFS km (purple), NAM 12 km (black), WRF-EMS (NAM forced) (10 km - red, 4.5 km - green, and 1.5 km - blue), and WRF-EMS (GFS forced) (10 km – pink).

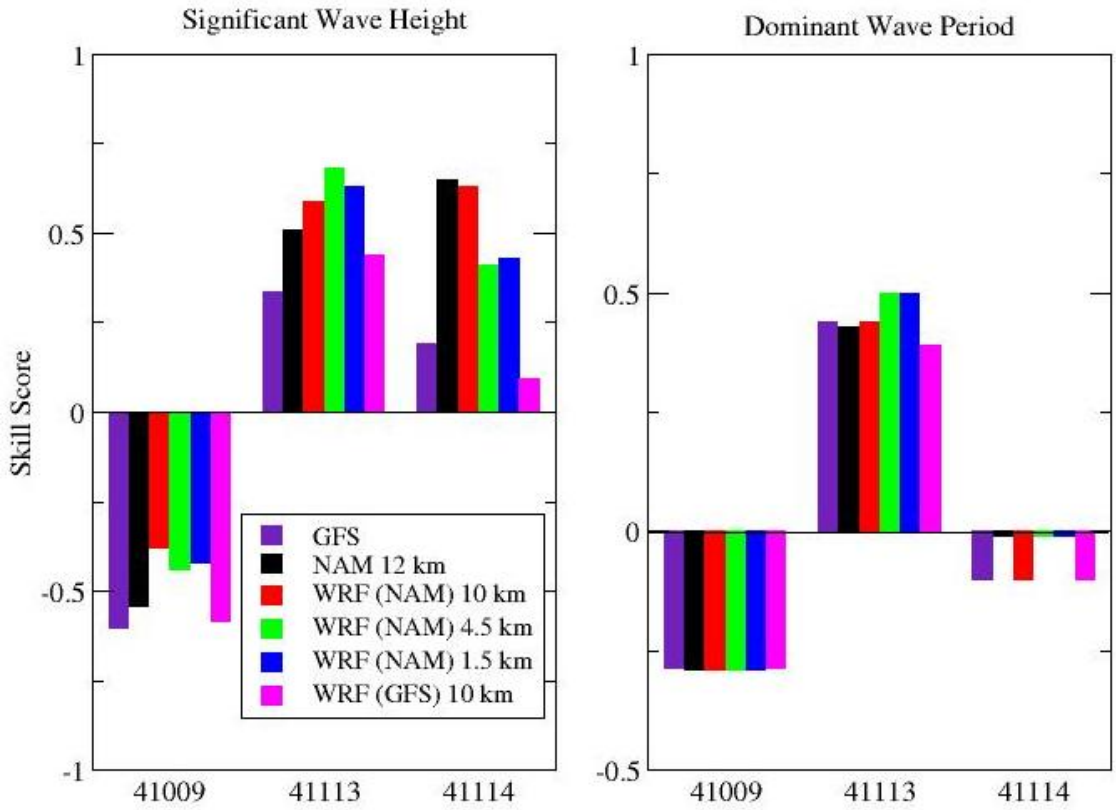

Fig. 38: Skill score for Tier 1 (Tropical Storm Fay 20 August 2008) CMS-Wave Significant Wave Height (m, left) and Dominant Wave Period (s, right) forecasts at NDBC buoys 41009, 41113, and 41114. Wind forcing: GFS (purple) NAM 12 km (black), WRF-EMS (10 km - red, 4.5 km - green, and 1.5 km - blue)

In terms of the skill score, all of the options used to force the CMS-Wave produced an improvement in the significant wave height forecasts at both nearshore buoys and dominant wave period forecasts at buoy 41113 when compared to WW3. Three of the models used to force CMS-Wave (NAM, WRF-NAM 4.5 km and 1.5 km) were very close to the dominant wave period forecasts produced by WW3 at buoy 41114. Issues in forecasting dominant wave period at buoy 41114 is also observed in Figure 37 in terms of RMSE. Observations at buoy

41114 (plotted in the bottom graph of Figure 36) show spikes in the dominant wave period (from 4 s to 10 s) which are possibly due to the swell component of the waves (typically longer periods) dominating over the wind component. Further investigation is required to determine if this is occurring at buoy 41114.

Although the forcing obtained from each of the three NAM initialized WRF simulations did not produce the best wind forecasts at buoy 41009 (Figs. 25 and 26), they did produce improved significant wave height and dominant wave period forecasts at buoy 41113 compared to those of WW3 (Fig. 38). Because buoys 41113 and 41114 do not report wind information, the connection between the quality of the wind forcing and wave forecasts is not clear. The wind evaluation at buoy 41009 may not apply to the nearshore buoys where the influence of the land may have a more profound impact on atmospheric model wind forecasts.

In terms of significant wave height at buoy 41009 for the Tier 1 event, the WRF-NAM also performed better than the other models used to force CMS-Wave, even though it was not an improvement over WW3. For Tropical Storm Fay the GFS or WRF-GFS 10 km wind forcing produced improved significant wave height forecasts at the nearshore buoys when compared to WW3, but were not as much of an improvement over WW3 compared to the NAM and WRF-NAM forecasts. This reveals that while the GFS and WRF-GFS 10 km are better at forecasting winds at buoy 41009 it is not necessarily indicative of improved performance in the

nearshore region - pointing out the need for wind observations in the nearshore region to further evaluate the quality of the wind forcings in the coastal zone.

Ultimately, the wave results indicate that there is not enough of a difference between the WRF-NAM resolutions to run the WRF at high resolution. Either the NAM or WRF-NAM 10 km seem to be sufficient in most cases, with perhaps exceptions for tropical cyclone scenarios – for which the GFS might exhibit better forecast track skill.

3.3: Resulting Wave Model Variability

As discussed in depth in sections 3.1.1.1 to 3.1.1.3, the expected variability or standard deviation in forecast wave height is represented by the dashed curves in Figures 11a and 11b. The resulting variability within CMS-Wave (WRF-NAM 10 km wind forcing), as well as the WW3, is now shown for buoy 41009 in Figures 39a-d. All data presented in Figures 39a-d are for Tier 3 48 h average forecasts and observations valid at buoy 41009. Figures 39a, 39b, and 39d display the same theoretical forecast and standard deviation curves from 11a with the addition of wind speed versus wave height comparisons:

a – GFS wind speed forecasts (WW3 wind forcing) vs. WW3 forecast H_s

b – WRF-NAM 10 km wind speed (CMS-Wave wind forcing) vs. CMS-Wave forecast H_s

d – Buoy observed wind speed vs. observed H_s

Figure 39d presents the observed variability in significant wave height due to wind speed, bounded by the theoretical standard deviation curves. Compare this to Figures 39a and 39b which compare wind forcing to resulting significant wave height forecasts for WW3 and CMS-Wave.

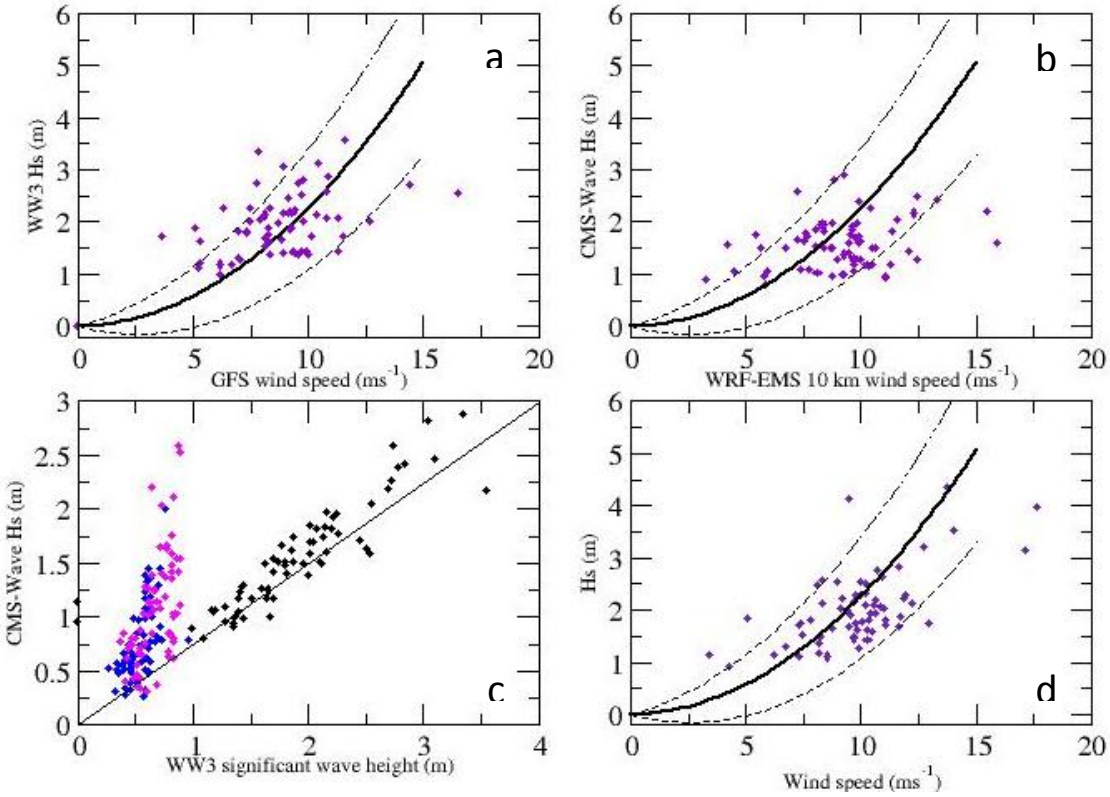

Figs. 39a-d: Figure 11a theoretical curves are plotted in Figures 39a, 39b, and 39d. Figures 39a-d all display 48 h averaged data for each Tier 3 wind event valid at buoy 41009. A – GFS forecast wind speed (ms^{-1}, WW3 wind forcing) versus WW3 forecast H_s (m), B – WRF-NAM 10 km forecast wind speed (ms^{-1}, CMS-Wave wind forcing) versus CMS-Wave forecast H_s (m). C - WW3 forecast Hs (m, CMS-Wave wave forcing) versus resulting CMS-Wave forecast H_s (m) (Buoy 41009 – black, 41113 – blue, 41114 – pink). D - Observed wind speed (ms^{-1}) versus observed H_s (m).

The majority of both observation (Fig. 39d) and forecast comparisons for both wave models (Figs. 39a and 39b) lie within the theoretical bounds discussed

earlier (Fig. 11a). Figure 39c compares the buoy 41009, 41113, and 41114 WW3 forecasted H_s (CMS-Wave wave forcing) to the resulting CMS-Wave forecasted H_s - showing how strongly the CMS-Wave is influenced at buoy 41009 by its boundary conditions from the WW3 but not at either of the nearshore buoys. Given a particular significant wave height forecast from WW3 at either of the nearshore buoys, there is significant variability in the resulting CMS-Wave forecast which, instead of coming from the WW3, it comes from a combination of varying bottom topography and the wind forcing (in this case WRF-NAM 10 km).

The next section will summarize the results as presented here, and in previous sections, to provide recommendations for the configuration of the coupled forecast system.

4. SUMMARY

A high-resolution atmosphere-wave coupled nearshore forecasting system for the National Weather Service was developed and evaluated in this study. A set of atmospheric forcing options (GFS, NAM, NWS generated GFE, and four configurations of the WRF), the WW3 wave forcing, and the resulting wave forecasts from CMS-Wave were examined across 213 48 h forecasts from August 2008 to March 2009, which included 67 wind events and one tropical storm. All forecasted wind and wave values were compared to observations at three buoys located within the study area (41009, 41113, and 41114 seen in Fig. 6). The following bulleted items will summarize the results collected from model validations at the buoys:

- Significant spatial variability was observed within each forecast wave domain wind field from NAM and WRF but no addition variability was added by increasing the resolution of the WRF model. Even with the single point time series limitation, five CMS-Wave model domains seem to be sufficient for capturing the variability within the wind fields (see single point time series versus domain average results in Figure 14). Future work may want to investigate the ability of ingesting a gridded wind field into the CMS-Wave model to further capture the wind variability and improve the wave forecasts.

- On a daily basis the GFS model performs well in forecasting winds at the offshore buoy (41009) but without wind observations at either of the nearshore buoys (41113 and 41114) this may not be the case over coastal waters. The difference in performance at buoy 41009 between the GFS and both the NAM model and WRF-NAM 10 km is small, thus, the daily performance analysis results are not clear on which model is the best. Wave model results were therefore the determining factor in which atmospheric model would be best to use in the coupled forecast system.

- For the Tier 1 Tropical Storm Fay event the GFS and WRF-GFS handled the storm better than the NAM and WRF-NAM, suggesting that the GFS would be preferable during tropical cyclone events.

- No significant difference exists between the various resolutions of the WRF model – indicating there is no need to increase the horizontal resolution. Since the 10 km WRF domain takes approximately five minutes to run and the 4.5 km WRF domain (with the 1.5 km nest) takes approximately four hours, the computational expense of the higher resolutions is too large for an operational forecast system.

- The coastal WW3 product performs well at the offshore buoy (41009), but with issues in forecasting waves in the nearshore (see Fig. 27) CMS-Wave can still improve upon the wave forecasts in the coastal region.

- For the Tier 3 wind events: In terms of significant wave height at the nearshore buoys, the NAM forced CMS-Wave model runs had the greatest improvement over the WW3 at both buoys. All three WRF-NAM resolutions also outperformed WW3 in terms of wind speed at the nearshore buoys, while both NAM and WRF-NAM outperformed WW3 in terms of dominant wave period at buoy 41113. Issues in forecasting dominant wave period at buoy 41114 must still be examined (Fig. 29). CMS-Wave issues in forecasting at buoy 41009 were to be expected as CMS-Wave was not designed for the open ocean.

- For the Tier 1 Tropical Storm Fay event (Figs. 35 and 36): All atmospheric model forcings outperformed WW3 in the nearshore, with the exception in dominant wave period at buoy 41114. Although the GFS and WRF-GFS 10 km performed well in terms of wind speed forecasts at buoy 41009, they did not provide the best forcings at the nearshore buoys – the NAM and WRF-NAM outperformed the GFS and WRF-GFS.

- The theoretical wave height variability discussed in sections 3.1.1.1 and 3.1.1.2 was indeed observed in the CMS-Wave forecasts at buoy 41009 (Figs. 39a-d), as well as in the WW3.

Based on the summarized results the following recommendations for the configuration of the coupled forecast system are shown in Table 14.

Table 14. Summarized study results and recommendations for the coupled forecast system (components, models, and resolutions).

Component	Model and Resolution
Atmospheric model (Wave model wind forcing)	WRF-NAM 10 km (00 UTC NAM forced WRF, 10 km resolution)
Wave model wave forcing	18 UTC coastal WW3 product
Number of wave domains	Five (this is specific to the Melbourne NWSFO forecast zones)

These recommendations are for a once daily setup of the coupled forecast system but can easily be accommodated for multiple daily forecasts. The 48 h wave forecast data from the recommended configuration would be available to the forecasters around 04 UTC. For operational runtime considerations the 18 UTC NAM could be used to force the WRF, which would make the data available around 22 UTC. The locations, shapes, and sizes of the wave grids can be further modified to fit the NWS forecast zone needs.

Future work on the coupled forecast system should focus on the following aspects:

- Researching the gridded wind field input option for the CMS-Wave or other wave model.
- Fall and winter analysis of the NWS generated GFE winds as a wave model forcing option.

- The incorporation of a flow model (M2D) into the forecast system.
- Analysis of forecast skill as a function of forecast hour.

The high-resolution atmosphere-ocean coupled forecast system is slated for transition and implementation at the National Weather Service (NWS) Forecast Offices in Melbourne and Miami, FL in late 2009. The forecast system will provide quality high resolution short-term gridded wave forecasts for the NWS marine area of responsibility. Taking advantage of the higher wave model resolution, the system will support the creation of enhanced, value-added products. The detailed information will help coastal forecast offices meet the increasing demands of a growing marine industry and boating community.

5. References

Blumberg, A. F., S. Fan, T. Herrington, M. Bruno, A. Cope, Q. Ahsan, and H. Li, 2005: A Coastal Wave Forecasting System for New Jersey and Long Island Waters. 6th Conference on Coastal Atmospheric and Oceanic prediction and Processes, 85th American Meteorological Society Annual Meeting, 9-13 January 2005, San Diego, CA.

Booij, N., R. C. Ris, and L. H. Holthuijsen (1999), A third-generation wave model for coastal regions 1. Model description and validation, *J. Geophys. Res.*, 104(C4), 7649–7666.

Buttolph, A. M., Reed, C. W., Kraus, N. C. , Ono, N., Larson, M., Camenen, B., Hansen, H., Wamsley, T., and Zundel, A. K.,. 2006. Two-Dimensional Depth-Averaged Circulation Model CMS-M2D: Version 3.0, Report 2, Sediment Transport and Morphology Change. Coastal Inlets Research Program Technical Report ERDC- CHL-TR-06-, U.S. Army Engineer Research and Development Center, Vicksburg, Mississippi.

Cavaleri, L., 2006: Wave Modeling: Where to Go in the Future. *Bull. Amer. Meteor. Soc.*, **87**, 207 – 214.

Chen, S.S., J.F. Price, W. Zhao, M.A. Donelan, and E.J. Walsh, 2007: The CBLAST-Hurricane Program and the Next-Generation Fully Coupled Atmosphere–Wave–Ocean Models for Hurricane Research and Prediction. *Bull. Amer. Meteor. Soc.*, **88**, 311–317.

Clancy, R., J. Kaitala, and L. Zambresky, 1986: The Fleet Numerical Oceanography Center Global Spectral Ocean Wave Model. *Bull. Amer. Meteor. Soc.*, **67**, 498–512.

Dong, C., and L.Y. Oey, 2005: Sensitivity of Coastal Currents near Point Conception to Forcing by Three Different Winds: ECMWF, COAMPS, and Blended SSM/I–ECMWF–Buoy Winds. *J. Phys. Oceanogr.*, **35**, 1229–1244.

Group, T.W., 1988: The WAM Model - A Third Generation Ocean Wave Prediction Model. *J. Phys. Oceanogr.*, **18**, 1775–1810.

Hodur, R.M., 1997: The Naval Research Laboratory's Coupled Ocean/Atmosphere Mesoscale Prediction System (COAMPS). *Mon. Wea. Rev.*, **125**, 1414–1430.

Høyer, J. L. and J. W. Nielsen, 2006: Satellite Significant Wave Height Observations in Coastal and Shelf Seas. 15 Years of Progress in Radar Altimetry Symposium, 812.

Hsu, S. A., Eric A. Meindl, and David B. Gilhousen, 1994: Determining the Power-Law Wind- Profile Exponent under Near-Neutral Stability Conditions at Sea, Applied Meteorology, Vol. 33, No. 6, June 1994.

Hsu, H.m., L.Y. Oey, W. Johnson, C. Dorman, and R. Hodur, 2007: Model Wind over the Central and Southern California Coastal Ocean. *Mon. Wea. Rev.*, **135**, 1931–1944.

Janssen, P. A. E. M., G. J. Komen, and W. J. P. De Voogt (1984), An Operational Coupled Hybrid Wave Prediction Model, *J. Geophys. Res.*, 89(C3), 3635–3654.

Janssen, P.A.E.M., B. Hansen, and J.R. Bidlot, 1997: Verification of the ECMWF Wave Forecasting System against Buoy and Altimeter Data. *Wea. Forecasting*, **12**, 763 – 784.

Johnson, H.K., H.J. Vested, H. Hersbach, J. Højstrup, and S.E. Larsen, 1999: The Coupling between Wind and Waves in the WAM Model. *J. Atmos. Oceanic Technol.*, **16**, 1780 – 1790.

Khandekar, M., and R. Lalbeharry, 1996: An Evaluation of Environment Canada's Operational Ocean Wave Model Based on Moored Buoy Data. *Wea. Forecasting*, **11**, 137–152.

Lin, L., H. Mase, F. Yamada, and Z. Demirbilek. 2006. *Wave-action balance diffraction (WABED) model tests of wave diffraction and reflection at inlets.* Coastal Inlets Research Program, ERDC/CHL CHETN-III-73. Vicksburg, MS: U.S. Army Engineer Research and Development Center.

Makin, V. K., and V. N. Kudryavtsev (1999), Coupled sea surface-atmosphere model 1. Wind over waves coupling, *J. Geophys. Res.*, 104(C4), 7613–7623.

Mase, H. 2001. Multi-directional random wave transformation model based on energy balance equation. *Coastal Engineering Journal* 43(4), 317-337.

Mase, H., and T. Kitano. 2000. Spectrum-based prediction model for random wave transformation over arbitrary bottom topography. *Coastal Engineering Journal* 42(1), 111-151.

Mase, H., K. Oki, T. Hedges, and H. J. Li. 2005. Extended energy-balance-equation wave model for multi-directional random wave transformation. *Ocean Engineering* 32, 961-985.

Nicolini, T. and G. Crawford, 2005: A High Resolution Nearshore Wave Model for Northwestern California. NWS Cooperative Project, final report.

Ris, R. C., L. H. Holthuijsen, and N. Booij (1999), A third-generation wave model for coastal regions 2. Verification, *J. Geophys. Res.*, 104(C4), 7667–7681.

Rozumalski, R. 2006: SOO/STRC WRF Environmental Modeling System users guide, http://strc.comet.ucar.edu/wrf/index.htm.

Tolman, H. L., 2002g: User manual and system documentation of WAVEWATCH-III version 2.22. NOAA / NWS / NCEP / MMAB Technical Note **222**, 133 pp.

Tracy, B. and A. Cialone, 2004: Comparison of Gulf of Mexico Wave Information Studies (WIS) 2-G Hindcast with 3-G Hindcasting. 8th International Workshop on Wave Hindcasting and Forecasting, C2.